LOW TEMPERATURE WATER GAS SHIFT REACTION OVER PROMOTED Pt-BASED CATALYSTS

by

Fatma Akpınar

B.S. in Ch.E., Yıldız Technical University, 2005

Submitted to the Institute for Graduate Studies in
Science and Engineering in partial fulfillment of
the requirements for the degree of
Master of Science

Graduate Program in Chemical Engineering

Boğaziçi University

2009

to my family

ACKNOWLEDGEMENTS

First of all, I would like to thank to my thesis advisor Assoc. Prof. Ramazan Yıldırım for his endless advice, support and encouragement during my thesis. It is my pleasure working with him and unforgettable experience in my life. Also I want to thank to my co-advisor Prof. Zeynep İlsen Önsan for her guidance.

I want to thank to my thesis committee members, Prof. Ahmet Erhan Aksoylu, Assist. Prof. Abdullah Kerem Uğuz and Prof. Ayşe Nilgün Akın who read and comment about my thesis.

Very special thanks to my graduate friends Melek Selcen Başar, Mehtap Demir, Funda Dikman, Seval Özdemir and Sevinç Tuna. The time passed full-up and enjoyable with them. Their friendship, valuable advices and supports motivated me during my experiments.

I wish to thank to Hacer Güneş who worked before me and taught the system where my experiments were carried out. Also I would like to thank CATREL team members Burcu Selen Çağlayan, Tuğba Davran Candan and Feyza Gökaliler for their experimental assistance.

Cordial thanks for Bilgi Dedeoğlu, Nurettin Bektaş and Yakup Bal for their technical assistance and help. Genuine thanks to Fatma Odak and Melike Gürbüz for their help.

I would like to thank my family for their support, patience, encouragement and trust in me throughout my entire education. My father, mother and brother have all been a great source of love for me. My thesis is dedicated to them.

Financial support is provided by TÜBİTAK through Project 105M034 and Boğaziçi University through BAP-06M104.

ABSTRACT

LOW TEMPERATURE WATER GAS SHIFT REACTION OVER PROMOTED Pt-BASED CATALYSTS

The aim of this study was to investigate the effects of various second promoters on Pt-Co/Al_2O_3 and Pt-Ce/Al_2O_3 catalysts for water gas shift reaction. For this purpose, seven metal oxides were used as the second promoters. Ni, K and Co were employed as the second promoter for Pt-Ce/Al_2O_3 and Ce, Mg, Mn, Fe and Zr were employed for Pt-Co/Al_2O_3. Pt-Co/Al_2O_3, Pt-Ce/Al_2O_3 were also studied for comparison. The catalysts were prepared by wetness impregnation method with 1.25 weight per cent promoter and 1.4 weight per cent platinum. The catalytic activity tests were conducted in a microreactor flow system. Total 100 ml/min gas reacted over 0.25 gr catalyst. Four different gas streams were used in experiments; one containing no CO_2 and H_2, one containing CO_2 only, one containing H_2 only and the last one containing both CO_2 and H_2. In addition, the effect of temperature and H_2O/CO ratio was also investigated. It was found that Ni, K and Co addition to Pt-Ce/Al_2O_3 catalyst decreased the CO conversion while Ce, Mn, Fe and Zr addition to Pt-Co/Al_2O_3 improved the activity. Mg addition, however, did not have any significant impact in the absence of CO_2 and H_2. The conversion dropped in all the cases in the presence of CO_2. The smallest decrease was observed in K containing catalyst. The activity of catalysts decreased more in the presence of H_2 than CO_2. With the addition of H_2, the biggest and the smallest decreases were seen on Pt-Ce/Al_2O_3 and Pt-Co-Mg/Al_2O_3 catalysts, respectively. The presence of both CO_2 and H_2 had negative effects on all the catalysts studied. The effect of temperature at 275 and 250°C were also tested over Pt-Ce/Al_2O_3, Pt-Co-Ce/Al_2O_3, Pt-K-Ce/Al_2O_3 and Pt-Co-Fe/Al_2O_3 catalysts and the activity decreased with decreasing temperature for all the catalysts. Finally the effect of H_2O/CO ratio was tested on Pt-Ce/γ-Al_2O_3 and Pt-Co-Fe/γ-Al_2O_3 at 275°C and it was found that CO conversion increased significantly as the H_2O/CO ratio increased from 2 to 3 over Pt-Ce/γ-Al_2O_3. On the other hand, no change was observed on Pt-Co-Fe/γ-Al_2O_3 catalyst.

ÖZET

KATKILANDIRILMIŞ PLATİN BAZLI KATALİZÖRLER ÜZERİNDE DÜŞÜK-SICAKLIK SU-GAZI GEÇİŞ REAKSİYONU

Bu çalışmanın amacı düşük sıcaklık su-gazı geçiş reaksiyonu için çeşitli ikinci katkıların Pt-Ce/Al_2O_3 ve Pt-Co/Al_2O_3 üzerindeki etkilerinin incelenmesidir. Bu amaçla yedi farklı geliştirici kullanılmıştır. Ni, K ve Co ikinci katkı olarak Pt-Ce/Al_2O_3 katalizörüne, Ce, Mg, Mn, Fe ve Zr ise Pt-Co/Al_2O_3'e eklenmiştir. Bunlara ilave olarak Pt-Ce/Al_2O_3 ve Pt-Co/Al_2O_3 katalizörleri de karşılaştırma amacıyla hazırlanmış ve çalışılmıştır. Katalizörler 1.25 ağırlık yüzdesi katkı ve 1.4 ağırlık yüzdesi platin içerecek şekilde emdirme yöntemi ile hazırlanmıştır. Katalitik aktive testleri akışlı bir microreaktör sisteminde, , 0.25 gr katalizör üzerinden 100 ml/dakika besleme gazı geçirilerek yürütülmüştür. Deneylerde, CO_2 ve H_2 içermeyen, CO_2 içeren, H_2 içeren ve son olarak hem CO_2 hem de H_2 içeren olmak üzere dört farklı gaz karışımı kullanılmış, ayrıca, sıcaklık ve H_2O/CO oranının etkileri de incelenmiştir. Pt-Ce/Al_2O_3 katalizörüne Ni, K ve Co eklenmesi ile aktivitenin düştüğü ancak buna karşın Pt-Co/Al_2O_3 katalizörüne Ce, Mn, Fe ve Zr eklenmesiyle artığı gözlenmiştir. Mg'nin ise Pt-Co/Al_2O_3'nun performansı üzerine kayda değer bir etkisi olmamıştır. Beklendiği gibi CO_2 varlığında bütün katalizörler üzerinde CO dönüşümü düşmüş, K içeren katalizör bundan en az etkilenen olmuştur. H_2 ilavesi ise CO dönüşümünü CO_2 ilavesinden çok daha fazla düşürmüştür. H_2 eklenmesiyle en büyük ve en küçük düşme sırasıyla Pt-Ce/Al_2O_3 ve Pt-Co-Mg/Al_2O_3 katalizörlerinde görülmüştür. CO_2 ve H_2 'nin birlikte eklendiği durumlarda ise en büyük aktivite düşüşü yaşanmıştır. Reaksiyon sıcaklığının etkisini görmek amacıyla Pt-Ce/Al_2O_3, Pt-Co-Ce/Al_2O_3, Pt-K-Ce/Al_2O_3 ve Pt-Co-Fe/Al_2O_3 katalizörleri 275 ve 250°C'de de test edilmiş ve bütün katalizörler için sıcaklığın düşmesiyle aktivitenin de düştüğü görülmüştür. 275°C'de H_2O/CO oranının iki den üç'e çıkartılmasıyla ise Pt-Ce/γ-Al_2O_3 üzerinde CO dönüşümünün önemli ölçüde arttığı gözlenmiş, Pt-Co-Fe/γ-Al_2O_3 katalizörü üzerinde ise herhangi bir değişiklik olmamıştır.

TABLE OF CONTENTS

ACKNOWLEDGMENTS iv
ABSTRACT v
ÖZET vi
LIST OF FIGURES ix
LIST OF TABLES xv
LIST OF SYMBOLS/ABBREVIATIONS xix
1. INTRODUCTION 1
2. LITERATURE SURVEY 4
2.1. Fuel Cells 4
2.2. Water-Gas Shift Reaction 7
2.2.1. High-Temperature Water-Gas Shift Reaction 10
2.2.2. Low-Temperature Water-Gas Shift Reaction 16
2.3. Platinum Catalyst 22
2.3.1. Support Effect on the Catalyst 22
2.4. Catalyst Preparation Methods 24
2.4.1. Precipitation 24
2.4.2. Sol-Gel Method 25
2.4.3. Impregnation 25
2.4.4. Wet Impregnation 25
2.4.5. Incipient Wetness Impregnation 25
3. EXPERIMENTAL WORK 27
3.1. Materials 27
3.1.1. Chemicals 27
3.1.2. Gases and Liquids 28
3.2. The Experimental Set-Up 28
3.2.1. Catalyst Preparation System 29
3.2.2. Microflow Reactor System 29
3.2.3. Product Analysis System 30
3.3. Catalyst Preparation 31
3.4. Catalytic Activity Measurements 33

4. RESULTS AND DISCUSSION 35
4.1. Effect of Promoter Type in the Absence of CO_2 and H_2 36
4.1.1. 1.4wt.%Pt-1.25wt.%X-1.25wt.%Ce/Al_2O_3 (X=None, Co, K, Ni) at 300°C 36
4.1.2. 1.4wt.%Pt-1.25wt.%Co-1.25wt.%X/Al_2O_3 (X=None, Ce, Fe, Mg, Mn, Zr) at 300°C 42
4.2. Effect of Promoter Type in the Presence of CO_2 48
4.2.1. 1.4wt.%Pt-1.25wt.%X-1.25wt.%Ce/Al_2O_3 (X=None, Co, K, Ni) at 300°C 48
4.2.2. 1.4wt.%Pt-1.25wt.%Co-1.25wt.%X/Al_2O_3 (X=None, Ce, Fe, Mg, Mn, Zr) at 300°C 53
4.3. Effect of Promoter Type in the Presence of H_2 59
4.3.1. 1.4wt.%Pt-1.25wt.%X-1.25wt.%Ce/Al_2O_3 (X=None, Co, K, Ni) at 300°C 59
4.3.2. 1.4wt.%Pt-1.25wt.%Co-1.25wt.%X/Al_2O_3 (X=None, Ce, Fe, Mg, Mn, Zr) at 300°C 64
4.4. Effect of Promoter Type in the Presence of CO_2 and H_2 69
4.4.1. 1.4wt.%Pt-1.25wt.%X-1.25wt.%Ce/Al_2O_3 (X=None, Co, K, Ni) at 300°C 69
4.4.2. 1.4wt.%Pt-1.25wt.%Co-1.25wt.%X/Al_2O_3 (X=None, Ce, Fe, Mg, Mn, Zr) at 300°C 74
4.5. Effect of Reaction Temperature in the Presence of CO_2 and H_2 80
4.6. Effect of H_2O/CO Ratio in the Presence of CO_2 and H_2 89
5. CONCLUSIONS AND RECOMMENDATIONS 92
5.1. Conclusions 92
5.2. Recommendations 93
REFERENCES 94

LIST OF FIGURES

Figure 2.1. Schematic diagram of the PEM fuel cell 5

Figure 3.1. The impregnation system 29

Figure 3.2. The reactor and furnace system 30

Figure 3.3. The microreactor flow and product analysis system 31

Figure 4.1. CO conversion over 1.4wt.%Pt-1.25wt.%Ce/γ-Al_2O_3 catalyst at 300°C 37

Figure 4.2. CO conversion over 1.4wt.%Pt-1.25wt.%Co-1.25wt.%Ce/γ-Al_2O_3 catalyst at 300°C 38

Figure 4.3. CO conversion over 1.4wt.%Pt-1.25wt.%K-1.25wt.%Ce/γ-Al_2O_3 catalyst at 300°C 39

Figure 4.4. CO conversion over 1.4wt.%Pt-1.25wt.%Ni-1.25wt.%Ce/γ-Al_2O_3 catalyst at 300°C 40

Figure 4.5. CO conversion at the 60th minute for Pt-X-Ce/Al_2O_3 at 300°C..... 42

Figure 4.6. CO conversion over 1.4wt.%Pt-1.25wt.%Co/γ-Al_2O_3 catalyst at 300°C 43

Figure 4.7. CO conversion over 1.4wt.%Pt-1.25wt.%Co-1.25wt.%Fe/γ-Al_2O_3 catalyst at 300°C 44

Figure 4.8. CO conversion over 1.4wt.%Pt-1.25wt.%Co-1.25wt.%Mg/γ-Al_2O_3 catalyst at 300°C 45

Figure 4.9. CO conversion over 1.4wt.%Pt-1.25wt.%Co-1.25wt.%Mn/γ-Al_2O_3 catalyst at 300°C 46

Figure 4.10. CO conversion over 1.4wt.%Pt-1.25wt.%Co-1.25wt.%Zr/γ-Al_2O_3 catalyst at 300°C 47

Figure 4.11. CO conversion at the 60th minute for Pt-Co-X/Al_2O_3 at 300°C 48

Figure 4.12. CO conversion comparison for Pt-Ce/γ-Al_2O_3 catalyst with CO_2 and without CO_2 at 300°C 49

Figure 4.13. CO conversion comparison for Pt-Co-Ce/γ-Al_2O_3 catalyst with CO_2 and without CO_2 at 300°C 50

Figure 4.14. CO conversion comparison for Pt-K-Ce/γ-Al_2O_3 catalyst with CO_2 and without CO_2 at 300°C 51

Figure 4.15. CO conversion comparison for Pt-Ni-Ce/γ-Al_2O_3 catalyst with CO_2 and without CO_2 at 300°C 52

Figure 4.16. CO conversion comparison at the 60^{th} minute for Pt-X-Ce/γ-Al_2O_3 catalysts with CO_2 and without CO_2 at 300°C..... 53

Figure 4.17. CO conversion comparison for Pt-Co/γ-Al_2O_3 catalyst with CO_2 and without CO_2 at 300°C 54

Figure 4.18. CO conversion comparison for Pt-Co-Fe/γ-Al_2O_3 catalyst with CO_2 and without CO_2 at 300°C 55

Figure 4.19. CO conversion comparison for Pt-Co-Mg/γ-Al_2O_3 catalyst with CO_2 and without CO_2 at 300°C 56

Figure 4.20. CO conversion comparison for Pt-Co-Mn/γ-Al_2O_3 catalyst with CO_2 and without CO_2 at 300°C 57

Figure 4.21. CO conversion comparison for Pt-Co-Zr/γ-Al_2O_3 catalyst with CO_2 and without CO_2 at 300°C 58

Figure 4.22. CO conversion comparison at the 60^{th} minute for Pt-Co-X/γ-Al_2O_3 catalysts with CO_2 and without CO_2 at 300°C..... 58

Figure 4.23. CO conversion comparison for Pt-Ce/γ-Al_2O_3 catalyst with H_2 and without H_2 at 300°C..... 60

Figure 4.24. CO conversion comparison for Pt-Co-Ce/γ-Al_2O_3 catalyst with H_2 and without H_2 at 300°C 61

Figure 4.25. CO conversion comparison for Pt-K-Ce/γ-Al_2O_3 catalyst with H_2 and without H_2 at 300°C 62

Figure 4.26. CO conversion comparison for Pt-Ni-Ce/γ-Al_2O_3 catalyst with H_2 and without H_2 at 300°C 63

Figure 4.27. CO conversion comparison at the 60^{th} minute for Pt-X-Ce/γ-Al_2O_3 catalysts with H_2 and without H_2 at 300°C 63

Figure 4.28. CO conversion comparison for Pt-Co/γ-Al_2O_3 catalyst with H_2 and without H_2 at 300°C 64

Figure 4.29. CO conversion comparison for Pt-Co-Fe/γ-Al_2O_3 catalyst with H_2 and without H_2 at 300°C 65

Figure 4.30. CO conversion comparison for Pt-Co-Mg/γ-Al_2O_3 catalyst with H_2 and without H_2 at 300°C 66

Figure 4.31. CO conversion comparison for Pt-Co-Mn/γ-Al_2O_3 catalyst with H_2 and without H_2 at 300°C 67

Figure 4.32. CO conversion comparison for Pt-Co-Zr/γ-Al_2O_3 catalyst with H_2 and without H_2 at 300°C 68

Figure 4.33. CO conversion comparison at the 60th minute for Pt-Co-X/γ-Al_2O_3 catalysts with H_2 and without H_2 at 300°C 69

Figure 4.34. CO conversion comparison for Pt-Ce/γ-Al_2O_3 catalyst with CO_2&H_2 and without CO_2&H_2 at 300°C 70

Figure 4.35. CO conversion comparison for Pt-Co-Ce/γ-Al_2O_3 catalyst with CO_2&H_2 and without CO_2&H_2 at 300°C 71

Figure 4.36. CO conversion comparison for Pt-K-Ce/γ-Al_2O_3 catalyst with CO_2&H_2 and without CO_2&H_2 at 300°C 72

Figure 4.37. CO conversion comparison for Pt-Ni-Ce/γ-Al_2O_3 catalyst with CO_2&H_2 and without CO_2&H_2 at 300°C 73

Figure 4.38. CO conversion comparison at the 60th minute for Pt-X-Ce/γ-Al_2O_3 catalysts with CO_2&H_2 and without CO_2&H_2 at 300°C 74

Figure 4.39. CO conversion comparison for Pt-Co/γ-Al_2O_3 catalyst with H_2 and without H_2 at 300°C 75

Figure 4.40. CO conversion comparison for Pt-Co-Fe/γ-Al_2O_3 catalyst with CO_2&H_2 and without CO_2&H_2 at 300°C 76

Figure 4.41. CO conversion comparison for Pt-Co-Mg/γ-Al_2O_3 catalyst with CO_2&H_2 and without CO_2&H_2 at 300°C 77

Figure 4.42. CO conversion comparison for Pt-Co-Mn/γ-Al_2O_3 catalyst with CO_2&H_2 and without CO_2&H_2 at 300°C 78

Figure 4.43. CO conversion comparison for Pt-Co-Zr/γ-Al_2O_3 catalyst with CO_2&H_2 and without CO_2&H_2 at 300°C 79

Figure 4.44. CO conversion comparison at the 60^{th} minute for Pt-Co-X/γ-Al_2O_3 catalysts with CO_2&H_2 and without CO_2&H_2 at 300°C 79

Figure 4.45. Equilibrium curve of the water-gas shift reaction for as feed gas composition of 5%CO, 10% H_2O, 10%CO_2 and 40%H_2 in He..... 80

Figure 4.46. CO conversion comparison for Pt-Ce/γ-Al_2O_3 catalyst at different temperatures 81

Figure 4.47. CO conversion versus temperature over 1.4wt.%Pt-1.25wt.%Ce/γ-Al_2O_3 with respect to equilibrium (60 minutes time-on-stream) 82

Figure 4.48. CO conversion comparison for Pt-Co-Ce/γ-Al_2O_3 catalyst at different temperatures 83

Figure 4.49. CO conversion versus temperature over 1.4wt.%Pt-1.25Co-1.25wt.% Ce/γ-Al_2O_3 with respect to equilibrium (60 minutes time-on-stream)..... 84

Figure 4.50. CO conversion comparison for Pt-K-Ce/γ-Al_2O_3 catalyst at different temperatures 85

Figure 4.51. CO conversion versus temperature over 1.4wt.%Pt-1.25wt.%K-1.25wt. %Ce/γ-Al_2O_3 with respect to equilibrium (60 minutes time-on-stream).. 86

Figure 4.52. CO conversion comparison for Pt-Co-Fe/γ-Al_2O_3 catalyst at different temperatures 87

Figure 4.53. CO conversion versus temperature over 1.4wt.%Pt-1.25wt.%Co-1.25 %Fe/γ-Al_2O_3 with respect to equilibrium (60 minutes time-on-stream).. 88

Figure 4.54. CO conversion comparison at the 60^{th} minute for Pt-X-Ce/γ-Al_2O_3 and Pt-Co-X/γ-Al_2O_3 catalysts with CO_2&H_2 and without CO_2&H_2 at 300, 275, 250°C 89

Figure 4.55. Effect of H_2O/CO ratio on CO conversion at 275°C over 1.4wt.%Pt-1.25wt%Ce/γ-Al_2O_3 catalyst..... 90

Figure 4.56. Effect of H_2O/CO ratio on CO conversion at 275°C over 1.4wt.%Pt-1.25wt%Co-Fe/γ-Al_2O_3 catalyst 91

LIST OF TABLES

Table 2.1. WGS catalyst requirements for mobile and stationary applications 10

Table 3.1. Chemicals used in catalyst preparation 27

Table 3.2. Applications and specifications of the gases used 28

Table 3.3. Applications and specifications of the liquids used 28

Table 3.4. Calcination procedures of catalysts 32

Table 3.5. Reduction program for Pt/X/Ce/γ-Al_2O_3 catalyst (X= None, K, Ni, Co) and Pt/Co/X/γ-Al_2O_3 catalyst (X=None, Ce, Fe, Mg, Mn, Zr) 33

Table 3.6. Reaction conditions for catalytic activity tests 34

Table 4.1. CO conversion results for Pt-Ce/γ-Al_2O_3 at 300°C 36

Table 4.2. CO conversion results for Pt-Co-Ce/γ-Al_2O_3 at 300°C 38

Table 4.3. CO conversion results for Pt-K-Ce/γ-Al_2O_3 at 300°C 39

Table 4.4. CO conversion results for Pt-Ni-Ce/γ-Al_2O_3 at 300°C 40

Table 4.5. CO conversion results for Pt-Co/γ-Al_2O_3 at 300°C 42

Table 4.6. CO conversion results for Pt-Co-Fe/γ-Al_2O_3 at 300°C 44

Table 4.7. CO conversion results for Pt-Co-Mg/γ-Al_2O_3 at 300°C 45

Table 4.8. CO conversion results for Pt-Co-Mn/γ-Al_2O_3 at 300°C 46

Table 4.9. CO conversion results for Pt-Co-Zr/γ-Al_2O_3 at 300°C 47

Table 4.10. CO conversion results for Pt-Ce/γ-Al_2O_3 at 300°C 49

Table 4.11. CO conversion results for Pt-Co-Ce/γ-Al_2O_3 at 300°C 50

Table 4.12. CO conversion results for Pt-K-Ce/γ-Al_2O_3 at 300°C 51

Table 4.13. CO conversion results for Pt-Ni-Ce/γ-Al_2O_3 at 300°C 52

Table 4.14. CO conversion results for Pt-Co/γ-Al_2O_3 at 300°C 53

Table 4.15. CO conversion results for Pt-Co-Fe/γ-Al_2O_3 at 300°C 54

Table 4.16. CO conversion results for Pt-Co-Mg/γ-Al_2O_3 at 300°C 55

Table 4.17. CO conversion results for Pt-Co-Mn/γ-Al_2O_3 at 300°C 56

Table 4.18. CO conversion results for Pt-Co-Zr/γ-Al_2O_3 at 300°C 57

Table 4.19. CO conversion results for Pt-Ce/γ-Al_2O_3 at 300°C 59

Table 4.20. CO conversion results for Pt-Co-Ce/γ-Al_2O_3 at 300°C 60

Table 4.21. CO conversion results for Pt-K-Ce/γ-Al_2O_3 at 300°C 61

Table 4.22. CO conversion results for Pt-Ni-Ce/γ-Al_2O_3 at 300°C 62

Table 4.23. CO conversion results for Pt-Co/γ-Al_2O_3 at 300°C 64

Table 4.24. CO conversion results for Pt-Co-Fe/γ-Al_2O_3 at 300°C 65

Table 4.25. CO conversion results for Pt-Co-Mg/γ-Al_2O_3 at 300°C 66

Table 4.26. CO conversion results for Pt-Co-Mn/γ-Al_2O_3 at 300°C 67

Table 4.27. CO conversion results for Pt-Co-Zr/γ-Al_2O_3 at 300°C 68

Table 4.28. CO conversion results for Pt-Ce/γ-Al_2O_3 at 300°C 70

Table 4.29. CO conversion results for Pt-Co-Ce/γ-Al_2O_3 at 300°C 71

Table 4.30. CO conversion results for Pt-K-Ce/γ-Al_2O_3 at 300°C 72

Table 4.31. CO conversion results for Pt-Ni-Ce/γ-Al_2O_3 at 300°C 73

Table 4.32. CO conversion results for Pt-Co/γ-Al_2O_3 at 300°C 74

Table 4.33. CO conversion results for Pt-Co-Fe/γ-Al_2O_3 at 300°C 75

Table 4.34. CO conversion results for Pt-Co-Mg/γ-Al_2O_3 at 300°C 76

Table 4.35. CO conversion results for Pt-Co-Mn/γ-Al_2O_3 at 300°C 77

Table 4.36. CO conversion results for Pt-Co-Zr/γ-Al_2O_3 at 300°C 78

Table 4.37. CO conversion results for Pt-Ce/γ-Al_2O_3 at different reaction temperatures 81

Table 4.38. CO conversion over 1.4%Pt-1.25%Ce/γ-Al_2O_3 at different reaction temperatures (60 minutes time-on-stream) 82

Table 4.39. CO conversion results for Pt-Co-Ce/γ-Al_2O_3 at different reaction temperatures 83

Table 4.40. CO conversion over 1.4%Pt-1.25%Co-1.25%Ce/γ-Al_2O_3 at different reaction temperatures (60 minutes time-on-stream) 84

Table 4.41. CO conversion results for Pt-K-Ce/γ-Al_2O_3 at different reaction temperatures 85

Table 4.42. CO conversion over 1.4%Pt-1.25%K-1.25%Ce/γ-Al_2O_3 at different reaction temperatures (60 minutes time-on-stream) 86

Table 4.43. CO conversion results for Pt-Co-Fe/γ-Al_2O_3 at different reaction temperatures 87

Table 4.44. CO conversion over 1.4%Pt-1.25%Co-1.25%Fe/γ-Al_2O_3 at different reaction temperatures (60 minutes time-on-stream) 88

Table 4.45. CO conversion results for Pt-Ce/γ-Al_2O_3 at different H_2O/CO ratios at 275°C 90

Table 4.46. CO conversion results for Pt-Co-Fe/γ-Al_2O_3 at different H_2O/CO ratios at 275°C 91

LIST OF SYMBOLS / ABBREVIATIONS

R	Ideal Gas Constant
T	Temperature
ΔH	Enthalpy of the Reaction
ΔG	Gibbs Free Energy of Reaction
ρ	Density
W/F	Residence Time
AFCs	Alkaline Fuel Cells
ATR	Autothermal Reforming
CeMimp	Cerium Containing Mordenites Impregnation
CeMin	Cerium Containing Mordenites in Situ
CeMss	Cerium Containing Mordenites Solid-State Ion Exchange
CeMTi	Ceria Modified Mesoporous Titania
DP	Deposition-Precipitation
DSS	Daily Start-up and Shut-down
HT	High-Temperature
HTCs	High-Temperature Catalysts
HTS	High-Temperature Shift
HTSR	High-Temperature Shift Reaction
LTCs	Low-Temperature Catalysts
LTSR	Low-Temperature Shift Reaction
LT-WGS	Low-Temperature Water Gas Shift Reaction
MCFCs	Molten Carbonate Fuel Cells
PAFCs	Phosphoric Acid Fuel Cells
PEMs	Proton Exchange Membrane Fuel Cells
POX	Direct Partial Oxidation
RWGS	Reverse Water Gas Shift
SEM	Scanning Electron Microscopy
SOFCs	Solid Oxide Fuel Cells

SR	Steam Reforming
STEM	Scanning Transmission Electron Microscopy
TPO	Temperature- Programmed Oxidation
WGS	Water Gas Shift

1. INTRODUCTION

The increasing energy needs and environmental concerns increase the demand for cleaner and more efficient energy systems (Jo *et al*., 2009). The traditional fossil energy sources such as oil and natural gas are limited, the demand and supply will have to be balanced by alternative energy sources in the near future. The hydrogen based energy technologies such as fuel cells seem to be promising alternatives (European commission report, 2003). Polymer electrolyte membrane fuel cell (PEMFC) is considered to be the most promising technology with immediate/potential market exploitation (Ding and Chan, 2009).

Fuel processing is the most convenient method of supplying hydrogen in the absence of a suitable infrastructure for hydrogen. Fuel processors generate hydrogen from hydrocarbons by either steam reforming or autothermal reforming. Besides hydrogen and carbon dioxide, 8-12%CO was generated with the reforming steps. This CO must be converted with the help of steam to CO_2 and hydrogen via the water gas shift (WGS) reaction before a final clean-up step that can reduce the CO content to <10–50 ppm for the fuel cell. Such low CO levels are needed at the fuel cell anode to efficiently carry out the electrochemical oxidation of hydrogen (Ruettinger *et al*., 2003).

The WGS reaction is moderately exothermic and strongly controlled by thermodynamic equilibrium at high temperatures. The equilibrium conversion is favored under low temperatures and is independent of pressure (Adrover *et al*., 2009). The reaction rate is constrained by kinetics at low temperatures and highly performing catalysts are necessary to provide high activity (Fiorot et al., 2007). WGS is commercially achieved in a two-step process: a high temperature shift (HTS) ranges of 623–723K using a Fe–Cr catalyst and a low temperature shift (LTS) at the temperatures lower than 573K using a Cu–Zn catalyst. The existing Cu–Zn catalyst has lower potential for WGS because of its low activity. It is deactivated by daily start-up and shut down (DSS) operations under oxidizing atmospheres (Sekine *et al*., 2009).

Two stage WGS is technically complex and inappropriate for mobile applications. Thus a single-stage WGS is desirable. Supported noble metal (Au, Rh, Pt and Pd) based catalysts seems to be promising single stage WGS catalysts. They have some advantages such as, robustness, operating at higher temperatures, less sensitive to poisons and more active than Fe/Cr catalysts (Azzam *et al*., 2007a).

On the other hand, the high costs of the noble metals are disadvantages in WGS. To overcome this disadvantage the oxides of metals such as ceria, cobalt, iron, nickel, potassium are used as the promoter. The idea behind using promoters is to combine Pt's activeness and promoters' properties such as oxygen storage capacity, and durability.

Besides the metals, promoters and supports, the preparation process is also very important in the catalytic activity. The precipitation, impregnation, ion exchange and sol-gel methods can be used for catalyst preparation. Among these methods, the impregnation of porous support materials with solutions of active components is the best-known one, especially for preparing supported noble metal catalysts (İnce, 2004).

Moreover, the possibility of methane formation from hydrogen and CO in reformate, which would decrease the H_2/CO ratio, should be also considered when designing new catalysts for WGS (Duarte de Farias *et al*., 2008).

The impregnation method is simply impregnating of porous support materials with a solution of active components. If a second noble metal with or without a promoter is going to be employed, impregnation can be done as co-impregnation or sequential impregnation. The impregnated catalysts have many advantages; their pore structure and specific surface area are largely determined by the supporting material, controlled metal loading, and reproducibility.

The aim of this thesis was to investigate the effects of various promoters for Pt/Al_2O_3 catalyst for water gas shift reaction. Eight promoters were used for experiments; Ceria, Cobalt, Nickel, Potassium, Magnesium, Manganese, Iron, Zirconium. Mostly these promoters used as couples, only $Pt\text{-}Co/Al_2O_3$ and $Pt\text{-}Ce/Al_2O_3$ were prepared for

comparison. All catalysts were prepared by impregnation method. A microreactor flow system is used for the catalytic activity measurements.

This thesis contains five chapters. Chapter 2 includes a literature survey on fuel cells, high and low temperature water gas shift reactions characteristics, catalysts used in WGS, platinum catalyst, support effects and catalyst preparation methods. In chapter 3, the experimental work for catalyst preparation and activity tests are shown. The results and discussions are given in chapter 4. The conclusions of this work and recommendations for future work are presented in chapter 5.

2. LITERATURE SURVEY

The citizens and companies of the world need a secure supply of energy at an affordable price in order maintaining the current standards of living. At the same time, the negative effects of energy use, particularly fossil fuels, on the environment must be reduced. That is why we must focus on developing alternative energy sources, on reducing dependence fossil fuels while reducing the energy consumption. The hydrogen based energy conversion technologies such as fuel cells seem to be one of the promising alternatives for the future (European commission report, 2003). This way, the air pollution can be controlled by reducing CO and NO_x emissions (Önsan, 2007).

2.1. Fuel Cells

Fuel cells are quite efficient and very clean energy conversion devices as compared with fuel combustion for primary power generation (Ruettinger *et al*., 2003).

Fuel cells, which are electrochemical devices, are used to produce electricity, heat and water by combining fuel with oxygen. By this process the chemical energy is converted to electrical energy directly. The fuel cells are more efficient than conventional heat engines. Besides, the production of CO_2, NO_x and particulate pollutants are reduced because of the fuel cells' non-combustion features (Fuelcell energy, 2008).

Internal combustion engines are used to generate mechanical and electrical energy by changing chemical energy to thermal energy. But they are less efficient than fuel cells, due to conversion of thermal energy to mechanical energy, which is limited by Carnot Cycle (Fuel cells, 2008).

The fuel cells can be classified depending on the type of electrolyte and the operation temperature. The proton exchange membrane fuel cells (PEMs) operate at ~ 80˚C, Alkaline fuel cells (AFCs) operate at ~ 100˚C, Phosphoric acid fuel cells (PAFCs) operate at ~

200˚C, Molten carbonate fuel cells (MCFCs) operate at ~ 650˚C, Solide oxide fuel cells (SOFCs) operate at 800- 1100˚C (Fuel cell handbook, 2000).

All the fuel must be converted to hydrogen before entering the fuel cell in low temperature applications. In addition, CO is harmful for the anode catalyst of low temperature fuel cells, for example for PEM. In high temperature, on the other hand, CO and even CH_4 can be converted to hydrogen or even directly oxidized electrochemically (Fuel cell handbook, 2004).

The PEM fuel cells draw attention among the five fuel cells in areas such as stationary power generators, portable devices, and the transportation sector. In addition, PEM fuel cells have a low operating temperature, sustained operation at a high current density, low weight, compactness, the potential for low cost and volume, long stack life, fast start-ups and suitability for discontinuous operation (Wee, 2007).

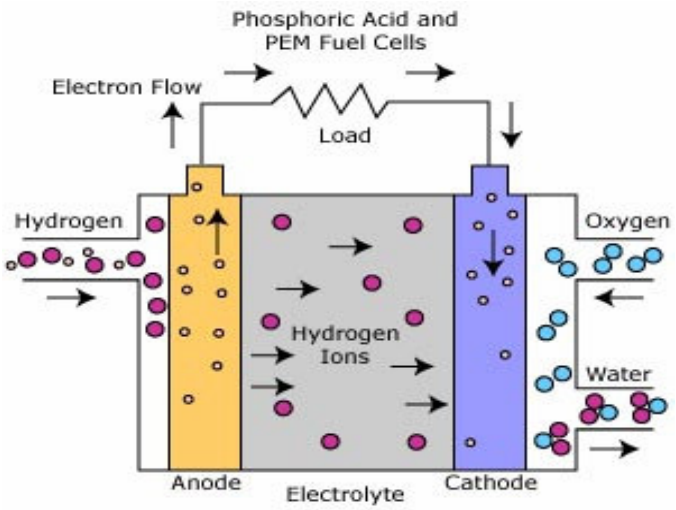

Figure 2.1. Schematic diagram of PEM fuel cell

All fuel cells have the same basic principle. As fuel (hydrogen) flows into anode, hydrogen gas separates into hydrogen ions and electrons. While the hydrogen ions pass through the electrolyte with the help of catalyst, electrons cannot pass through the electrolyte, flow through an external circuit. At the cathode side, hydrogen ions combine with oxygen and electrons. As a result water is produced. The reactions at the electrodes are as follows:

$$H_2 \rightarrow 2H^+ + 2e^- \text{ (anode)} \quad (2.1)$$

$$O_2 + 4H^+ + 4e^- \rightarrow 2H_2O \text{ (cathode)} \quad (2.2)$$

$$2H_2 + O_2 \rightarrow 2H_2O \text{ (overall)} \quad (2.3)$$

Fuel processors are used to produce hydrogen from hydrocarbons, the process also produces CO_2, which can cause greenhouse effect and CO, which is harmful for anode catalyst (Wee, 2006). This CO can be converted to CO_2 and hydrogen with the water gas shift reaction (WGS) (Ruettinger *et al*., 2003). Hydrogen production processes employed in the fuel processors are steam reforming, direct partial oxidation and autothermal reforming (Önsan, 2007).

SR: *CnHmOp* + *steam* → carbon oxides + hydrogen $\Delta HR > 0$ (2.4)

POX: *CnHmOp* + *air* → carbon oxides + hydrogen + nitrogen $\Delta HR < 0$ (2.5)

ATR: *CnHmOp* + *steam* + *air* → carbon oxides + hydrogen + nitrogen $\Delta HR \leq 0$ (2.6)

Steam reforming (SR) is highly endothermic reaction, which would demand an extra thermal energy and the gas expands in this reaction. To obtain maximum conversion, the steam reforming must be carried out at high temperature, low pressure and high steam to hydrocarbon ratio (Zhou *et al*., 2009). However, this route shows some disadvantages such as the formation of by-products and strong catalyst deactivation (Silva *et al*., 2008).

Autothermal reforming (ATR) is a modified version of steam reforming (SR), with a combination of partial oxidation. The overall reactor efficiency and the process flexibility can be increased by ATR (Ding and Chan, 2009).

Partial oxidation systems have fast start up and response time, which make them attractive for following rapidly varying loads. Moreover, the POX reactor which does not need the indirect addition of heat by a heat exchanger is more compact than a steam reformer (Silva *et al*., 2008).

The anodes produced with the latest technology are tolerant up to 100 ppm CO in the feed gas but the fuel processor's reformate contains more CO than 100 ppm (1-3%)in addition to hydrogen and carbon dioxide (Ladebeck and Wagner, 2003). Hence CO must be converted with the help of steam to CO_2 and hydrogen by the water gas shift (WGS) reaction before a final clean-up step which can reduce the CO content to <10–50 ppm. Fuel cell anode then efficiently carries out the electrochemcial oxidation of hydrogen in the absence of high levels of CO (Ruettinger *et al*., 2003).

Altough the water–gas shift reaction is well established in conventional large steady-state operations, a new and more active catalyst should be developed to utilize this technology in the fuel cell applications (Silva *et al.*, 2008).

2.2. Water Gas Shift Reaction

The water gas shift (WGS), which is widely used in the chemical industry, is one of the oldest catalytic processes. Recently, there is more concern in this process due to its application in clean power generation systems based on proton exchange membrane (PEM) fuel cells (Andreeva *et al*., 2002).

The water–gas shift reaction (WGS) has been applied in large steady-state operations such as ammonia production plants (Duarte de Farias *et al*., 2008). In fuel processing, the water-gas shift reaction is an important reaction that increases the hydrogen content of reformate gas streams and removes carbon monoxide which poisons PEM fuel cell anode catalysts (Pierre *et al*., 2007).

The hydrogen from reformed gas typically contains about 10% CO. Conversion of CO by the water gas shift, both increases the hydrogen yield and reduces the CO concentration from ~10% to ~0.5–1% with the following reaction (Luengnaruemitchai *et al*., 2003).

$$CO\ (g) + H_2O\ (g) \leftrightarrow H_2\ (g) + CO_2\ (g); \qquad (2.7)$$

$$\Delta H = -41.2\ kJ.mol^{-1} \text{ and } \Delta G = -28.6\ kJ.mol^{-1}$$

The WGS reaction (2.7) is a reversible so that the WGS reaction is balanced with the reverse WGS reaction. In the Reverse Water Gas Shift (RWGS) reaction CO_2 is used as reactant to form CO which is a valuable material in many chemical processes. Aside from the industry requirement, the RWGS reaction can occur in many reactions whenever CO_2 and H_2 are present in a reaction mixture. The reverse WGS reaction (RWGS) can be preferred in controlling of CO_2 emission (Yablonsky *et al*., 2008). In addition, because the WGS reaction is important in the industry, the study of RWGS catalysts is helpful for designing and developing WGS catalysts. The copper-based catalysts and Pt/CeO_2 are effective for RWGS. RWGS reaction is an endothermic reaction. Therefore, the formation of CO at high temperatures will be easier than low temperatures (Luhui *et al*., 2008).

The WGS reaction is exothermic and thermodynamically favorable at lower temperatures according to Le Chatelier's principle. On the other hand, kinetically, the catalysts are not so active to attain the equilibrium at low temperatures. The thermodynamics of the WGS reaction are well known that, at high temperatures, the conversion is equilibrium limited while the low temperatures it is kinetically limited (Luengnaruemitchai *et al*., 2003).

The WGS equilibrium constant at 600°C is nearly 80 times greater than the WGS equilibrium constant at 200°C. The water content is an important parameter in converting CO. The water amount in the WGS reactor can be changed by controlling the amount added at the reformer or by injecting water before or between stages of the WGS reaction. In contrast, the CO, CO_2 and H_2 concentrations are more dependent on the reformer operation, which in turn determines the thermodynamic limitations (Ladebeck and Wagner, 2003).

The pressure effect is insignificant while considering pressure range used for fuel processing because of equimolar WGS reaction (equation 2.7). The pressure can be increased from 3 to 30 atm without any thermodynamic effect on the CO conversion. On the other hand, the equilibrium CO concentration is lower at 300 atm. However it is not useful to increase the pressure to take advantage of the slightly higher equilibrium CO conversion (Ladebeck and Wagner, 2003).

Another issue is the possibility of methane formation from hydrogen and CO in reformate, which would decrease the H_2/CO ratio, that should also be evaluated when designing new catalysts for hydrogen purification by WGS reaction (Duarte de Farias *et al*., 2008).

The WGS reaction can be categorized according to the reaction temperatures which are the high-temperature shift reaction (HTSR) and the low-temperature shift reaction (LTSR). The high-temperature shift reaction temperature changes from 350 to 500°C, whereas low-temperature shift reaction temperature is between 150 and 250°C. WGSR is an exothermic reaction, and at high temperatures, the reaction tends to shift to the left side which leads to a lower CO conversion. Alternatively, the reaction rate or Arrhenius law is temperature-dependent, at high temperature; a high level CO conversion will be obtained. When high-temperature catalysts (HTCs) are employed, the hydrogen generation or CO conversion always rises with increasing reaction temperature. In contrast, if the low-temperature catalysts (LTCs) are utilized, the hydrogen production may rise or reach to a maximum point and then decline when the reaction temperature is pushed higher. These observations reveal that WGSR depends strongly on the nature of the adopted catalysts. This is attributed to the fact that different extents of activation energy are diminished when various catalysts are applied. Moreover, the optimal distribution in hydrogen generation using the LTCs is a consequence of balance between Le Chatelier's principle and Arrhenius law (Chen *et al*., 2008a). Two stage water gas shift, which is currently practiced at industrial scales, is not an appropriate choice for mobile applications because of its technical complexity and the multiple stages involved. A single-stage WGS conversion is thus desirable (Azzam *et al*., 2007a).

There are many difficulties in applying WGS catalysts successfully to fuel processing. The requirements of WGS catalysts, which are used for fuel cells and industrial applications, are quite different (Table 2.1). For mobile applications operability, size, weight and cost targets are very important. On the other hand, for stationary applications larger volumes and higher costs are acceptable to compete with the cost of electricity. But it is clear that catalyst and reactor technology developed for mobile fuel cells will be integrated into stationary applications making them more economically viable (Ladebeck and Wagner, 2003).

The pyrophoricity (temperature rise when exposed to air) and complicated activation steps of commercial WGS catalysts make them inappropriate for use in fuel cell systems. Thus, the need for new catalysts for WGS has motivated many researchers (Lim *et al*., 2009).

Table 2.1. WGS catalyst requirements for mobile and stationary applications

WGS catalyst attribute	Mobile application	Stationary application
Volume reduction	Critical, <0.1 l kW−1	Not as constrained
Weight reduction	Critical, <0.1 kgkW−1	Not as constrained
Cost	Critical, <$1kW−1	Not as critical
Rapid response	Critical, <15 s	Load following
Nonpyrophoric	Important	Eliminate purging
Attrition resistance	Critical	No constraint
Selectivity	Critical	Important
No reduction required	Critical	Important
Oxidation tolerant	Critical	Important
Condensation tolerant	Important	Important
Poison tolerant	Desired	Desired
Pressure drop	Important	Important

2.2.1. High-Temperature Water Gas Shift Reaction

High temperature WGS converters are operated between 300 - 450°C and used to reduce the CO content first to 3%-4%. At high temperatures CO conversion is equilibrium limited. In industry, Fe-Cr based high temperature WGS catalysts are used due to their low cost, long life, and acceptable sulfur tolerance. The existing WGS catalysts have many disadvantages such as their sensitivity to air and their low activity, which dictates higher temperature of operation, or large reactor volumes (Natesakhawat *et al*., 2006).

The HTS stage is carried out over three catalytic fixed beds of chromia-doped iron oxides, commercialized as hematite (α-Fe_2O_3). Magnetite (Fe_3O_4) which is found to be the

active phase is produced by reducing hematite. This reaction is highly exothermic and should be controlled to avoid the production of metallic iron, which may catalyze undesirable reactions such as hydrocarbon generation. In industrial processes, large amounts of steam are used to inhibit the metallic iron formation. However, this requires high operational costs which lead to the need for developing the catalyst in the active phase (Quadro *et al*., 1999).

$$3Fe_2O_3 + H_2 \rightarrow 2Fe_3O_4 + H_2O \qquad (2.8)$$

High-temperature (Fe_3O_4/Cr_2O_3) WGS catalysts cannot be used in power generation systems for transportation and residential applications because of their volume and weight and also due to the requirements for reduced start-up times, durability under steady state and transient conditions and stability to condensation and poisons. Fe/Cr catalyst for high temperature (HT) condition has lots of weakness. Before reduction it requires activation, it has the pyrophoric (loses activity was happened when exposed to air or steam) nature. In addition, certain range of temperature condition requires different type of catalyst. Finally, the catalyst must be separated during the system shutdown (Halim *et al*., 2005).

Commercial Fe/Cr/Cu and Cu/Zn/Al catalysts must be activated before operation using a specific process to control reduction of the oxides to the catalytically active state. The activity and life of the catalyst strongly depend on the right activation. Also steam condensation and re-oxidation of the catalysts must be prevented at shutdown. There are some ways to increase the lives of WGS catalysts which are training of plant operators on the careful startup, inert purging to prevent condensation and sequestration during shutdown of industrial reactors. By this way the lives of WGS catalysts increase from months to years (Ladebeck and Wagner, 2003).

There are lots of studies in high temperature water gas shift reaction. In Fe–Cr catalysts, Cu promoter's state was investigated which was changed from 0.17 to 1.5wt.%. It was found that Cu was in the metallic phase. However, it reoxidized easily when exposed to the atmosphere (Kappen *et al*., 2001).

Rhodes *et al*. (2002) examined the activity of catalysts based on Fe_3O_4/Cr_2O_3 where 2wt.% of B, Cu, Ba, Pb, Hg, and Ag were contained in the catalysts and prepared by co-

precipitation. It was observed that adding Hg, Ag, or Ba between 350 - 440°C was useful. This could be due to their different ionic sizes compared to that of Fe^{2+}, influencing the electronic structure of the active Fe^{3+} center. They discovered that B would poison the activity slightly, whereas the other additives could increase the activity and thereby increase the performance of the WGS reaction. Despite its high WGS activity, the toxic Hg-promoted catalyst will not be considered as a commercial HTS catalyst. Although Fe–Cr catalysts have been widely used in the HTS reaction, the role of the Cr_2O_3 addition on the stabilization of the catalyst structure is still unclear.

There are more environmental concerns about chromium which has been used as a stabilizer in high temperature shift catalysts and to end this concerns new harmless catalysts are needed. Araujo and Rangel (2000) investigated the catalytic performance of Al-doped Fe-based catalyst with small amounts of copper (Cu≈3 wt.%). The aluminum and copper-doped iron catalyst was prepared by coprecipitation–impregnation method and studied at 370°C. As a result this catalyst showed similar catalytic activity compared to the commercial Fe–Cr–Cu catalyst.

Sol–gel method to synthesize Fe-Al-Cu was used by Zhang *et al* (2008). At this method a gel was composed of an organic iron precursor with Al and Cu. This gel provided a uniform distribution of promoters in the iron oxide matrix. Fe-Al-Cu catalysts was prepared by sol–gel synthesis technique and compared with 2-step and 1- step Fe-Al-Cu catalysts. The highest catalytic activity was obtained by sol–gel method which created more oxygen vacancies during the WGS reaction and that this facilitated the oxidation and reduction cycle and thus enhanced the WGS reaction rate.

Pereira *et al*. (2008) used chromium-doped magnetite catalyst for water gas shift reaction to compare the precipitation and impregnation methods. By preparing the catalyst with these two methods, the catalysts show different textural and catalytic properties towards the water gas shift reaction. However, chromium can preserve the specific surface area during WGS reaction and delay the metallic iron production which does not connected with the preparation method. On the other hand, chromium causes a decrease in activity per area, depending on the preparation method. This can be due to its ability in making the production of Fe^{2+} species more difficult. The most active catalyst can be obtained by

adding chromium by impregnation, which leads to a large amount of total chromium in the solid and then a catalyst with high specific surface area is produced.

Thorium- and copper-doped magnetite is an efficient catalyst in HTS reaction. Costa *et al*. (2002) investigated the using thorium instead of chromium in iron- and copper-based catalysts. It was found that the thorium and copper-doped catalyst at the conditions H_2O/CO = 0.6 and 370°C was more active than the commercial Fe–Cr–Cu catalyst. In these solids copper acts as a structural promoter whereas thorium prevents sintering and the production of metallic iron which can catalyze undesirable reactions. However, thorium damages some active sites and decreases the activity per area. The most active catalyst is obtained when both thorium and copper are present in the solid. It is more active and selective than a chromium- and copper-doped commercial catalyst. Also this catalyst has some advantages like being non-toxic, having better performance, reducing energy consumption.

Natesakhawat *et al*. (2006) tested chromium-free iron-based catalysts for high-temperature water-gas shift reaction (HTS). Two-step co-precipitation–impregnation and one-step co-precipitation methods were used to prepare chromium-free iron-based catalysts by adding aluminium and copper. Aluminium is a promising chromium replacement to act as a textural promoter and stabilizes the magnetite phase. Copper can be used as a structural promoter for high temperature Fe-based catalyst to enhance the catalytic activity. The effect of Cu as promoter is found to be strongly dependent on the preparation method.
Cr-free iron-based catalyst (NBC-1) was studied by Liu *et al*. (2005) for the high-temperature WGS reaction. It is a good alternative to traditional Fe-Cr WGS catalysts. Iron in the fresh NBC-1 catalyst is present as γ-Fe_2O_3. During reduction and reaction, most of the γ-Fe_2O_3 in the catalyst is transformed to the Fe_3O_4 with perfect structure. It is postulated that Fe_3O_4 acts as active phase for WGS reaction. Desorption of the CO_2 and CO adsorbed on the NBC-1 surface takes place less than 300°C and over 400°C for the H_2O.

Lei *et al*. (2006) investigated rhodium promotion of the high-temperature WGS reaction on iron/chromium oxide catalysts. The activities per gram were compared at temperatures from 350 to 500°C. The feed composed of 9%H_2O, 9%CO, balance N_2. It

was found that the rhodium promoted sample is almost five times more active as the unpromoted one at 350°C and 1.5 times more active at 500°C.

Djinovic *et al*. (2008) investigated the influence of CuO loading and catalyst pretreatment procedure to derive an optimal CuO-CeO2 catalyst for water gas shift (WGS) reaction, and to study in detail structure–activity relationships. Nanostructured catalyst samples prepared by co-precipitation and 10, 15 and 20 mol% CuO content were examined in the temperature range of 180 – 400°C. Strong surface structure–activity dependence in WGS reaction was observed for all catalyst samples. It was found that increasing CuO content results in higher extent of CeO_2 reduction, which has a positive effect on H_2 production during the WGS reaction. Increasing calcinations temperature on the other hand reduces BET surface area, induced by CuO sintering and agglomeration of CeO_2 particles resulting in a negative effect on H_2 production. Distinctive WGS activity dependence on surface acidity of examined solids was observed for all CuO loadings.

Hu *et al*. (2000) investigated the effect of cerium oxide in promoting the reductive behavior of iron-based shift catalyst by using temperature-programmed reduction method. On the reduced catalyst, they elucidated that water could be decomposed to form hydrogen and adsorbed hydroxyl groups, and carbon monoxide reacted with hydroxyl groups to produce hydrogen and carbon dioxide simultaneously.

The effect of cerium on the properties of zirconia-supported platinum catalysts was studied by Querino *et al*. (2005). Zirconia-supported platinum, pure or doped with cerium, are efficient catalysts to WGSR at high temperatures. The activity is proportional with the amount of steam and the highest conversion is obtained under the largest amount of steam. The most active catalyst is obtained when zirconia is doped with cerium. This solid has some advantages like being non-toxic and having higher activity, in comparison to the commercial catalyst with high chromium toxicity.

Germani *et al*. (2005) prepared platinum/ceria/alumina catalysts by a sol–gel method. These catalysts are very active for the water-gas shift reaction between 300 and 400°C. The influence of the amount of platinum and ceria as well as the effect of a binder on the catalytic performance has been investigated. The catalysts prepared containing about 1 or

2wt.% of Pt and 10 and 20 wt.% of CeO_2. Hardly any influence of the amount of ceria as well as the effect of a binder on the catalytic performance has been observed.

Goguet *et al*. (2004) investigated the effect of carbon deposition in the deactivation of a 2%Pt/CeO_2 under RWGS conditions by an accelerated ageing procedure consisting of measuring the catalyst activity (under 1%CO_2, 4%H_2, 300°C) before and after exposure to CO, CO_2, H_2, or CH_4 at 400°C. Exposure to CO led to severe deactivation while exposure to CO_2, CH_4, or H_2 led to moderate or no deactivation. Additional activity measurements performed before and after exposure to CO followed by subsequent temperature-programmed oxidation (TPO) showed that exposure to increasing amounts of CO led to increased deposits of carbon and deactivation. No evidence for metal sintering was found. Additional TPO following catalyst exposure to RWGS conditions evidenced the deposition of carbonaceous deposits under the RWGS reactant mix.

Damyanova and Bueno (2003) prepared Pt catalysts supported on mixed CeO_2-Al_2O_3 carriers with different CeO_2 loading (0.5–10.3wt.%) with wetness impregnation method. It was shown that pretreatment temperature and the concentration of CeO_2 in the support influences significantly on the morphology of Pt. XRD showed the formation of nanocrystallites of Pt on the surface of alumina and low-loaded CeO_2 (≤6wt.%) samples at higher temperature of calcination (1073K). Amorphous Pt was observed in all reduced samples. The effect of CeO_2 loading on the catalytic behavior of supported Pt catalysts in the reaction of CO_2 reforming of CH_4 was determined. Addition of cerium oxide results in improvement of catalytic performance for the reforming of methane with CO_2. Pt catalyst with 1 wt.% of CeO_2 exhibited the highest specific activity and stability, due to the increase in the metal–support interface area, caused by the higher Pt dispersion.

The water gas shift activity of bimetallic Pt-Ni/Al_2O_3 catalyst was investigated the temperature between 200-450°C by Çağlayan and Aksoylu. The feed consist of 3%CO and 6%-10%H_2O. It is observed that increasing Ni content and H_2O/CO ratio shifted carbon monoxide conversion toward lower reaction temperatures. Also no detectable methane formation was seen. The results showed that Pt-Ni/Al_2O_3 catalysts are highly selective and active for water gas shift reactions (Çağlayan and Aksoylu, 2009).

2.2.2. Low-Temperature Water Gas Shift Reaction

The low-temperature WGS reaction is expected to reduce the CO content of reformate from 3%-4% to less than 1%. Cu-ZnO/Al_2O_3 catalyst is used at the temperature between 200-250°C. However, Cu-ZnO/Al_2O_3 catalysts have been designed for a large-scale steady-state operation; they are not suitable for fuel cell power systems with duty cycles including frequent start-ups and shut-downs, because they require in situ reductive pretreatment with careful temperature control owing to the high exothermicity of the process; moreover, they are deactivated by steam condensation and poisoned by traces of sulfur and halides (Önsan, 2007).

A Cu/ZnO/Al_2O_3 catalyst is used industrially in the WGSR reaction and, with some modifications, for methanol synthesis. As the synthesis gas contains H_2/CO/CO_2, the following reactions may occur during the catalytic process:

$$H_2O + CO \leftrightarrow CO_2 + H_2 \quad (2.8)$$

$$CO + 2H_2 \leftrightarrow CH_3OH \quad (2.9)$$

$$CO_2 + 3H_2 \leftrightarrow CH_3OH + H_2O \quad (2.10)$$

The reaction of displacement of the water gas can be represented by reaction (2.8) and methanol synthesis by reactions (2.9) and (2.10).

The catalysts in the low temperature shift reaction must be more active than in the high temperature shift reaction, because the process is kinetically controlled at lower temperatures (Mhadeshwar and Vlachos, 2005).

At lower temperatures, higher CO conversions are obtained because of the exothermic nature of the water gas shift reaction. The WGS equilibrium constant is nearly 80 times greater at 600°C than 200°C (Ladebeck and Wagner, 2003).

From the thermodynamic perspective, the WGS reaction is more efficient at low temperature, high water and low hydrogen concentration (Ladebeck and Wagner, 2003).

Advanced low-temperature shift catalysts are needed to supply CO-free hydrogen to the PEM fuel cell to avoid the use of expensive H_2-permeable membranes. A very good WGS catalyst is cerium oxide loaded with platinum metals. Cerium oxide-based WGS catalysts have attracted increasing attention primarily because of the high oxygen-storage capacity of ceria and modified ceria. In practice, the role of CeO_2 is not limited to storage of oxygen. The picture is much more complicated, with ceria serving as a stabilizer of both the noble metal and alumina, as well as a promoter of several reactions including the water-gas shift and carbon monoxide oxidation (Li *et al*., 2000).

Idakiev *et al*. (2007) reported new gold catalytic system prepared on ceria-modified mesoporous titania (CeMTi) used as water gas shift (WGS) reaction catalyst. Gold-based catalysts with different gold content (1–5wt.%) were synthesized by DP of gold hydroxide on mixed metal oxide support. The catalytic activity of the gold-based catalysts was evaluated in the water-gas shift reaction at wide temperature range of 140–300°C. The WGS activity of the catalyst Au/CeMTi is significantly higher than that of the gold catalysts supported on simple oxides, mesoporous TiO_2 (Au/MTi) and CeO_2 (Au/Ce). It is also observed that the degree of CO conversion increases with the gold loading on ceria-modified mesoporous titania. The Au/ceria-modified mesoporous titania catalytic system is found to be efficient catalyst for WGS reaction.

Tabakova *et al*. (2000) examined Au/ZrO_2 catalysts and reported high activity, along with Au/Fe_2O_3, for the low temperature shift reaction. They concluded that the activity of gold/metal oxide catalysts depended on both the dispersion of gold as well as the nature and textural structure of the support. That is, the best activity was obtained on well-crystallized ZrO_2 and Fe_2O_3, and much lower activity on poorly crystallized oxides, such as ZrO_2, ZnO, and Fe_2O_3–ZnO, and Fe_2O_3–ZrO_2 mixed oxides.

Goerke *et al*. (2004) described high CO conversion rates at low temperature with $5\%Ru/ZrO_2$ coated in a microchannel reactor. The water gas shift reaction at 250–300°C using a Ru/ZrO_2 catalyst allowed to reduce the CO content by more than 95%.

Iida and Igarashi (2006) obtained enhanced activity by promoting Pt/ZrO_2 with Re to form a bimetallic catalyst. Since Re/ZrO_2 alone did not exhibit significant WGS activity, they concluded that the increased activity must be due to Re having a synergistic effect with Pt.

Iida *et al*. (2006) examined the catalytic activities for water gas shift reaction at low temperature (LT-WGS) and the characteristics of Pt/TiO_2 (R: rutile) catalysts prepared from various Pt precursors, As a result, it was found that the Pt/TiO_2 (R) catalysts prepared from $H_2PtCl_6.6H_2O$ and $Pt(C_5H_7O_2)_2$ had relatively high catalytic activities. Further, catalytic activity is proportional with Pt dispersion of the catalysts. This result suggested that LT-WGS reaction on Pt/TiO_2 (R) is structure insensitive, unrelated to the type of Pt precursor used.

Yahiro *et al*. (2007) investigated the influence of support (Al_2O_3, MgO, SiO_2-Al_2O_3, SiO_2-MgO, b-zeolite, and CeO_2) of Cu-ZnO catalysts for the low-temperature water–gas shift reaction. Supported Cu-ZnO catalysts were prepared by impregnation method. The activity of Cu-ZnO catalysts for the water gas shift (WGS) reaction was largely influenced by the kind of support; Cu-ZnO catalysts supported on Al_2O_3, MgO, and CeO_2 showed high activity, while those on SiO_2-Al_2O_3, SiO_2-MgO and b-zeolite showed less activity in the temperature range 423–523K. It was concluded that the reducibility of CuO is one of the important factors controlling the activity of the WGS reaction over the supported CuO-ZnO catalysts.

Nagai *et al*. (2006) investigated water-gas shift (WGS) reaction over nickel–molybdenum (Ni–Mo) carbide catalysts at 453K. The 873 K-carburized $Ni_{0.25}Mo_{0.75}$ catalyst ($Ni_{0.25}Mo_{0.75}C$-873) exhibited the highest rate of CO conversion among the catalysts carburized at 823, 923, and 973K with various Ni contents.

Mohamed *et al*. (2005) prepared cerium containing mordenites catalysts by impregnation (CeMimp), solid-state ion exchange (CeMss) and in situ incorporation during synthesis (CeMin). Water gas shift reaction was carried out over various catalysts. The results obtained showed the presence of cerium silicate phase in case of CeMin sample. In case of CeMimp and CeMss, a separate CeO_2 phase was observed in a highly dispersed

state in the former than in the latter. CeMimp showed the highest catalytic activity followed by CeMss.

Venugopal *et al*. (2003) examined gold–ruthenium interactions. The water–gas-shift reaction has been carried out over Au–Ru supported on α-Fe_2O_3 catalyst the temperature between 373 and 513K at atmospheric pressure. It was found that Au–Ru/iron oxide activity was higher than Au/iron oxide and Ru/iron oxide catalysts.

Sekine *et al*. (2009) investigated the WGS activity of Pt Pd supported on perovskite oxides at 573K without pretreatment. Their activities varied depending on the kind of perovskite and loading metal. The WGS activity was not derived from Pt or Pd metals, or the perovskite oxide itself. The interaction between Pt or Pd, and the support promotes the WGS reaction. Results show that Pt/$LaCoO_3$ had high initial activity but deactivated immediately; Pd/LaCoO3 was less active than Pt/$LaCoO_3$ initially, but had superior stability. From STEM observation of the Pt, Pd/$LaCoO_3$, the active metal was shown not to be sintered during the reaction. The cause of deactivation of Pt/$LaCoO_3$ was attributed to reduction of Co and Pt. Regarding the Pd/LaCoO3 catalyst, although Co and Pd were reduced by the reaction gas, the activity of Pd/$LaCoO_3$ for WGS reaction was stable. Therefore, Pd was added to Pt/$LaCoO_3$ to maintain the high activity of Pt/$LaCoO_3$ and the high stability of Pd/$LaCoO_3$. The Pt and Pd loading weights were varied; ultimately, 0.5wt.%Pd/1wt.%Pt/$LaCoO_3$ showed the highest activity and stability for the WGS reaction.

The effect of the steam/carbon ratio on CO conversion was studied by Figueiredo *et al*. (2005). Cu/ZnO/Al_2O_3 catalysts prepared by reverse co-precipitation and an industrial catalyst were used for the low-temperature water gas shift reaction. The conversion of CO increased continuously with increasing steam/carbon ratio, until reaching a constant value. The CZA catalyst showed higher conversion than the commercial catalyst.

Yahiro *et al*. (2006) investigated the effect of calcination temperature on the catalytic activity for water gas shift (WGS) reaction for copper/alumina catalysts. The catalyst prepared by the impregnation method and calcined at 1073K, followed by the treatment in H_2 at 523K, showed a high activity for WGS reaction. The catalyst calcined at 1073K

contained both highly dispersed CuO and spinel $CuAl_2O_4$ particles. The former species was reduced by the treatment in H_2 at 523K to yield the highly dispersed metallic copper which would act as catalytically active sites in WGS reaction.

Radhakrishnan *et al*. (2006) examined the WGS activity of some noble metals (Pt, Pd, Ru, Rh, Ir, and Au) on ceria-zirconia oxides. They found that Pt is the most active. However, they pointed out that the activity of the catalysts is highly dependant on the synthesis methods.

The activity patterns for WGS reactions over supported precious metal catalysts were measured by Lei *et al*. (2005). Seven oxides promoted by Pt were tested and Cr_2O_3 had the highest activity. Furthermore, in a comparison of five different metals as promoters for Fe/Cr oxide, the most active promoter was found to be Rh.

Luengnaruemitchai *et al*. (2003) studied catalytic low-temperature water gas shift (WGS) reaction over the Pt/CeO_2, Au/CeO_2 and Au/Fe_2O_3 catalysts. The activity of these catalysts was tested in the composition of 4%CO, 2.6–20%H_2O and helium in the range of 120–360°C. It was found that CO and H_2O concentrations have significant effects on the catalytic activity. The $1\%Pt/CeO_2$ was substantially more active than other catalysts in the presence of 20%H_2O.

Du *et al*. (2008) achieved highly efficient Cu–Mn spinel catalysts for water gas shift (WGS) reaction by a single step urea-nitrate combustion method. A series of doped Cu–Mn-M catalysts (M=Ce, Zr, Zn, Fe, Al) were prepared by the same method. It was found that WGS activities depend strongly on the natures of the dopant employed despite of their lower content, varying in the order of Zr>Fe>non-doped>Ce>Al>Zn. In addition, Zr-doped Cu–Mn catalyst with 5wt.% content showed the best catalytic performance and, optimal stability exposed to oxygen-stream and on-stream operation. It indicates that ZrO_2 is an effective promoter for Cu–Mn catalyst, and the catalytic performances are related to the existence of a $Cu_{1.5}Mn_{1.5}O_4$ phase and ease reducibility of the catalysts.

Guo *et al*. (2009) prepared the $Cu/ZnO/Al_2O_3$ catalysts by the coprecipitation method, and evaluated in the water gas shift (WGS) reaction. The $Cu/ZnO/Al_2O_3$ catalyst

prepared at the calcination temperature of 450°C showed the best activity and stability, with the decrement of the CO conversion of only 12.8% after three shut-down/start-up cycles. Deactivation of the $Cu/ZnO/Al_2O_3$ catalysts is attributed to the blocking or deterioration of the active sites by $Zn_6Al_2(OH)_{16}CO_3.4H_2O$ resulting from the degeneration of the oxides under cyclic operations. Removal of the hydroxycarbonate species by calcination in air followed by re-reduction could restore the steady-state WGS activity; however, the regenerated catalyst underwent much severe deactivation in subsequent shut-down/start-up operation.

Luhui *et al*. (2008) investigated reverse water gas shift reaction over co-precipitated $Ni-CeO_2$ catalysts. The Ni-Ce catalysts with different Ni contents were prepared by a co-precipitation method. 2wt.%$Ni-CeO_2$ showed excellent catalytic performance in terms of activity, selectivity, and stability for RWGS reaction. The results indicated that, in $Ni-CeO_2$ catalysts, there were three kinds of nickel, nickel ions in ceria lattice, highly dispersed NiO and bulk NiO.

Lilong *et al*. (2008) prepared multiple-metal catalysts (Ni-Mn-Ce-K/bauxite) by impregnation for water gas shift (WGS) reaction. The results indicated that the addition of 7.5%CeO_2 improved the activity of the WGS reaction obviously, and also increased the specific surface area and pore volume of the catalysts. The addition of CeO_2 decreases the reduction temperature, enhanced the adsorption and activation of H_2O, and improved the adsorption content of CO.

Yeragi *et al*. (2006) carried water-gas-shift reaction over a series of Mn-promoted Cu/Al_2O_3 catalysts in the temperature range of 448–533K. The catalysts were characterized suitably by various techniques. The catalyst containing 8.55wt.%Mn was found to be the most active one. A maximum CO conversion of 90% was obtained over this catalyst at 513K with a CO space-time of 5.33h. The catalysts were found to be structure sensitive for the low-temperature water-gas shift reaction.

Panagiotopoulou *et al*. (2006) prepared Pt/CeO_2 and Pt/Al_2O_3 catalysts with variable metal loading in the range of 0.1–5.0wt.% and tested for their catalytic activity. It is observed that catalytic activity does not depend on Pt loading or crystallite size.

2.3. Platinum Catalyst

Platinum is a noble metal. The concentrations of platinum in the soil, water and air are very little. Platinum is a lustrous silvery-white, malleable, ductile metal and a member of group 10 of the periodic table of the elements. It has the third highest density, behind osmium and iridium.

Platinum is unaffected by air and water, but will dissolve in hot *aqua* regia, in hot concentrated phosphoric and sulphuric acids, and in molten alkali. It is as resistant as gold to corrosion and tarnishing. Indeed, platinum will not oxidize in air no matter how strongly it is heated. It melts at 1093°C. Owing to its high melting point and its resistance to the action of most chemicals, no single acid will act on it. A mixture of nitric and hydrochloric acid (aqua regia) will dissolve it.

Supported noble metal-based (e.g., Pt) catalysts are reported as promising single-stage WGS catalysts because they

(i) are robust,
(ii) can operate at higher temperatures where the kinetics is more favorable,
(iii) are less sensitive to poisons (Cl and S),
(iv) are more active than the HTS catalysts,
(v) are stable during start-up – shutdown cycles

Due to availability and cost of noble metals, Pt is often the metal chosen. Since Pt is not able to activate water, bifunctional, hydrophilic oxide supported catalysts are needed, where platinum activates CO and support activates H_2O (Azzam *et al*., 2007a).

2.3.1. Support Effect on the Catalyst

The nature of oxide supports has a crucial effect on the performance of Pt-based catalysts in the water–gas shift reaction. Supports both determine the activity of the catalyst, and influence their stability. The role of the support oxide is to activate water, completing the WGS reaction sequence (Azzam *et al*., 2007b).

In general, it is agreed that both the metal and the support play essential roles in the WGS reaction. CO and H_2O are two reactants in WGS reaction, H_2O is more difficult to activate because of its thermodynamic stability. Metals such as Cu and Fe are reported to undergo oxidation by water, thereby activating it. However, Pt does not interact chemically with water because the PtO_x that would be formed is not thermodynamically stable at WGS temperatures. Thus, for Pt based WGS catalysts, a hydrophilic oxide support is essential to adsorb and activate water. Therefore, such catalysts are bifunctional, with platinum activating CO and the support activating H_2O (Azzam *et al*., 2007a).

A critical parameter, which determines the catalytic activity, is the nature of the support. The mesoporous materials with different compositions, new pore systems and novel properties have attracted considerable attention because of their remarkably large surface areas and narrow pore size distributions, which make them ideal candidates for catalysts. Other than their chemical properties, another advantage of this kind of new materials while being used as supports for metallic catalysts relies on their well-defined pore size which can limit the growth of metal or metal oxide particles (Idakiev *et al*., 2007).

Azzam *et al*. (2007a) investigated the roles of support on catalyst activity and stability. They found that among the catalysts studied, Pt/TiO_2 was the most active. Activity followed the order Pt on TiO_2 > $T_{i0.5}Ce_{0.5}O_2$ > $_{Ce0.5}Zr0.5O2$ > CeO_2 > $T_{i0.8}Ce_{0.2}O_2$ > $Ce_{0.8}Zr_{0.2}O_2$ > $T_{i0.5}Zr_{0.5}O_2$ > ZrO_2. Recalling that the order of activity for single-oxide supports was Pt/TiO_2 > Pt/CeO_2 > Pt/ZrO_2, it can be seen that mixed-oxide supports did not result in enhanced catalytic performance.

The catalytic performance of supported noble metals for the WGS reaction depends strongly on the nature of both the metallic phase and the metal oxide support. Platinum catalysts are generally more active than Ru, Rh, and Pd, and exhibit significantly higher activity when supported on ‘‘reducible’’ rather than on ‘‘irreducible’’ oxides. Titania-supported platimum is more active than the well-studied Pt/CeO_2 catalyst, especially in the temperature range of 200–250°C. When noble metals are dispersed on ‘‘reducible’’ oxides, such as CeO_2 and TiO_2, the apparent activation energy of the reaction does not depend on the nature of the metallic phase but only on the nature of the support. In contrast, E_a differs

from one metal to another when supported on an irreducible oxide, such as Al_2O_3 (Panagiotopoulou and Kondarides, 2006).

Activity may be further improved when the metal oxide (MO_x) is dispersed on a high surface area support, such as Al_2O_3 or TiO_2, because reducibility increases with decreasing MO_x crystallite size (Panagiotopoulou and Kondarides, 2007). Also high surface area reported to result in significant enhancement of activity, selectivity and stability of dispersed noble metals (Çağlayan and Aksoylu, 2009). The sintering behavior of precious metal particles on γ-Al_2O_3 strongly depends on the preparation method (Mitsui *et al.*, 2008).

2.4. Catalyst Preparation Methods

A heterogeneous catalyst is a composite material, characterized by the relative amounts of different components (active species, physical and/or chemical promoters, and supports); shape; size; pore volume and distribution; surface area. The optimum catalyst is the one that provides the necessary combination of properties (activity, selectivity, lifetime, ease of regeneration and toxicity) at an acceptable cost.

2.4.1. Precipitation

Precipitation is one of the most widely employed preparation methods and may be used to prepare either single component catalysts and supports or mixed catalysts. During precipitation the pH has to be adjusted and kept constant. Hydroxides and carbonates are the preferred precipitates because of their low solubility, easy decomposition and minimal toxicity and environmental problems.

Deposition-precipitation (DP) has been scarcely used to prepare platinum supported catalysts, while it is the preferred method to obtain active gold catalysts (Bamwenda *et al.*, 1997).

2.4.2. Sol-Gel Method

Sol–gel method is a homogeneous process which results in a continuous transformation of a solution into a hydrated solid precursor (hydrogel). The sol- gel method provides an interesting way to obtain solids with controlled surface area, porosity and surface acidity (Pecchi *et al*, 1997).

A unique characteristic of this method is that a solid bimetallic catalyst sample is prepared from a homogeneous solution that contains both the metal precursors and also the support precursor. This leads to a greater degree of control over catalyst preparation and one can "tailor make" catalysts to fit particular application (Balakrishnan and Gonzalez, 1994).

2.4.3. Impregnation

Impregnation is the procedure whereby a certain volume of solution containing the precursor of the active phase is contacted with the solid support, which, in a subsequent step, is dried to remove the imbibed solvent. Two methods of contacting may be distinguished, depending on the volume of solution: wet impregnation and incipient wetness impregnation.

2.4.3.1. Wet Impregnation

In wet impregnation, an excess of solution is used. After a certain time the solid is separated and the excess solvent is removed by drying. The composition of the batch solution will change and the release of debris can form a mud which makes it difficult to completely use the solution. The heat of adsorption is released in a short time.

2.4.3.2. Incipient Wetness Impregnation

In incipient wetness impregnation, the volume of the solution of appropriate concentration is equal or slightly less than the pore volume of the support. Control of the operation must be rather precise and repeated applications of the solution may be

necessary. The maximum loading is limited by the solubility of the precursor in the solution. For both methods the operating variable is the temperature, which influences both the precursor solubility and the solution viscosity and as a consequence the wetting time. The concentration profile of the impregnated compound depends on the mass transfer conditions within the pores during impregnation and drying (Campanati *et al*., 2003).

3. EXPERIMENTAL WORK

3.1. Materials

3.1.1. Chemicals

The chemicals used in the catalysts are listed in Table 3.1.

Table 3.1. Chemicals used in catalyst preparation

Chemicals	Formula	Grade	Source	Molecular Weight (g/mole)
Tetraammineplatinum (II) nitrate	$Pt(NH_3)_4(NO_3)_2$	Research	Aldrich	387.21
Cobalt Nitrate hexahydrate	$Co(NO_3)_2.6H_2O$	Extra Pure	Merck	291.04
Mangan(II)nitrate Tetrahydrate	$Mn(NO_3)_2.4H_2O$	Extra Pure	Merck	251.01
Zirconyl nitrate Hydrate	N_2O_7Zr	Extra Pure	Fluka	231.23
Magnesium nitrate Hexahydrate	$Mg(NO_3)_2.6H_2O$	Extra Pure	Merck	256.41
Nickel(II) nitrate hexahydrate	$Ni(NO_3)_2.6H_2O$	Extra Pure	Merck	290.81
Cerium(III) nitrate hexahydrate	$Ce(NO_3)_2.6H_2O$	Extra Pure	Merck	434.23
Iron(III) nitrate nonahydrate	$Fe(NO_3)_2.9H_2O$	Extra Pure	Merck	341.6
Potassium Carbonate	K_2CO3	Extra Pure	Merck	138.21
Aluminium Oxide	Al_2O_3	Extra Pure	ZeochmEU	101.96

3.1.2. Gases and Liquids

The liquids and gases used in this study are listed with their applications and specifications in the Table 3.2 and Table 3.3. All of the gases used in this study were supplied by BOS and HABAŞ Companies, Istanbul, Turkey**.**

Table 3.2. Applications and specifications of the gases used

Gas	Application	Specification
Carbon monoxide	Reactant, MS calibration	99.0% HABAŞ
Oxygen	Reactant, MS calibration	99.99% BOS
Carbon dioxide	Reactant, MS calibration	99.99% BOS
Hydrogen	Reactant, Reducing agent, MS calibration	99.99% BOS
Helium	Reactant (Inert), MS calibration	99.99% BOS

Table 3.3. Applications and specifications of the liquids used

Liquid	Application	Specification
Water	Reactant, cleaning	Distilled

3.2. The Experimental Set-Up

The experimental set-up consists of three parts:

- Catalyst Preparation System: Catalysts were prepared by co-impregnation method in this system.
- Microreactor Flow System: The system, in which catalytic activity tests were performed, was formed by mass flow controllers for gases, a pump for the water feed, a reactor and a programmable temperature controller.
- Analysis System: Reactant and product gases were analyzed by a Hiden Hal HPR-20 mass spectrometer equipped with a Faraday/Sem detector.

3.2.1. Catalyst Preparation System

Pt/X/Ce/Al_2O_3(X= None, K, Ni, Co), Pt/Co/X/Al_2O_3 (X= None, Ce, Fe, Mg, Mn, Zr) catalysts which had the same Pt contents were prepared by co-impregnation method. The catalyst preparation system consisted of Retsch UR1 ultrasonic mixer, a vacuum pump, a vacuum flask, a beaker, a Masterflex computerized-drive peristaltic pump and silicone tubing (Figure 3.1).

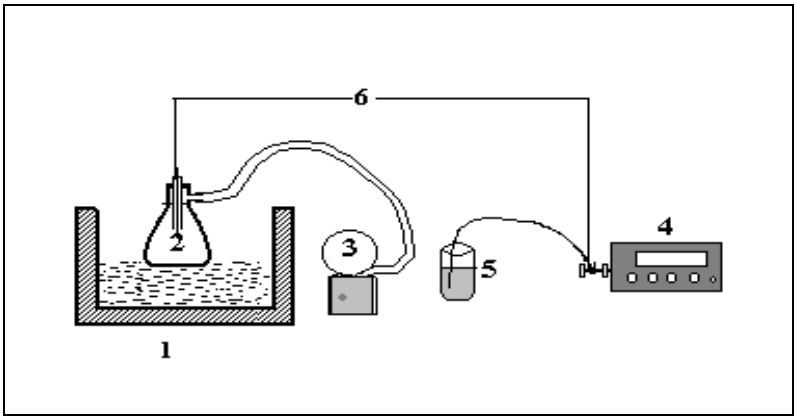

Figure 3.1. The impregnation system: 1.Ultrasonic mixer 2.Vacuum flask 3. Vacuum pump 4.Peristaltic pump 5.Beaker 6.Silicone tubing (Akın, 1996)

3.2.2. Microflow Reactor System

In the system, 1/4" stainless steel tubes were used until the water mixture region. Stainless steel tubes with 1/8" and 1/16" outer diameter were used in the mixture region. After that, tubes diameter increased to 1/8" and 1/4". The reaction gases which are CO, He, H_2 and CO_2 passed through 1/4" stainless steel tubes. The gases flow rates were measured by Brooks 5850E mass flow controller equipped with a 4-Channel Brooks 0154 Read Out unit. For all reaction gases, 30 psi input pressure was used for the best performance.

After passing flow controller region, the gases were mixed and sent to the reaction region include a down-flow 1/4" stainless steel fixed-bed reactor (Figure 3.2) which is 58.5 cm and placed in the furnace controlled to 0.5± K with Shimaden FP-21 programmable temperature controller. The K-type sheathed thermocouple was placed in the middle of the catalyst outside the microreactor. The fitting of the reactors, which were outside the

furnace, was isolated by ceramic wool to prevent heat loss and maintain stable reaction conditions.

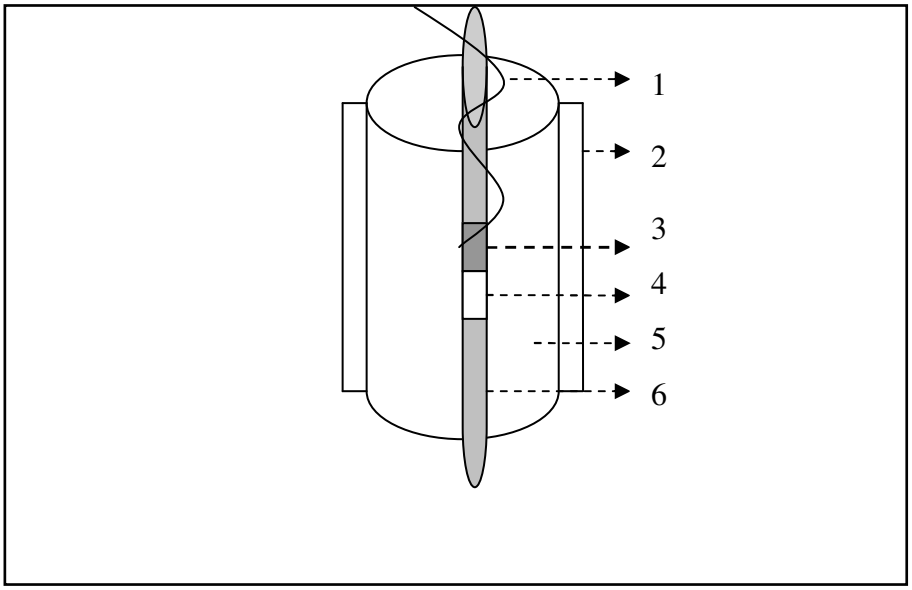

Figure 3.2. The reactor and furnace system: 1. Thermocouple, 2. Ceramic wool insulation, 3. Catalyst, 4. Catalyst bed, 5. Furnace 6. Reactor

The Jasco PU-2080 Plus HPLC pump was used for water pumping. The water temperature was controlled by Dixell single stage digital controller XT110C. Before the reaction, the reaction gases and distillated water were mixed for an hour to provide homogeneous mixture. Then the gas–stream mixture was fed to the reactor. The fed and produced water was separated by cold trap which was placed at the exit of the microreactor. The cold trap consisted of an ice box and coiled tubing to increase contact time of flow through a cold environment.

3.2.3. Product Analysis System

After the removal of the H_2O, the product stream was sent and analyzed by using a Hiden Hal 210 mass spectrometer connected to a personal computer and employing MASoft software. The entire microflow reaction system is presented in Figure 3.3.

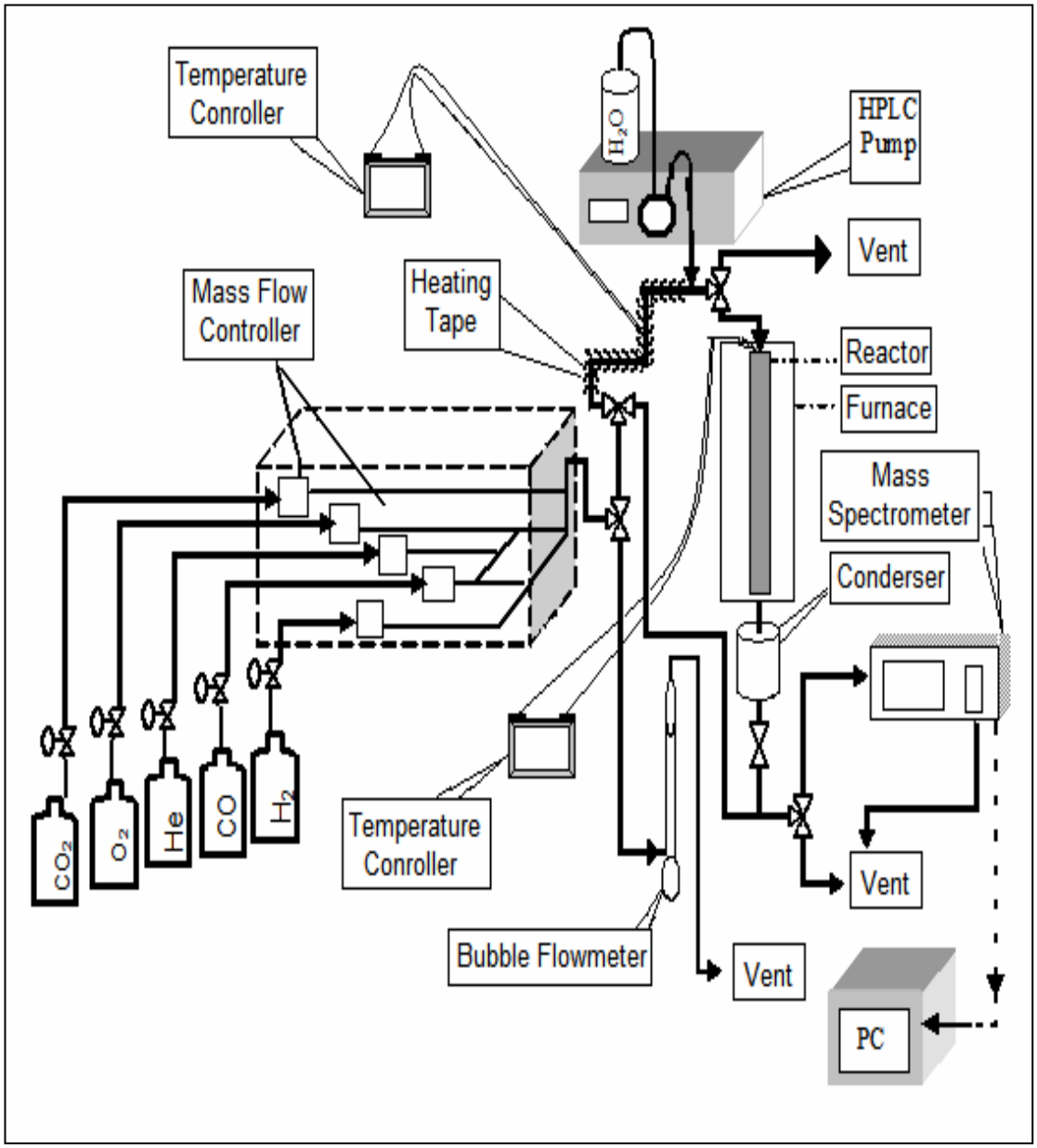

Figure 3.3. The microreactor flow and product analysis system

3.3. Catalyst Preparation

The Pt/X/Ce/Al_2O_3(X= None, K, Ni, Co) and Pt/Co/X/Al_2O_3(X= None, Ce, Fe, Mg, Mn, Zr) catalysts were prepared by incipient to wetness impregnation. The experiments were performed by these 9 different catalysts which had 1.4 weight per cent Pt and 1.25 weight per cent of each promoters. The catalyst preparation was composed of four steps:

- Evacuating the support

- Contacting the support with the precursor solution
- Drying of slurry
- Calcination

γ-alumina support was crushed and sieved into 45-60 mesh size (344-255 μm). γ-alumina was then dried in a furnace at 105°C for 1 hour and then calcined in a muffle furnace at 450°C for 5 hours. Before the impregnation, γ-alumina support was placed in a vacuum flask and was kept under vacuum for 30 min to remove the air in the support pores. The support material in the vacuum flask was mixed under vacuum with Retsch UR 1 ultrasonic mixer.

All the metal salts were dissolved in 1.21 ml of water per gram of alumina support, which is the amount of water to wet one gram alumina. The aqueous precursor solution was fed to the vacuum flask at a flow rate of 0.5 ml/min via silicone tubing using a Masterflex computerized-drive peristaltic pump. The slurry was mixed under vacuum by an ultrasound mixer to maintain uniform impregnation. The impregnated support was mixed for additional 90 min. The slurry obtained was dried at 115˚C overnight (16 hours). Then all the catalysts are calcined in the air using the procedure summarized in Table 3.4 depending on the promoter used.

Table 3.4. Calcination procedures of catalysts

Catalyst	Calcination Temperature	Calcination Time
Pt-Co/Al_2O_3	400˚C	2 hours
Pt-Co-Ce/Al_2O_3	400˚C	2 hours
Pt-Co-Mg/Al_2O_3	400˚C	4 hours
Pt-Co-Fe/Al_2O_3	300˚C	2 hours
Pt-Co-Mn/Al_2O_3	400˚C	5 hours
Pt-Co-Zr/Al_2O_3	400˚C	2 hours
Pt-Ce/ Al_2O_3	400˚C	2 hours
Pt-K-Ce/ Al_2O_3	450˚C	1 hour
Pt-Ni-Ce/ Al_2O_3	450˚C	2 hours

3.4. Catalytic Activity Measurements

Before the reaction, all catalysts were reduced and kept under the flow of He until the reaction test was performed. The temperature program used for the reductive pretreatment can be seen in Table 3.5.

Table 3.5. Reduction program for Pt/X/Ce/Al_2O_3 catalyst (X= None, K, Ni, Co) and Pt/Co/X/Al_2O_3 catalyst (X= None, Ce, Fe, Mg, Mn, Zr)

Segments	Starting and End Temperatures	Segment Gas
First Segment	Heating from 25°C to 400°C with a heating rate 5°C.min^{-1}	He with flow rate of 50 ml.min^{-1}
Second Segment (Reduction)	Keeping constant at 400°C for 2 h	H_2 with flow rate of 50 ml.min^{-1}
Third Segment	Flushing at 400°C for 1h to clean the catalyst surface	He with flow rate of 50 ml.min^{-1}
Fourth Segment	Cooling down to reaction temperature	He with flow rate of 25 ml.min^{-1}

The activity tests were carried out in the microreactor flow system shown in Figure 3.3. Prior to reaction, all the catalysts were heated from ambient temperature to 400°C under 50 ml/min helium stream. All the catalysts were reduced with H_2 before the reaction. After reduction, the reactor temperature was decreased to the reaction temperature (300°C) under inert helium flow and helium was trapped within the reactor until the reaction gases were sent to the reactor.

Four sets of reaction mixtures were used for catalytic activity test;

- First set consist of 5 ml/min CO, 10 ml/min H_2O and 85 ml/min He.
- The second set includes 5 ml/min CO, 10 ml/min H_2O, 40 ml/min H_2 and 45 ml/min He.
- The third set includes, 5 ml/min CO, 10 ml/min H_2O, 10 ml/min CO_2 and 75 ml/min He.

- In the last set, 5 ml/min CO, 10 ml/min H_2O, 40 ml/min H_2 , 10 ml/min CO_2 and 35 ml/min He were used.

The summary of the reaction conditions are given in Table 3.6, the results are presented and discussed in chapter 4.

Table 3.6. Reaction conditions for catalytic activity test

Parameter	Value
Catalyst Particle Size	45-60 mesh size (344-255µm)
Catalyst Amount	0,25 g
Reaction Temperature	300, 275, 250˚C
Reactant Total flow rate	100 ml/min
W/F Ratio	2.5 mg.min/ml

4. RESULTS AND DISCUSSION

Up to present, the platinum is the most frequently used metal among the noble metals (Pt, Ru and Rh) which are known as effective catalyst for water gas shift reaction (Gonzalez *et al*., 2008). There are lots of studies about bimetallic platinum based catalysts for water gas shift reaction. On the other hand, there is not enough study including trimetallic platinum based catalyst supported on alumina which is known as irreducible oxide.

Pt based bimettalic and trimetallic alumina supported catalysts were studied and the effect of promoters and Pt content was investigated for selective CO oxidation by Uğuz (2007). The catalytic activity of the same catalysts, which are Pt/X/Ce/Al_2O_3 (X= None, K, Ni, Co) and Pt/Co/X/Al_2O_3 (X= None, Ce, Fe, Mg, Mn, Zr) were tested for the water gas shift reaction in this study. The effects of promoter type, the temperature and H_2O/CO ratio were investigated for these nine catalysts. Considering that the water gas shift reaction activity is proportional to the CO conversion, the activity of the catalysts was expressed as CO conversion per cent defined as follows:

$$\text{CO conversion } (\%) = \frac{[CO]_{in} - [CO]_{out}}{[CO]_{in}} \times 100 \tag{4.1}$$

The amount of liquid water used in the experiments was calculated as:

$$V_{Steam(H_2O)} = \frac{V_{Liquid(H_2O)} \times \rho_{H_2O} \times R \times T}{M_{H_2O} \times P} \tag{4.2}$$

Where ρ=1000g.L^{-1}; P=1 atm; R=0.082 L.atm.mol^{-1}.K^{-1}; T=298K and M_{H2O}=18 g.mol^{-1}.

4.1. Effect of Promoter Type in the Absence CO_2 and H_2

4.1.1. 1.4wt.%Pt- 1.25wt.%X-1.25wt.%Ce/Al_2O_3 (X= None, Co, K, Ni) at 300˚C

Firstly, Pt-Ce/γ-Al_2O_3 bimetallic catalyst was tested for the activity of water gas shift reaction. Then the effect of three promoters on Pt-X-Ce/γ-Al_2O_3 (X= K, Ni, Co) which form trimetallic catalyst was investigated. The reactions were carried out at 300°C with these catalysts which were composed of 1.4wt.%Pt, 1.25wt.%Ce and 1.25wt.% of each promoter since these metal compositions were found to be effective for selective CO oxidation by Uğuz (2007). 5 per cent CO, 10 per cent H_2O, and He in balance (in the absence of CO_2 and H_2) were used as the feed. The results for Pt-Ce/Al_2O_3 catalyst are given in Table 4.1.

Table 4.1. Conversion results for Pt-Ce/γ-Al_2O_3 at 300˚C

Time (min)	% CO conversion
30	80.6
60	78.3
90	77.9
120	77.6
150	77.5
180	77.3

The conversion was about 80 per cent which was consistent with the thesis of Şen (2008). In her thesis, she used a catalyst with the same content along with the feed composition of 5 per cent CO, 5 per cent H_2O and He as balance. She obtained 74.6% maximum conversion after 2 hour reaction at 300°C. On the other hand, the selective CO oxidation was studied with the same catalyst at 80 and 110˚C and much smaller (approximately 14 per cent) CO conversion was obtained (Uğuz, 2007). The activity of Pt-Ce/Al_2O_3 catalyst did not change for three hours as a good sign of stability (Figure 4.1).

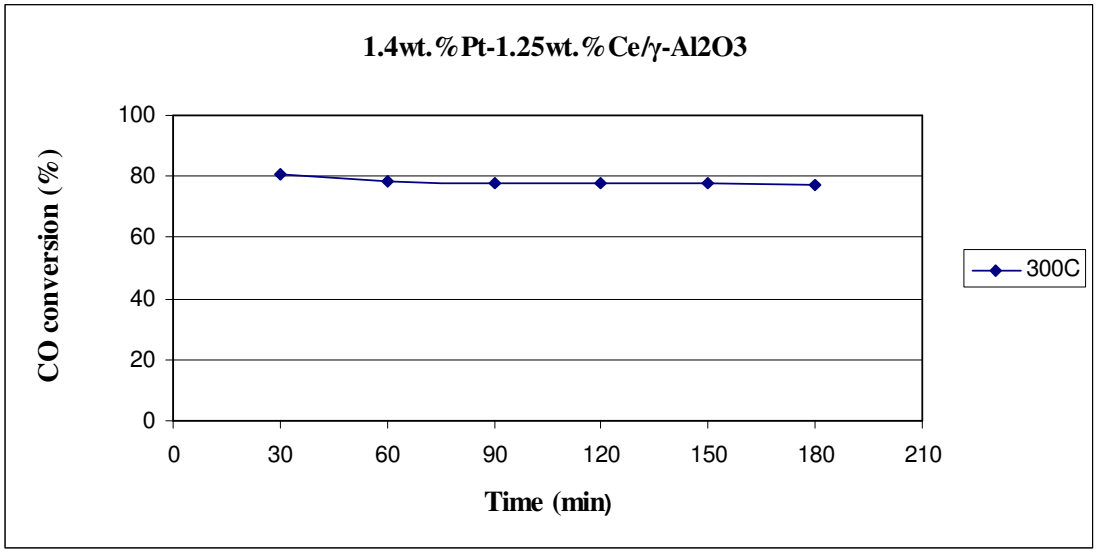

Figure 4.1. CO conversion over 1.4wt.%Pt-1.25wt.%Ce/γ-Al_2O_3 catalyst at 300°C

Panagiotopoulou and Kondarides (2007) investigated the catalytic activity of Pt-Ce/Al_2O_3 catalyst for the water gas shift reaction in the temperature range of 150-500°C. In the experiments, they used 100 mg catalysts with the particle diameter between 0.18 and 0.25 mm. The catalyst was prepared with 0.5wt.%Pt and 10wt.%Ce and the feed was composed of 3%CO and 10%H_2O. They found that CO conversion curve shifted toward lower temperatures in the presence of ceria compared to Pt/Al_2O_3. The ceria containing catalyst is more active at the temperature below 350°C. Approximately 50% CO conversion was obtained at 300°C. Pt/CeO_x/Al_2O_3 catalyst activity was one order of magnitude higher than Pt/Al_2O_3 catalyst at 250˚C.

The cobalt was found as effective promoter for Pt/Al_2O_3 catalyst in the selective CO oxidation reaction. In that reaction, catalytic activity was increased significantly with cobalt addition and 100% conversion was obtained at 110˚C (Uğuz, 2007). On the other hand, the cobalt addition decreased the water gas shift reaction activity as can be seen from Table 4.2. Maximum 60 per cent conversion was obtained with Pt-Co-Ce/γ-Al_2O_3 at 300˚C although the conversion was about 80% in the absence of Co (Table 4.1). The conversion was also slightly decreased with increasing time on stream after 90 minutes (Figure 4.2). However 60% CO conversion can be still considered significant.

Table 4.2. Conversion results for Pt-Co-Ce/γ-Al_2O_3 at 300˚C

Time (min)	% CO conversion
30	56.2
60	58.5
90	60
120	56.9
150	53.1
180	53.5

Panagiotopoulou and Kondarides (2007) also tested the activity of the cobalt containing Pt/Al_2O_3 catalyst. They recognized that while Pt/Co_3O_4 and Pt/Al_2O_3 catalysts reached equilibrium at 350 and 480˚C, respectively, Pt/CoO_x/Al_2O_3 catalyst reached equilibrium CO conversion at 330˚C. However, Pt/CoO_x/Al_2O_3 catalyst was less active than Pt/CeO_x/Al_2O_3 catalyst at 250˚C.

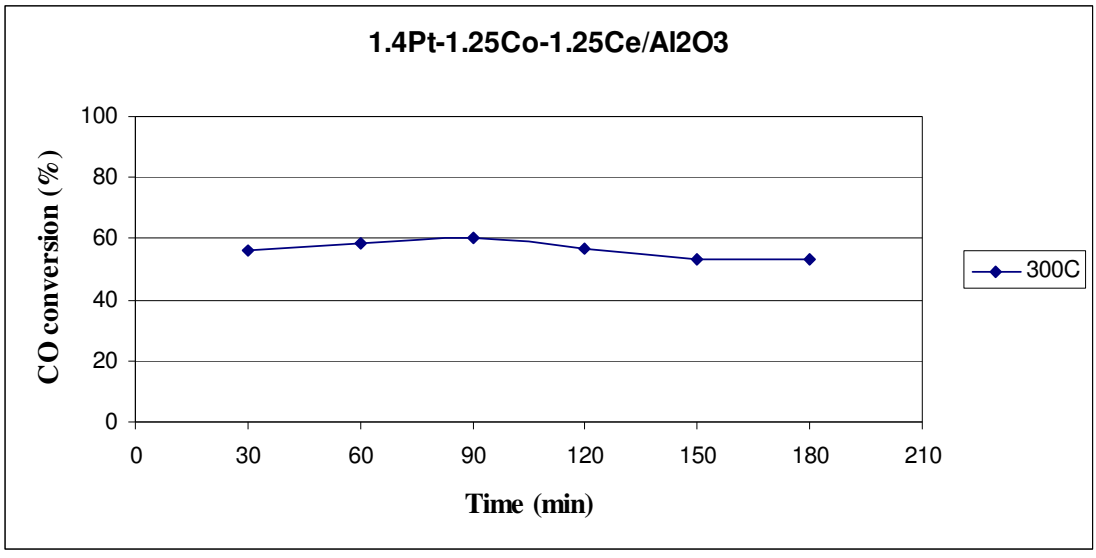

Figure 4.2. CO conversion over 1.4wt.%Pt-1.25wt.%Co-1.25wt.%Ce/γ-Al_2O_3 catalyst at 300°C

The potassium as the second promoter on Pt-Ce/Al_2O_3 catalyst was also tested for the water gas shift reaction, and its catalytic activity was found to be high (maximum CO conversion was about 63 %) although it was still lower than the Pt-Ce catalyst (resulted about 80 % conversion) without the second promoter indicating that K also decreased the

activity. It is observed that, the conversion of the catalyst was just about same during 3 hours as seen from Table 4.3. However Uğuz (2007) reported that K addition to Pt-Ce significantly increased the catalytic activity (as the conversion increased from 14% to about 70%) although the improvement was not as much as the Co addition (Uğuz, 2007).

Table 4.3. Conversion results for Pt-K-Ce/γ-Al_2O_3 at 300˚C

Time (min)	% CO conversion
30	62.6
60	60.2
90	59.8
120	60.3
150	54.9
180	62.1

Lee and Chen (1997) studied the additive effects on WGS. As promoter, Ce, Na and K were used. 150 mg catalyst was placed in the reactor with 0.4wt.%Pt content. The reaction was carried out at 550˚C under 0.31 air/fuel ratio. As a result, 81wt.%, 72wt.%, 65wt.%, 22wt.%CO conversion was observed with Pt-K_2O/Al_2O_3, Pt-Na_2O/Al_2O_3, Pt-CeO_2/Al_2O_3, Pt/Al_2O_3, respectively.

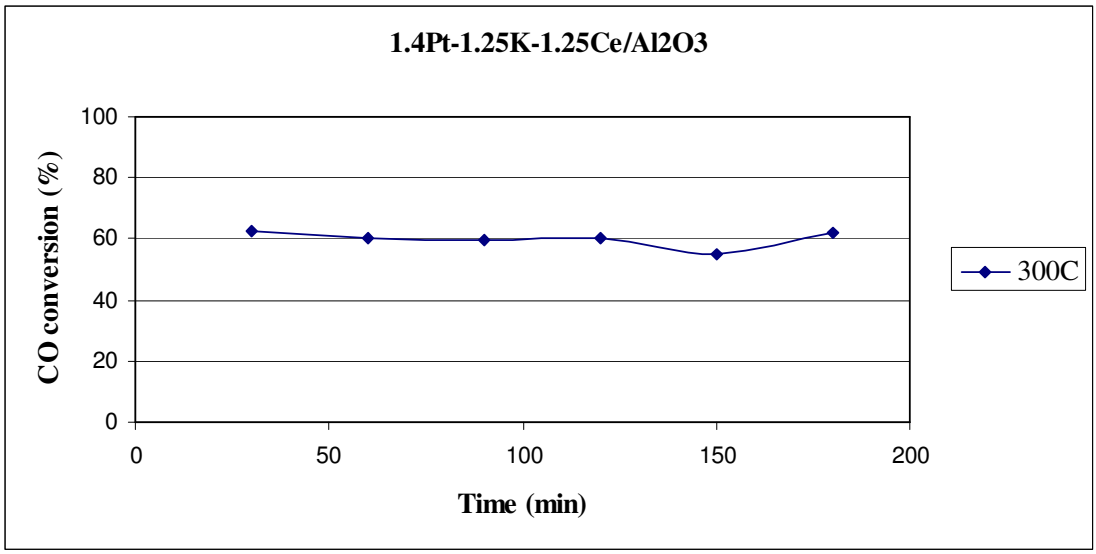

Figure 4.3. CO conversion over 1.4wt.%Pt-1.25wt.%K-1.25wt.%Ce/γ-Al_2O_3 catalyst at 300°C

Nickel is the last promoter used with ceria. Ni as the second promoter had nearly same as Co and K in WGS activity, which is significant although lower than that of Pt-Ce alone. It seems that Ni addition also has inverse effects on the WGS reaction although it was beneficial in the case of selective CO oxidation with the increase of CO conversion from 14% to about 90% (better than P and but less than Co) as reported by Uğuz (2007).The activity results obtained with Pt-Ni-Ce/γ-Al_2O_3 are shown in Table 4.4.

Table 4.4. Conversion results for Pt-Ni-Ce/γ-Al_2O_3 at 300˚C

Time (min)	% CO conversion
30	60.2
60	62.4
90	62.5
120	59.4
150	60.9
180	57.5

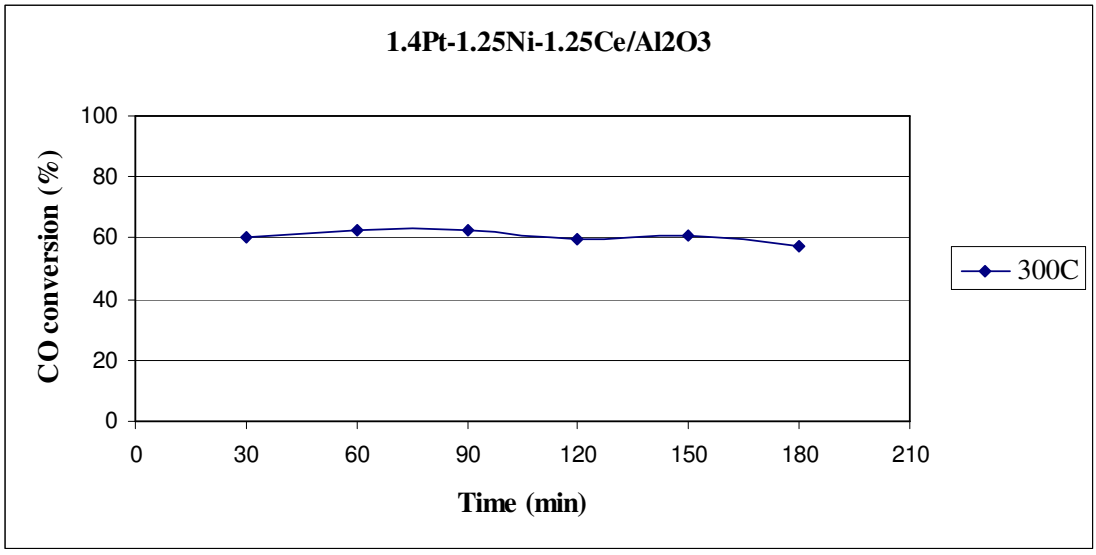

Figure 4.4. CO conversion over 1.4wt.%Pt-1.25wt.%Ni-1.25wt.%Ce/γ-Al_2O_3 catalyst at 300°C

Çağlayan and Aksoylu (2008) studied the water gas shift reaction over bimetallic Pt-Ni/Al_2O_3 catalyst. The reaction was conducted at the temperature between 200 and 450˚C with 3%CO and 10%H_2O and 87%N_2 as feed. They investigated different Ni contents

which were 5%, 10% and 15% and for all samples 2% Pt content was used. They found out that, as Ni content was increased, the catalyst reached to equilibrium curve at lower temperatures. Furthermore, nearly 98%CO conversion was obtained with 15%Ni content below 300˚C.

Panagiotopoulou and Kondarides (2007) investigated the catalytic activity of Pt-Ni/Al_2O_3 catalyst for the water gas shift reaction in the temperature range of 150-500°C. In the experiments, 100 mg catalysts which was prepared with 0.5wt.%Pt and 10wt.%Ni was used and their feed was composed of 3%CO and 10%H_2O. It was found out that Ni containing catalyst reached equilibrium curve at 350°C. Besides, the conversion of CO was approximately 22% at 300°C.

Haryanto *et al*. (2009) studied ceria promoted nickel catalyst supported on alumina (Ni/CeO_2-Al_2O_3) for low and high temperatures. The composition of catalyst was chosen as 4%Ni, 3%CeO_2 and 93%Al_2O_3. In the experiments, 1:3 CO/steam ratio was chosen. At low temperature (250°C), 96%CO conversion was observed which was close to equilibrium curve (99.6%) but stability of Ni catalysts was low. On the other hand, at high temperatures (450°C) with the same CO/steam ratio, the catalyst activity was observed as 95% where equilibrium conversion was 94%. The difference may have been the result of inaccuracy with flow rate reading which fluctuated from the set point during the experiment. Besides, undesirable methanation (CH_4) was observed with Ni catalyst.

The results obtained with all promoters are summarized in Figure 4.5. It is seen that promoter (Co, K and Ni) addition decreased the water gas shift reaction activity at 300°C. At the same time, the promoters' effects are quite close to each other at these reaction conditions.

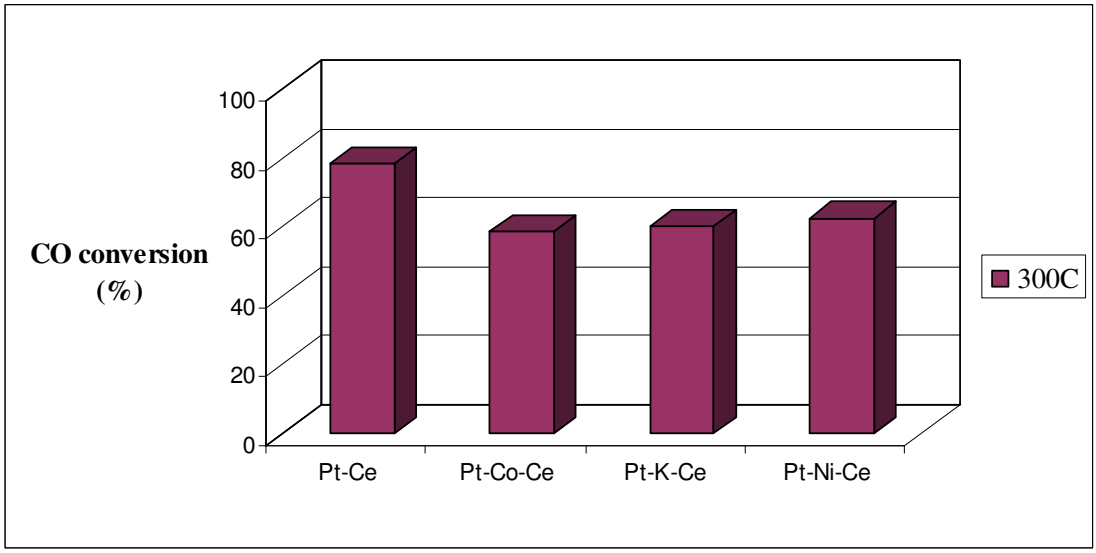

Figure 4.5. CO conversion at the 60th minute for Pt-X-Ce/γ-Al_2O_3 at 300 ˚C

4.1.2. 1.4wt.%Pt-1.25wt.%Co-1.25wt.%X/Al_2O_3 (X= None, Ce, Fe, Mg, Mn, Zr) at 300˚C

In this part, the ceria was replaced with some promoters in the Pt-Co system as it was studied for the selective CO oxidation by Uğuz (2007). The feed consisted of 5%CO, 10%H_2O, and He in balance (in the absence of CO_2 and H_2). The reactions were again carried out at 300°C.

Firstly, as the base catalyst, Pt-Co/Al_2O_3 activity was tested at 300˚C. As seen from Table 4.5, it had quite poor activity in WGS whereas, it was found to be a promising catalyst for selective CO oxidation at 80˚C with 99% conversion by Uğuz (2007).

Table 4.5. Conversion results for Pt-Co/γ-Al_2O_3 at 300˚C

Time (min)	% CO conversion
30	34.9
60	36.8
90	36.8
120	37.5
150	38.7
180	37.5

Panagiotopoulou and Kondarides (2007) also studied Co promoter on Pt/Al_2O_3 catalyst with the same conditions, as mentioned before. About 70%CO conversion was obtained at 300˚C with 0.5wt.%Pt and 10wt.%Co and the feed consisting of 3%CO and 10%H_2O. The difference between these results and the results obtained in this study may be attributed to the difference in the Co contents (1.25wt% versus 10wt%) or to the CO content of the feed although the Pt content of the catalyst they used was significantly lower than that is used in this thesis.

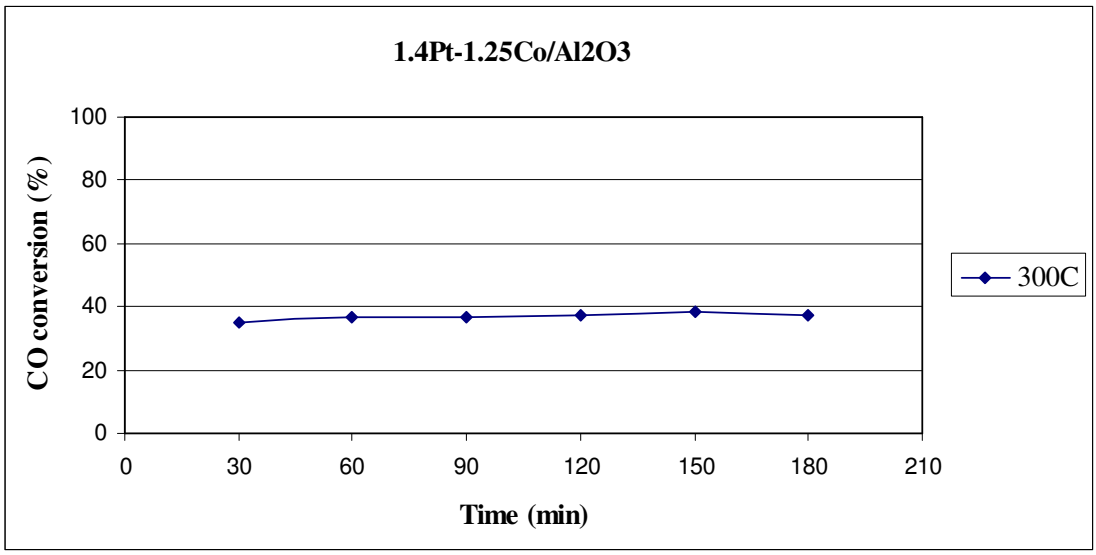

Figure 4.6. CO conversion over 1.4wt.%Pt-1.25wt.%Co/γ-Al_2O_3 catalyst at 300°C

The iron is also used in WGS reaction as promoter to increase the activity. The conversion of CO was nearly doubled with the addition of Fe to the Pt-Co/Al_2O_3 catalyst (Table 4.6). Cobalt is known as having high activity and selectivity but low WGS activity, whereas iron is known to be active for the WGS reaction (Lögdberg *et al.*, 2009). But, it was reported that CO conversion decreased slightly with the addition of Fe promoter in selective CO oxidation at 80˚C (Uğuz, 2007).

Table 4.6. Conversion results for Pt-Co-Fe/γ-Al_2O_3 at 300˚C

Time (min)	% CO conversion
30	66.2
60	68.2
90	65
120	67.9
150	66.4
180	66.3

Pt-Fe/Al_2O_3 catalyst activity for the water gas shift reaction was also studied between 150-500°C by Panagiotopoulou and Kondarides (2007). The catalyst' Pt and Fe loadings were 0.5% and 10%, respectively. Also 3%CO and 10%H_2O were used as feed composition. According to their results, Pt-Fe/Al_2O_3 catalyst was less active at low temperatures and with increasing the temperature CO conversion was increasing and closing to equilibrium curve. CO conversion was obtained below 10% at 300˚C and it was obtained as 90%, which reached equilibrium curve, at nearly 500˚C.

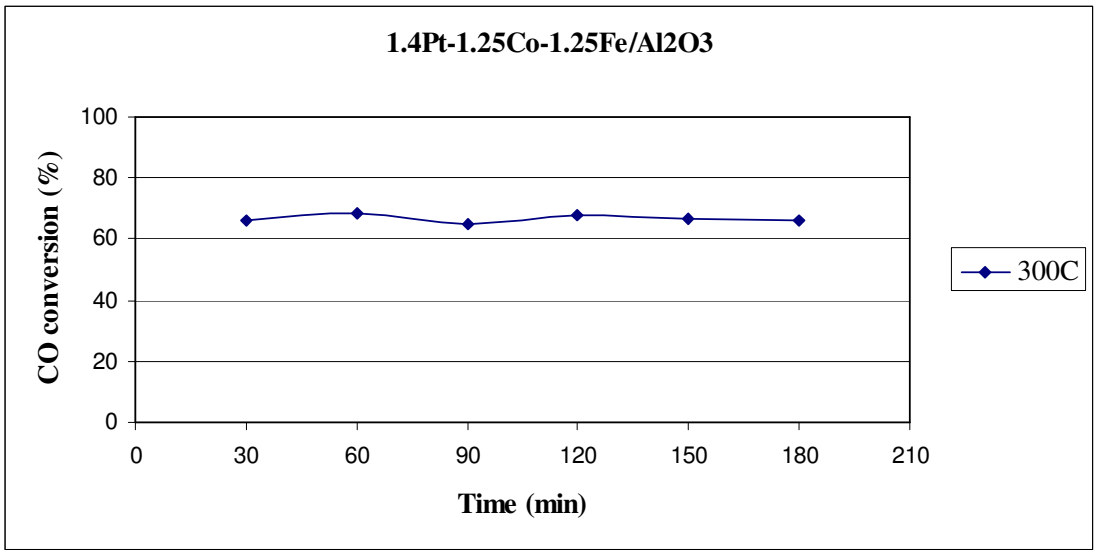

Figure 4.7. CO conversion over 1.4wt.%Pt-1.25wt.%Co-1.25wt.%Fe/γ-Al_2O_3 catalyst at 300°C

There was not any increase in the activity of Pt-Co/Al_2O_3 catalyst with the addition of magnesium (Table 4.7. and Figure 4.8). Yang *et al.*, (2006) also reported that the

magnesium promoter has a negative effect on WGS activity. Hence it can be concluded that using Mg as the second promoter is not beneficial although it was reported to enhance the activity of Pt-Co/Al_2O_3 catalyst in selective CO oxidation at 80˚C (Uğuz, 2007).

Table 4.7. Conversion results for Pt-Co-Mg/γ-Al_2O_3 at 300˚C

Time (min)	% CO conversion
30	37.5
60	36.1
90	35.6
120	36.5
150	35.1
180	36.1

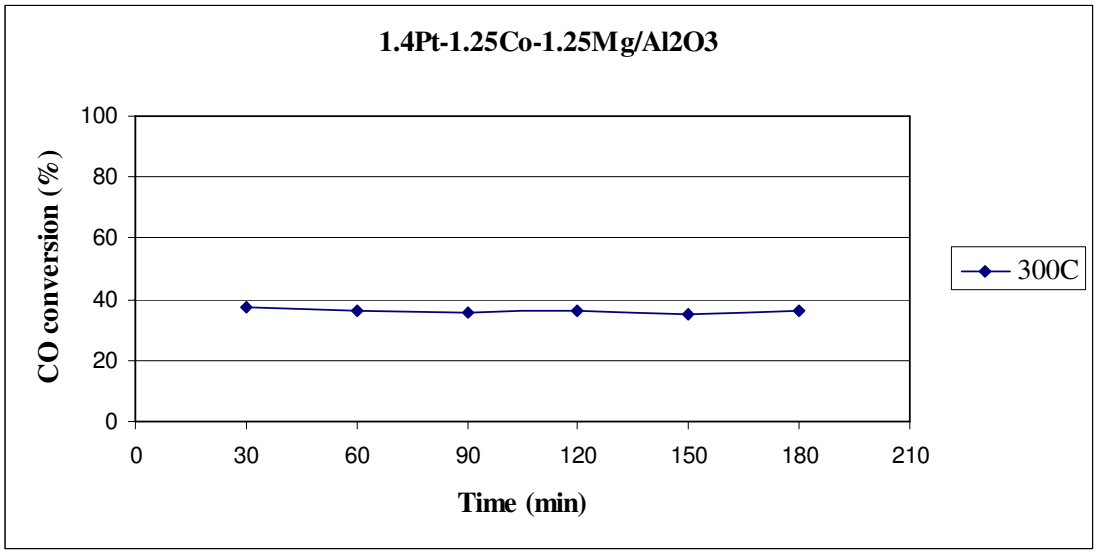

Figure 4.8. CO conversion over 1.4wt.%Pt-1.25wt.%Co-1.25wt.%Mg/γ-Al_2O_3 catalyst at 300°C

Panagiotopoulou *et al*. (2007) also investigated Pt/Ce-Mg-O catalyst between 100 and 550˚C with 3%CO, 10%H_2O and He in balance. Pt was loaded as 0.5wt.%. As a result, CO conversion with Mg was found as approximately 75% at 300˚C while Pt/CeO_2 showed 55% conversion at the same conditions. It was commented that the promoter addition increased the activity by increasing the reducibility. Apparently this was not the case in the present conditions.

Another promoter which was searched for its activity in the WGS was manganese. The activity of Pt-Co/Al_2O_3 catalyst increased with the addition of Mn promoter as compared Table 4.5 with Table 4.8. The addition of Mn to Pt-Co/Al_2O_3 also increased the CO conversion slightly in the selective CO oxidation (Uğuz, 2007).

Table 4.8. Conversion results for Pt-Co-Mn/γ-Al_2O_3 at 300˚C

Time (min)	% CO conversion
30	46.6
60	46.6
90	47.4
120	48.5
150	46.3
180	48.1

Mn was also tested by Panagiotopoulou and Kondarides (2007) in the Pt-Mn/Al_2O_3 catalyst for WGS with 0.5%Pt and 10%Mn loading, respectively. Reaction was carried out with 3%CO and 10%H_2O feed composition. They recognized that Pt-Mn/Al_2O_3 activity was less than Pt/Al_2O_3 activity in the temperature range of 250-500°C.

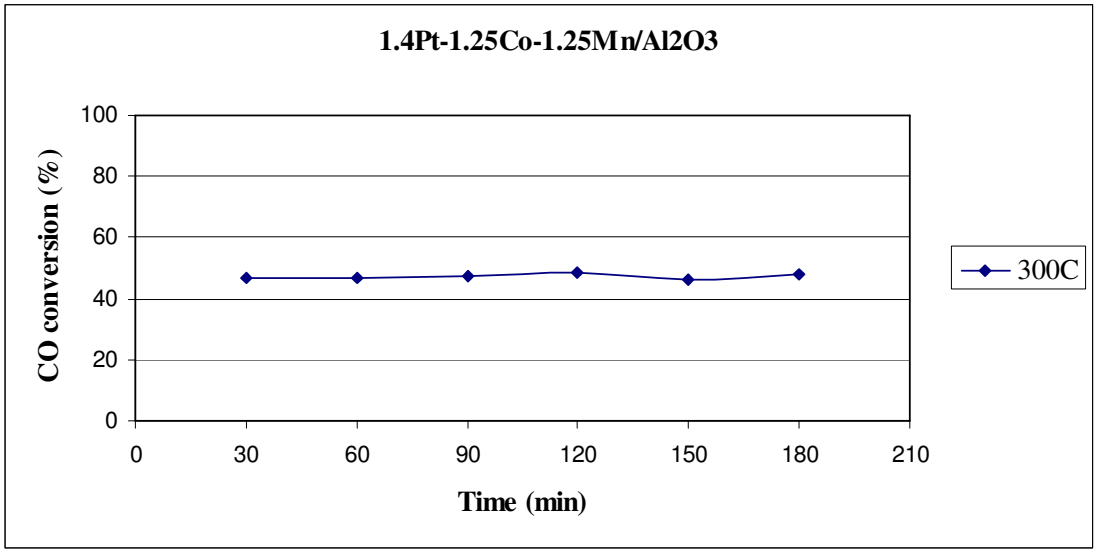

Figure 4.9. CO conversion over 1.4wt.%Pt-1.25wt.%Co-1.25wt.%Mn/γ-Al_2O_3 catalyst at 300°C

The last promoter tested for WGS was zirconium. Zr is also used as support in the literature. Zr addition to Pt-Co/Al_2O_3 did not improve the catalyst activity significantly. Just a few per cent increase was observed as seen from Table 4.9. Besides, Pt-Co-Zr/γ-Al_2O_3 catalyst was not active in selective CO oxidation, and after 1 hour, reaction rapid deactivation was observed (Uğuz, 2007). On the other hand, no deactivation was observed in the water gas shift reaction with Pt-Co-Zr/γ-Al_2O_3 catalyst.

Table 4.9. Conversion results for Pt-Co-Zr/γ-Al_2O_3 at 300˚C

Time (min)	% CO conversion
30	42.4
60	39.3
90	37
120	36.4
150	35.3
180	39.9

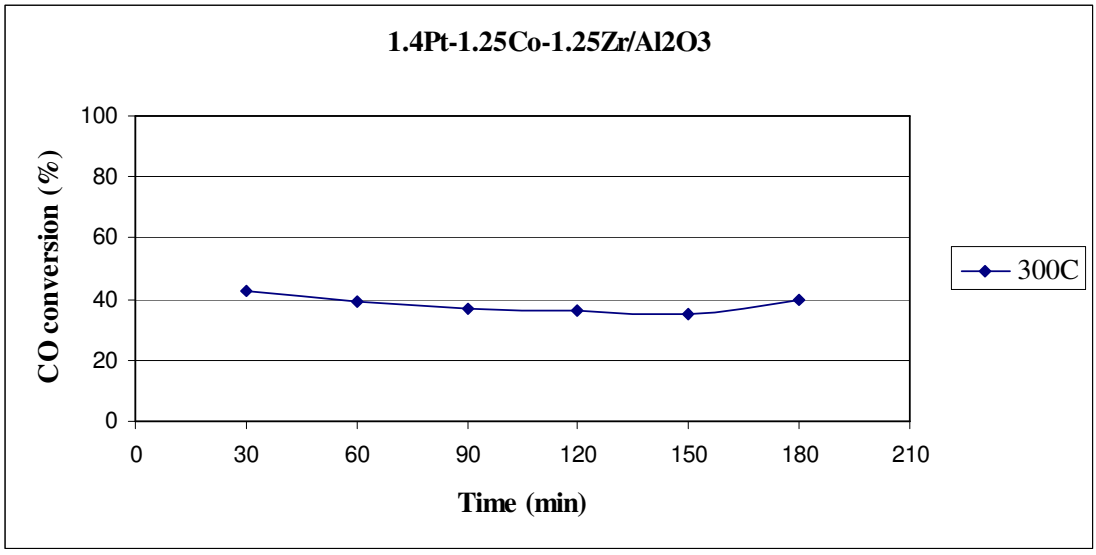

Figure 4.10. CO conversion over 1.4wt.%Pt-1.25wt.%Co-1.25wt.%Zr/γ-Al_2O_3 catalyst at 300°C

Panagiotopoulou and Kondarides (2007) investigated the Zr as promoter on the WGS at the same conditions, as mentioned before. They found out that Pt-Zr/Al_2O_3 had high WGS performance as compared to Pt/Al_2O_3 catalyst. Also, they obtained that Zr containing

catalyst was more active than Fe containing catalyst. This observation was not consistent with our results. This can be due to the effect of cobalt.

The CO conversion at the 60th minute time on stream for the six catalysts tested in this section is summarized in Figure 4.11. As seen from the figure, Fe and Ce containing catalysts are promising for water gas shift reaction and the addition of a second promoter (except Mg) to Pt-Co/Al_2O_3 catalyst improved the WGS activity.

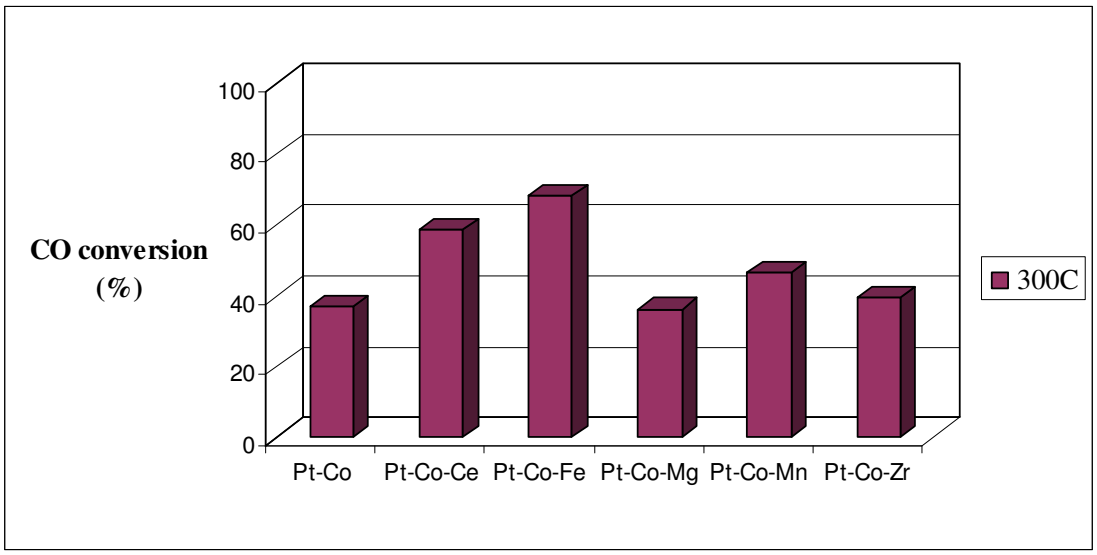

Figure 4.11. CO conversion at the 60th minute for Pt-Co-X/γ-Al_2O_3 at 300 ˚C

4.2. Effect of Promoter Type in the Presence of CO_2

4.2.1. 1.4wt.%Pt- 1.25wt.%X-1.25wt.%Ce/Al_2O_3 (X= None, Co, K, Ni) at 300˚C

In this section the effect of promoter type in the presence of CO_2 was investigated. CO conversion was expected to decrease in the presence of CO_2. The possible effect of CO_2 on WGS is that it can cause reverse water gas shift reaction, which produce CO by consuming H_2.

$$CO_2 + H_2 \leftrightarrow CO + H_2O \qquad (4.3)$$

Again the first experiment was done with Pt-Ce/Al_2O_3 by using 5%CO, 10%H_2O, 10%CO_2 and He in balance (in the absence of H_2). The activity results were given in Table 4.10. CO conversion decreased about 30 per cent with the addition of CO_2 (Figure 4.12). That means reverse water gas shift reaction was occurred. The CO conversion in the absence of CO_2 is also given in the same figure for comparison. Pt-Ce/Al_2O_3 catalyst was found to have the highest decrease in its activity among the catalyst studied as can be seen later.

Table 4.10. Conversion results for Pt-Ce/γ-Al_2O_3 at 300˚C

Time (min)	% CO conversion
30	51
60	50.2
90	48
120	49
150	47.7
180	48.4

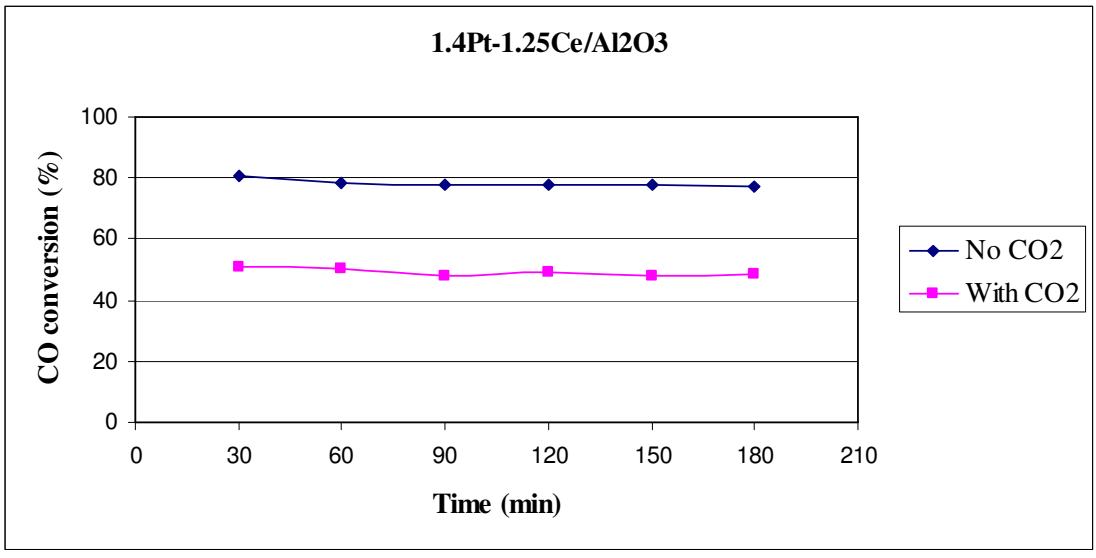

Figure 4.12. CO conversion comparison for Pt-Ce/γ-Al_2O_3 with CO_2 and without CO_2 at 300°C

The effect of CO_2 on Pt-Co-Ce/Al_2O_3 was less than Pt-Ce/Al_2O_3. Conversion decreased approximately 13 per cent closing the gap between this catalyst and Pt-Ce. The results are given in Table 4.11 and Figure 4.13

Table 4.11. Conversion results for Pt-Co-Ce/γ-Al_2O_3 at 300˚C

Time (min)	% CO conversion
30	45.3
60	45.8
90	44.1
120	44.5
150	42
180	49

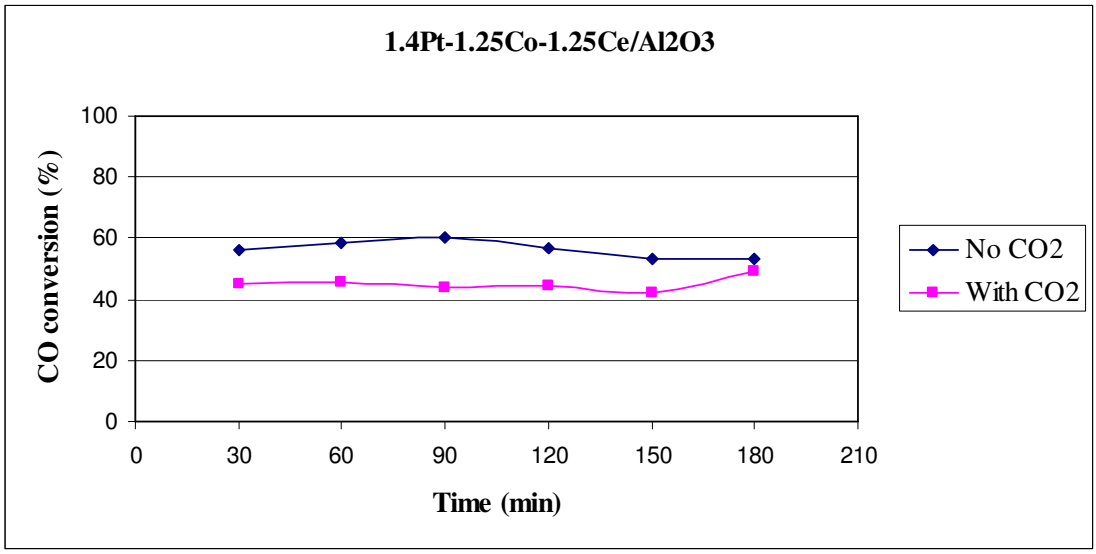

Figure 4.13. CO conversion comparison for Pt-Co-Ce/γ-Al_2O_3 with CO_2 and without CO_2 at 300°C

Minimum decrease (0.5 per cent) was observed in Pt-K-Ce/γ-Al_2O_3 catalyst with the addition of CO_2. Also K containing catalyst was found as the most active one in the presence of CO_2 making this catalyst a promising candidate for the realistic environment. Apparently the activity of the catalyst was very poor for the reverse water-gas shift reaction, where CO_2 reacts with H_2O and produce CO. The results could be seen from the Table 4.12 and Figure 4.14.

Table 4.12. Conversion results for Pt-K-Ce/γ-Al_2O_3 at 300˚C

Time (min)	% CO conversion
30	58.3
60	59.7
90	60.6
120	60.3
150	58.5
180	58.6

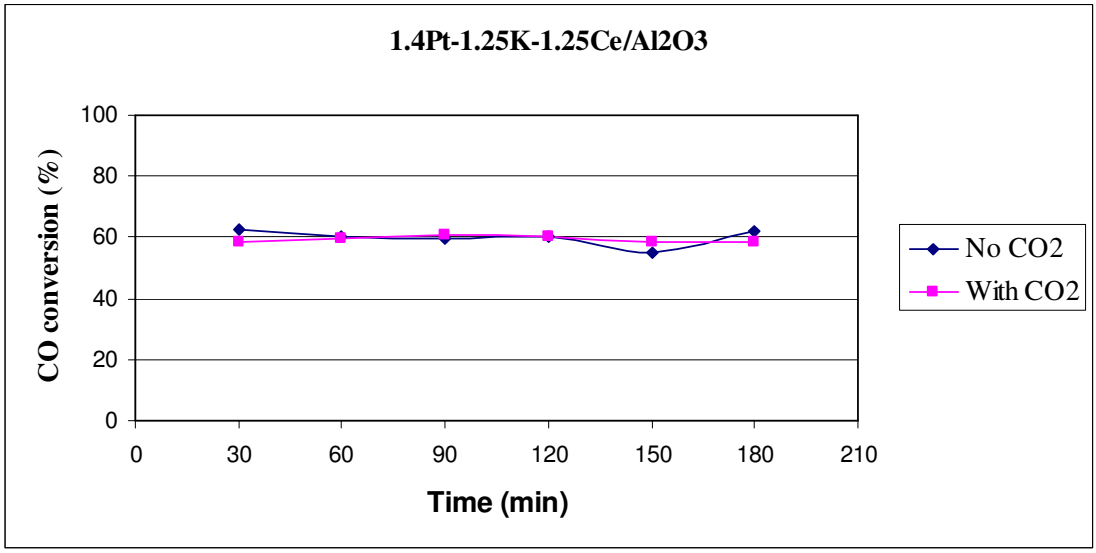

Figure 4.14. CO conversion comparison for Pt-K-Ce/γ-Al_2O_3 with CO_2 and without CO_2 at 300°C

Table 4.13 contains the results for Pt-Ni-Ce/Al_2O_3 catalyst with CO_2 in the feed stream. The effects of CO_2 addition to the feed on Pt-Ni-Ce/Al_2O_3 was also about 10 per cent decrease compare to the results obtained in the absence of CO_2 (Figure 4.15).

Table 4.13. Conversion results for Pt-Ni-Ce/γ-Al_2O_3 at 300˚C

Time (min)	% CO conversion
30	53.2
60	52.7
90	51.1
120	45.9
150	45.9
180	45.4

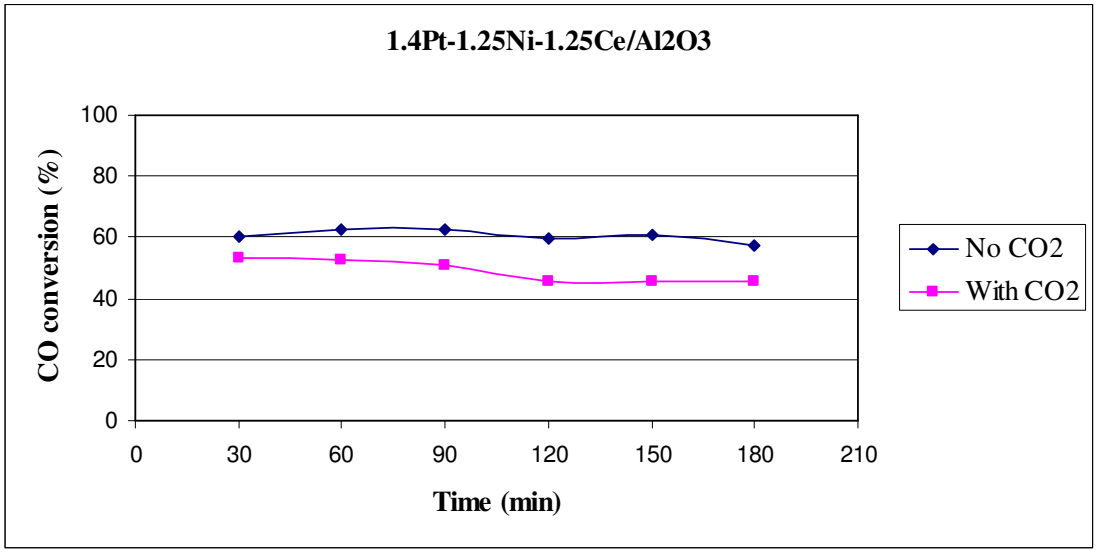

Figure 4.15. CO conversion comparison for Pt-Ni-Ce/γ-Al_2O_3 with CO_2 and without CO_2 at 300°C

The CO conversion value for all the catalyst tested in the presence of CO_2 is summarized in Figure 4.16. The conversion dropped in all the cases as expected. The decrease was the most and the least dramatic for none and K containing catalysts, respectively. Besides, the addition of K and Ni promoters increased the activity of catalysts in the presence of CO_2.

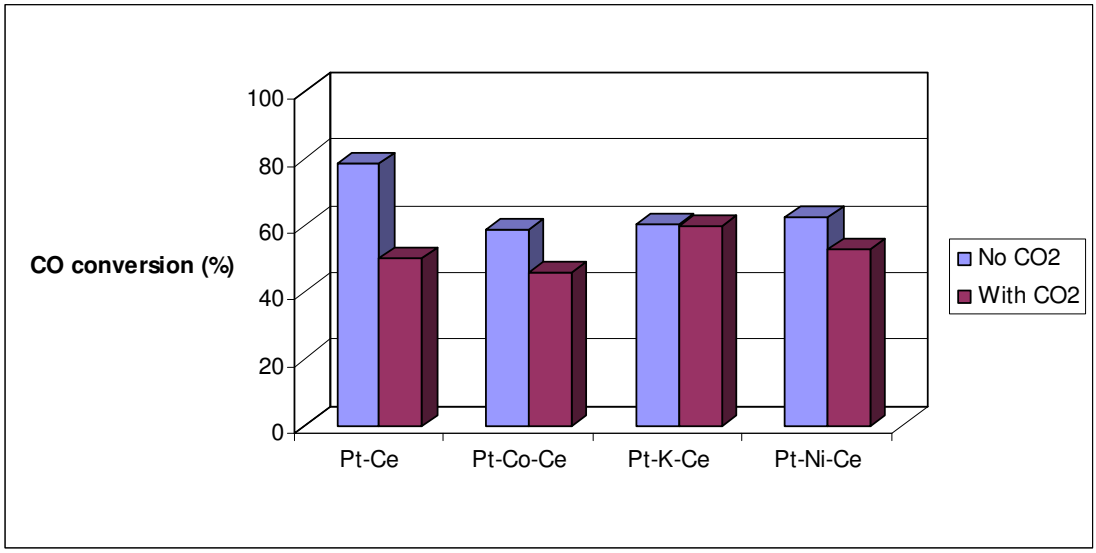

Figure 4.16. CO conversion comparison at the 60th minute for Pt-X-Ce/γ-Al_2O_3 with CO_2 and without CO_2 at 300˚C

4.2.2. 1.4wt.%Pt-1.25wt.%Co-1.25wt.%X/Al_2O_3 (X= None, Ce, Fe, Mg, Mn, Zr) at 300˚C

Firstly, the experiment was conducted with Pt-Co/Al_2O_3 as base catalyst and results were given in Table 4.14. After 1 hour, CO conversion decreased 10 per cent with the addition of CO_2 (Figure 4.17).

Table 4.14. Conversion results for Pt-Co/γ-Al_2O_3 at 300˚C

Time (min)	% CO conversion
30	30.6
60	26.4
90	30.9
120	30.2
150	33.6
180	36

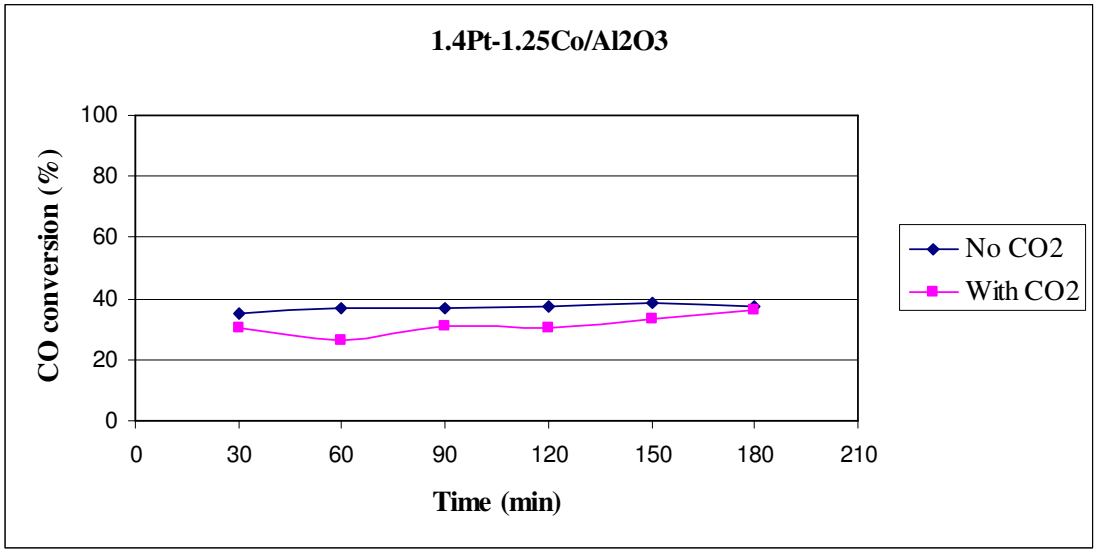

Figure 4.17. CO conversion comparison for Pt-Co/γ-Al_2O_3 with CO_2 and without CO_2 at 300°C

The Pt-Co-Fe/Al_2O_3 catalyst was also affected by the CO_2 addition significantly. As shown in Table 4.15 and Figure 4.18 CO conversion decreased to about 45%, which is 24% lower than the value obtained in the absence of CO_2.

Table 4.15. Conversion results for Pt-Co-Fe/γ-Al_2O_3 at 300˚C

Time (min)	% CO conversion
30	45.4
60	44.1
90	46.5
120	41.9
150	45.8
180	46.6

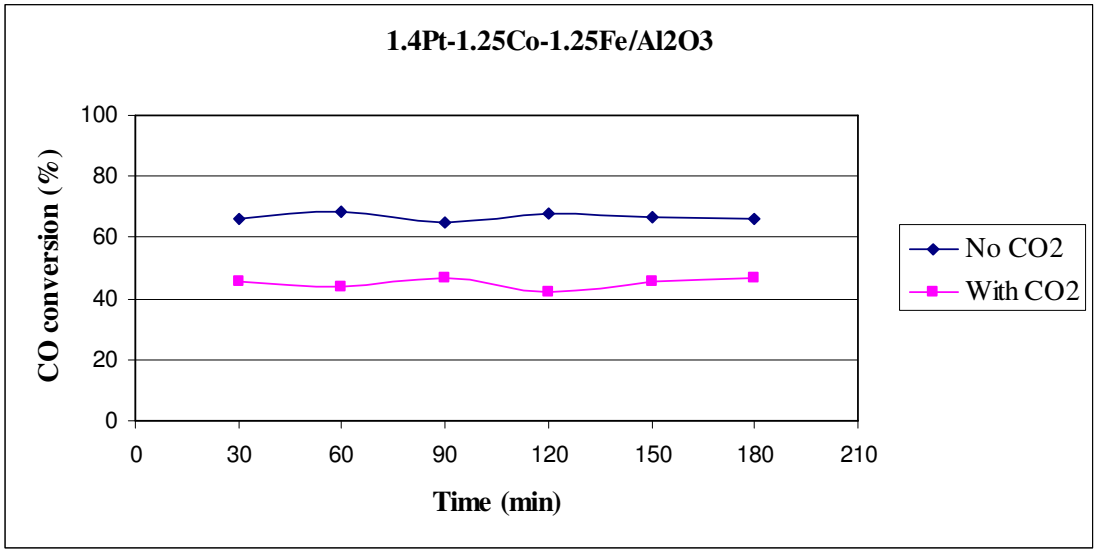

Figure 4.18. CO conversion comparison for Pt-Co-Fe/γ-Al_2O_3 with CO_2 and without CO_2 at 300°C

Table 4.16 contains the results for Pt-Co-Mg/Al_2O_3 catalyst with CO_2 in the feed stream. The effects of CO_2 addition to the feed on Pt-Co-Mg/Al_2O_3 was also about 3 per cent decrease as compared in the case of Pt-Co-Mg/Al_2O_3 in the absence of CO_2 (Figure 4.19).

Table 4.16. Conversion results for Pt-Co-Mg/γ-Al_2O_3 at 300˚C

Time (min)	% CO conversion
30	33.5
60	33.2
90	31
120	32.8
150	38.6
180	38.6

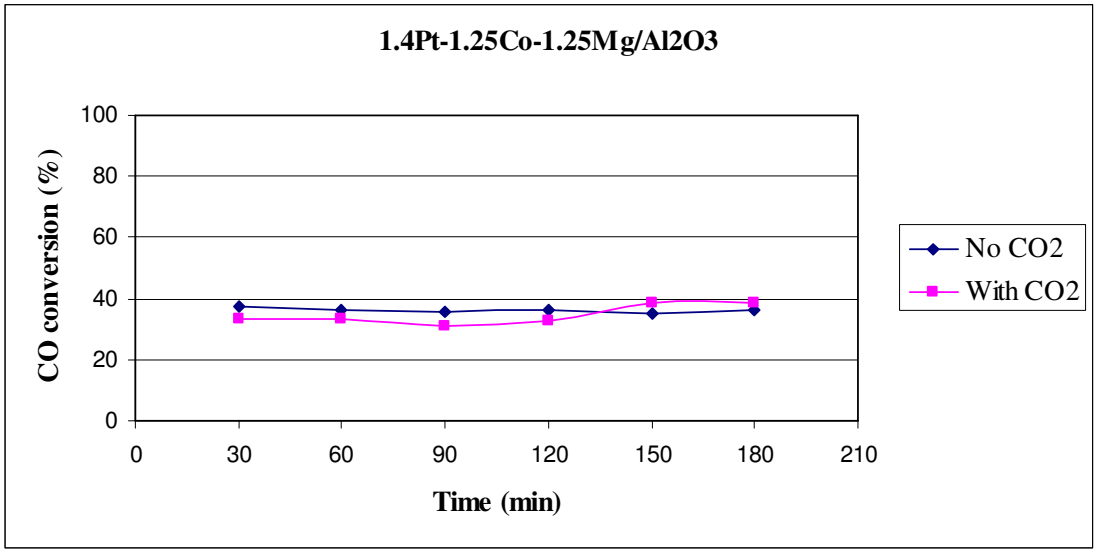

Figure 4.19. CO conversion comparison for Pt-Co-Mg/γ-Al_2O_3 with CO_2 and without CO_2 at 300°C

The CO conversion decreased 2.5 per cent in Pt-Co-Mn/Al_2O_3 when the 10% CO_2 added to the feed (Table 4.17 and Figure 4.20).

Table 4.17. Conversion results for Pt-Co-Mn/γ-Al_2O_3 at 300˚C

Time (min)	% CO conversion
30	45.4
60	44.1
90	42.7
120	42.7
150	39.1
180	42

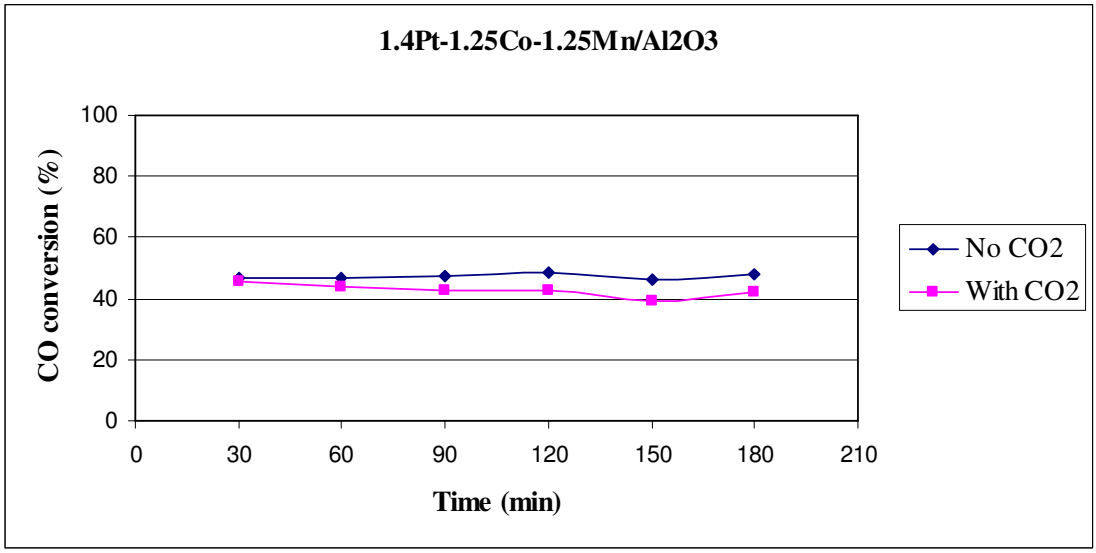

Figure 4.20. CO conversion comparison for Pt-Co-Mn/γ-Al_2O_3 with CO_2 and without CO_2 at 300°C

CO_2 addition is insignificant for Pt-Co-Zr/Al_2O_3 catalyst. The decrease in the activity was only 2 per cent. The results are given in Table 4.18 and Figure 4.21.

Table 4.18. Conversion results for Pt-Co-Zr/γ-Al_2O_3 at 300˚C

Time (min)	% CO conversion
30	34.2
60	37.6
90	37.2
120	34.7
150	39.1
180	36.5

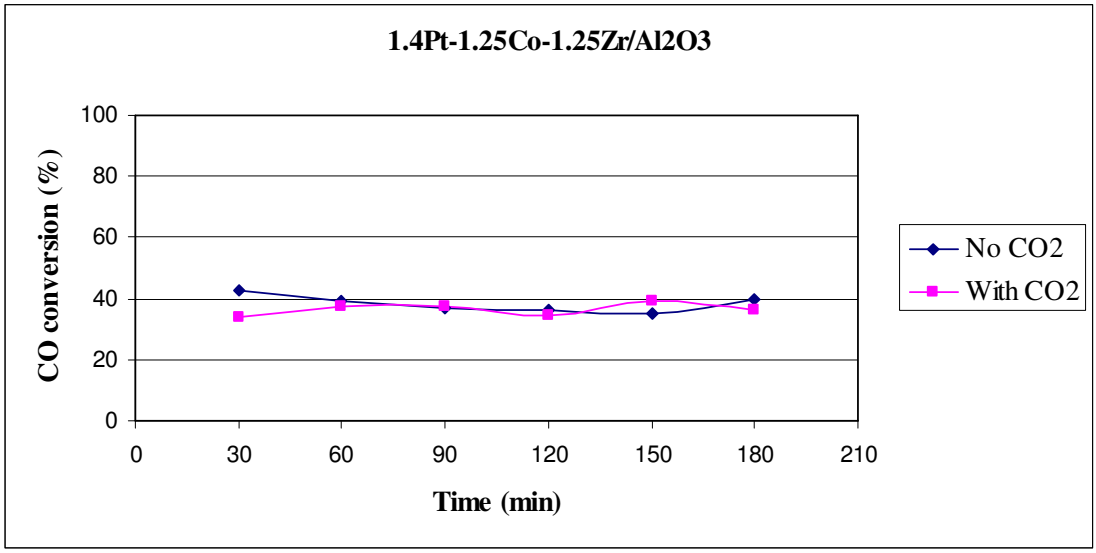

Figure 4.21. CO conversion comparison for Pt-Co-Zr/γ-Al_2O_3 with CO_2 and without CO_2 at 300°C

The CO conversion value for all the catalyst tested in the presence of CO_2 is summarized in Figure 4.22. The conversion was dropped in all the cases as expected. The decrease was more dramatic for the Fe containing catalysts and less for Zr containing catalyst. Moreover, promoter addition to cobalt containing catalyst increased the activity in the presence of CO_2. The increase was the most for Ce and the least for Mg.

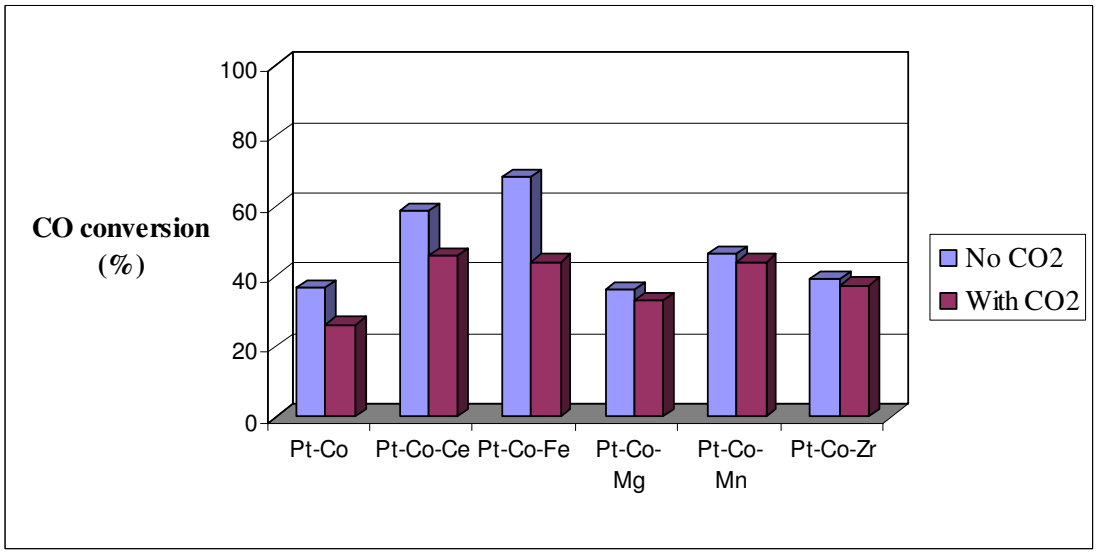

Figure 4.22. CO conversion comparison at the 60th minute for Pt-Co-X/γ-Al_2O_3 with CO_2 and without CO_2 at 300°C

4.3. Effect of Promoter Type in the Presence of H_2

4.3.1. 1.4wt.%Pt- 1.25wt.%X-1.25wt.%Ce/Al_2O_3 (X= None, Co, K, Ni) at 300˚C

In this section H_2 effect on different promoter types was investigated. CO conversion was expected to decrease in the presence of H_2 just as in the case of CO_2. But more decrease was expected with H_2 than CO_2.

The experiments were conducted with 5%CO, 10%H_2O, 40%H_2 and He in balance (in the absence of CO_2). Pt-Ce/Al_2O_3 was chosen as base catalyst to compare promoters' effects. As seen from Table 4.19, CO conversion decreased 53 per cent with H_2 addition. This decrease was the highest among the catalysts tested similar to the case of CO2. According to the results, the activity decreased more with the addition of H_2 than CO_2.

Table 4.19. Conversion results for Pt-Ce/γ-Al_2O_3 at 300˚C

Time (min)	% CO conversion
30	25.8
60	25.3
90	24.9
120	26.2
150	24.9
180	24.9

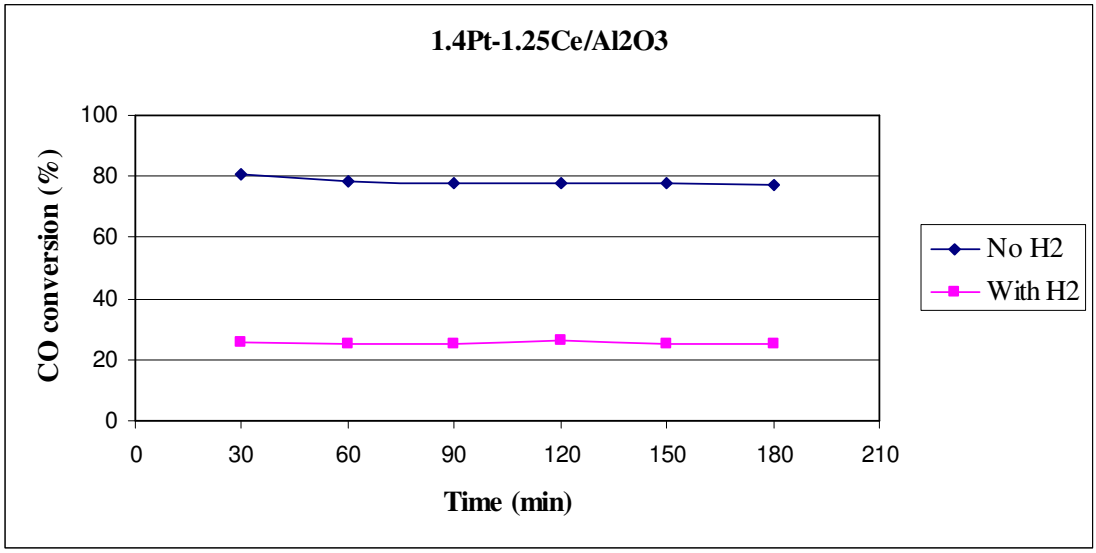

Figure 4.23. CO conversion comparison for Pt-Ce/γ-Al_2O_3 with H_2 and without H_2 at 300°C

The addition of cobalt as promoter to Pt-Ce/Al_2O_3 catalyst was also investigated and 40 per cent decrease was observed. The activity results for Pt-Co-Ce/Al_2O_3 were given in Table 4.20. The conversion dropped nearly 30% from approximately 45% to about 15-18% with H_2 addition.

Table 4.20. Conversion results for Pt-Co-Ce/γ-Al_2O_3 at 300˚C

Time (min)	% CO conversion
30	18
60	18
90	15.9
120	15.5
150	15.5
180	14.2

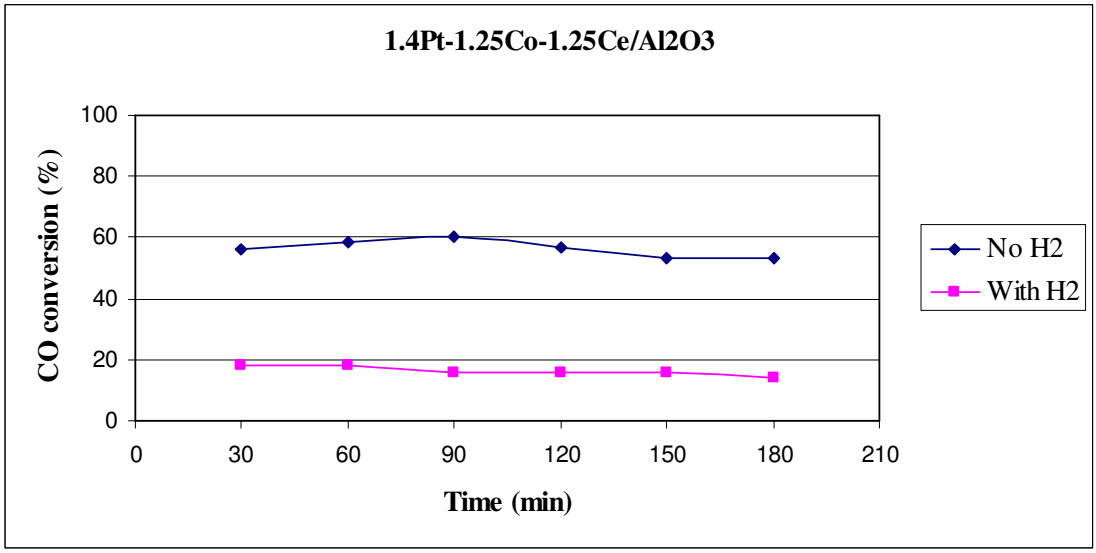

Figure 4.24. CO conversion comparison for Pt-Co-Ce/γ-Al_2O_3 with H_2 and without H_2 at 300°C

Table 4.21 contains the results for Pt-K-Ce/Al_2O_3 catalyst with 40%H_2 in the feed stream. The effects of CO_2 addition to the feed on Pt-K-Ce/Al_2O_3 was about 33 per cent decrease which was the lowest among the Ce containing catalysts (Figure 4.25).

Table 4.21. Conversion results for Pt-K-Ce/γ-Al_2O_3 at 300˚C

Time (min)	% CO conversion
30	25.7
60	27.4
90	28.3
120	28.8
150	30.5
180	28.3

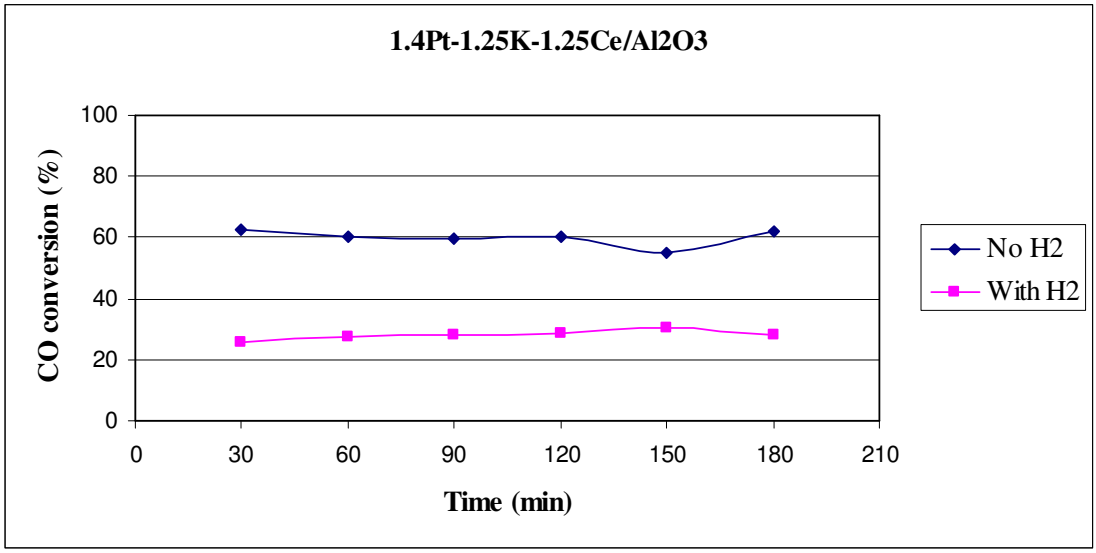

Figure 4.25. CO conversion comparison for Pt-K-Ce/γ-Al_2O_3 with H_2 and without H_2 at 300°C

42 per cent decrease was observed with Pt-Ni-Ce/Al_2O_3 catalyst with the addition of H_2 to the feed. The results could be seen from the Table 4.22 and Figure 4.26.

Table 4.22. Conversion results for Pt-Ni-Ce/γ-Al_2O_3 at 300˚C

Time (min)	% CO conversion
30	20.8
60	20.4
90	21.3
120	19.9
150	19.4
180	19.9

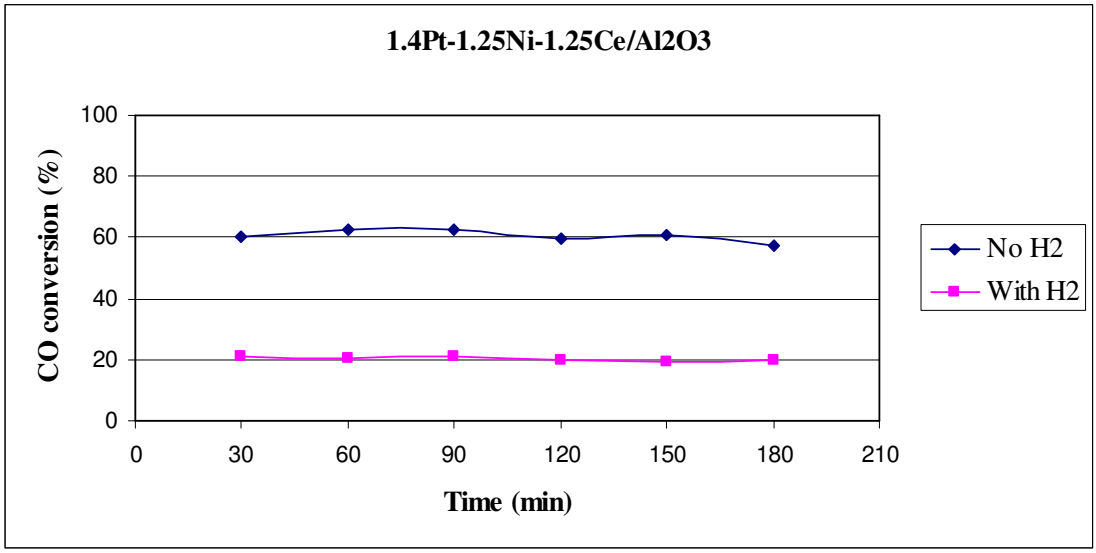

Figure 4.26. CO conversion comparison for Pt-Ni-Ce/γ-Al_2O_3 with H_2 and without H_2 at 300°C

The CO conversion value for all the catalyst tested in the presence of H_2 is summarized in Figure 4.27. The conversion dropped in all the cases as expected. The most decrease was seen on Pt-Ce/Al_2O_3 catalyst with the addition of H_2. Pt-Ce/Al_2O_3 and Pt-K-Ce/Al_2O_3 catalysts activity were quite close to each other.

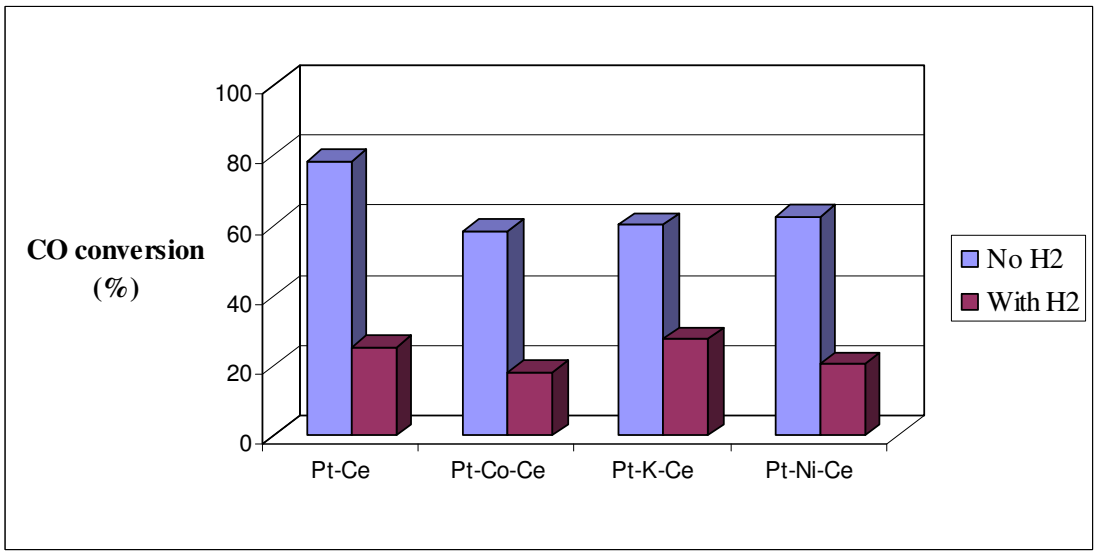

Figure 4.27. CO conversion comparison at the 60th minute for Pt-X-Ce/γ-Al_2O_3 with H_2 and without H_2 at 300˚C

4.3.2. 1.4wt.%Pt-1.25wt.%Co-1.25wt.%X/Al_2O_3 (X= None, Ce, Fe, Mg, Mn, Zr) at 300˚C

In this part, the water gas shift was carried out replacing Ce with various alternatives using a feed stream composition of 5%CO, 10%H_2O, 40%H_2, and He as balance.

First of all, Pt-Co/Al_2O_3 catalyst was prepared to compare the promoter effects. Pt-Co/Al_2O_3 exhibited 21 per cent decrease in its performance in the presence of H_2 (Table 4.23 and Figure 4.28).

Table 4.23. Conversion results for Pt-Co/γ-Al_2O_3 at 300˚C

Time (min)	% CO conversion
30	10.2
60	15.5
90	15.9
120	17.5
150	18.7
180	17.9

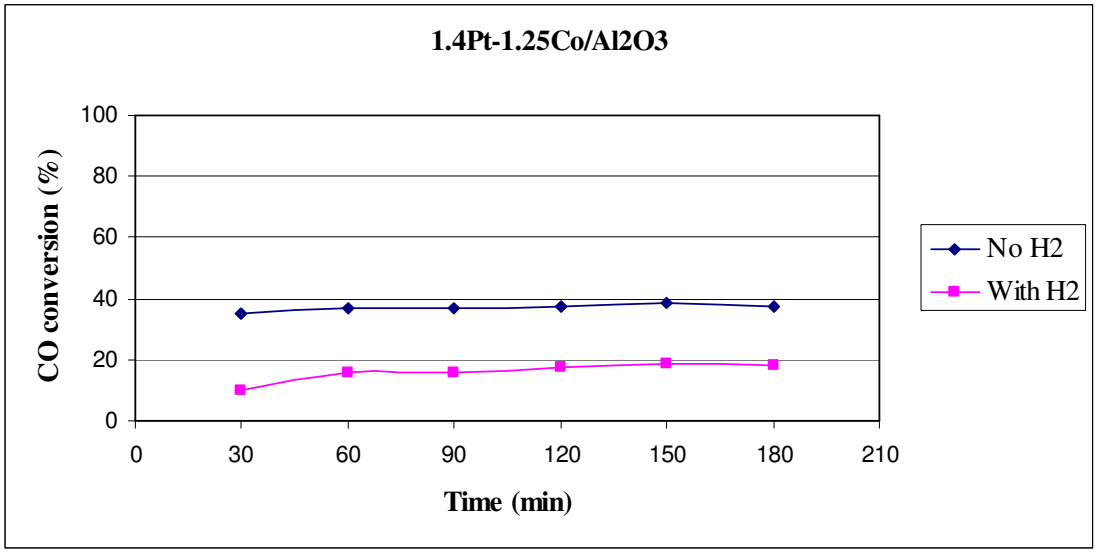

Figure 4.28. CO conversion comparison for Pt-Co/γ-Al_2O_3 with H_2 and without H_2 at 300°C

Table 4.24 contains the results for Pt-Co-Fe/Al_2O_3 catalyst in the presence of H_2. Fe was found as the most effective promoter among others. The highest decrease (46 per cent) was obtained over Pt-Co-Fe/Al_2O_3 catalyst with the addition of H_2 (Figure 4.29).

Table 4.24. Conversion results for Pt-Co-Fe/γ-Al_2O_3 at 300˚C

Time (min)	% CO conversion
30	22
60	22
90	23.6
120	23.6
150	23.6
180	23.2

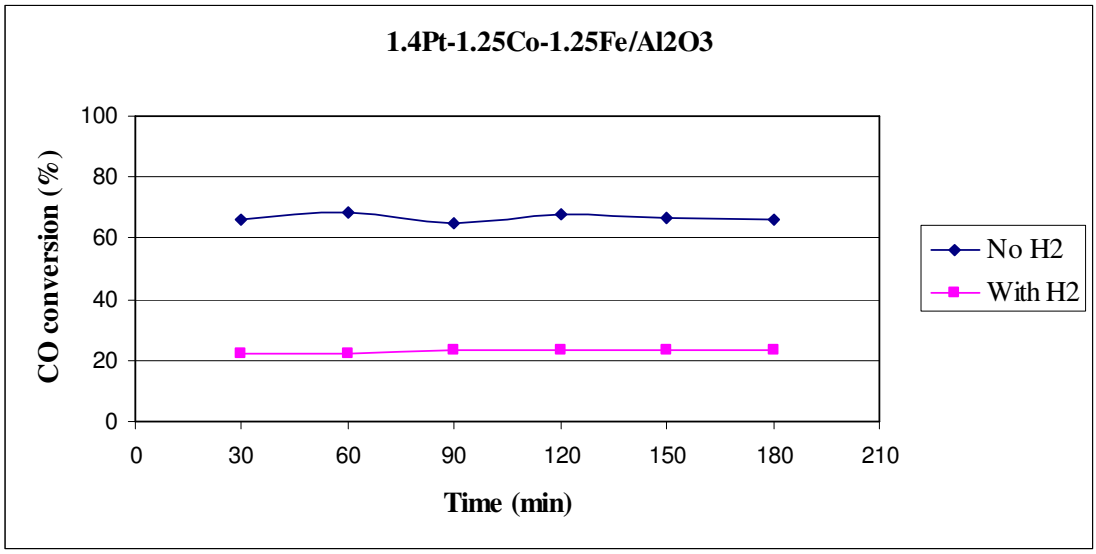

Figure 4.29. CO conversion comparison for Pt-Co-Fe/γ-Al_2O_3 with H_2 and without H_2 at 300°C

The CO conversion decreased 18 per cent in Pt-Co-Mg/Al_2O_3 when the 40% H_2 added to the feed (Table 4.25 and Figure 4.30).

Table 4.25. Conversion results for Pt-Co-Mg/γ-Al_2O_3 at 300˚C

Time (min)	% CO conversion
30	15
60	17
90	17.4
120	16.6
150	18.6
180	19.8

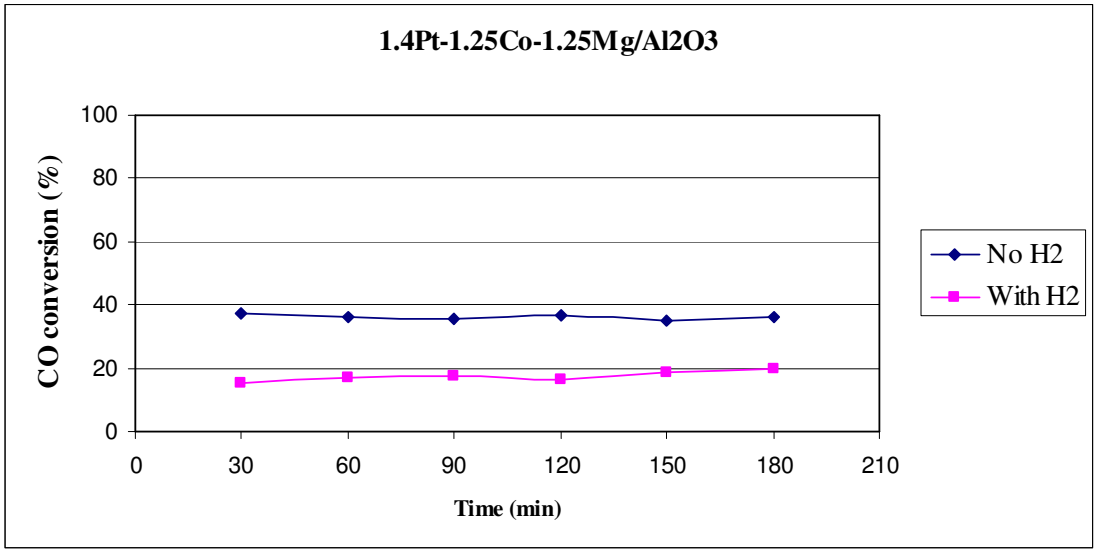

Figure 4.30. CO conversion comparison for Pt-Co-Mg/γ-Al_2O_3 with H_2 and without H_2 at 300°C

The Mn containing catalyst was found to be less effective than other catalysts and 32 per cent decrease was observed in the presence of H_2. The results were shown in Table 4.26 and Figure 4.31.

Table 4.26. Conversion results for Pt-Co-Mn/γ-Al_2O_3 at 300˚C

Time (min)	% CO conversion
30	14.4
60	13.9
90	13.4
120	13.4
150	13.9
180	14.4

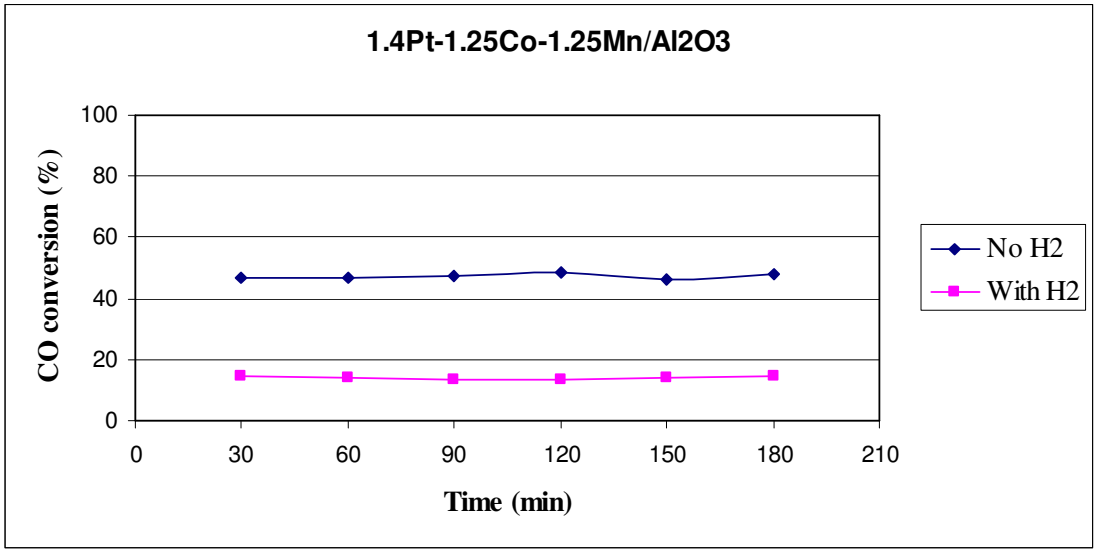

Figure 4.31. CO conversion comparison for Pt-Co-Mn/γ-Al_2O_3 with H_2 and without H_2 at 300°C

Like Pt-Co-Mn/Al_2O_3, the Pt-Co-Zr/Al_2O_3 catalyst was also affected by the H_2 addition. The results were shown in Table 4.27 and Figure 4.32.

Table 4.27. Conversion results for Pt-Co-Zr/γ-Al_2O_3 at 300˚C

Time (min)	% CO conversion
30	15
60	17.1
90	17.1
120	15
150	13.4
180	12.6

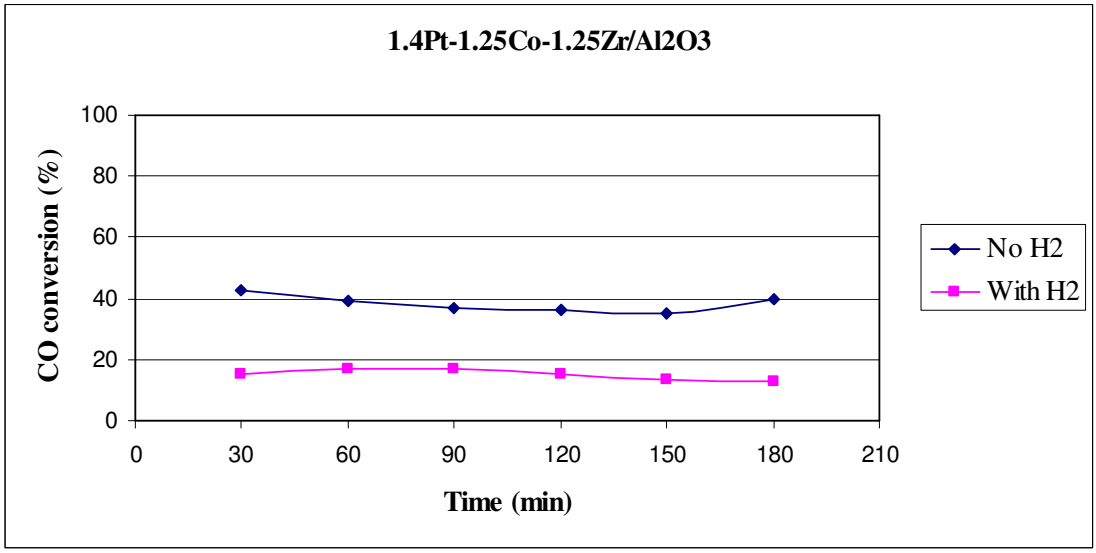

Figure 4.32. CO conversion comparison for Pt-Co-Zr/γ-Al_2O_3 with H_2 and without H_2 at 300°C

The CO conversion value for all the catalyst tested in the presence of H_2 is summarized in Figure 4.33. The conversion dropped in all the cases as expected. The decrease of Pt-Co-Fe/Al_2O_3 was more than other catalysts and the smallest decrease was observed with Pt-Co-Mg/Al_2O_3 catalyst with the addition of H_2.

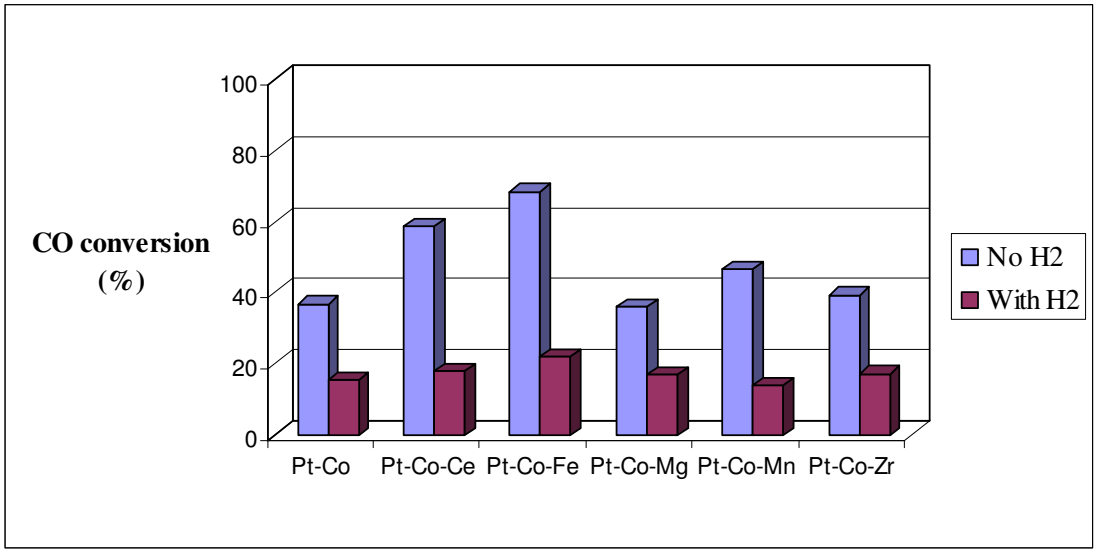

Figure 4.33. CO conversion comparison at the 60th minute for Pt-Co-X/γ-Al_2O_3 with H_2 and without H_2 at 300˚C

4.4. Effect of Promoter Type in the Presence of CO_2 and H_2

4.4.1. 1.4wt.%Pt- 1.25wt.%X-1.25wt.%Ce/Al_2O_3 (X= None, Co, K, Ni) at 300˚C

Under realistic reaction conditions, the feed contains significant amounts of hydrogen and carbon dioxide, and both have a negative effect on the activity. Hence the catalytic performance of the catalysts discussed in the previous sections was also investigated under realistic feed compositions. The experiments were conducted with 5%CO, 10%H_2O, 10%CO_2, 40%H_2 and He as balance.

The conversion results for Pt-Ce/Al_2O_3 are given in Table 4.28. The conversion decreased from 78% to 21% after 60 minutes with the addition of CO_2 and H_2. In the activity the biggest decrease was observed with Pt-Ce/Al_2O_3 catalyst among Ce containing catalysts.

Table 4.28. Conversion results for Pt-Ce/γ-Al_2O_3 at 300˚C

Time (min)	% CO conversion
30	18.2
60	21.2
90	13.8
120	14.3
150	16.3
180	16.3

Thinon *et al*. (2008) studied Pt/CeO_2/Al_2O_3 catalyst which was prepared with sol-gel method. In order to investigate the activity of catalyst at 250, 300 and 350°C, 0.9wt.% metal was loaded. The experiments were conducted with 10%CO, 10%CO_2, 20%H_2O, 30%H_2 and 30%Ar. As a result, 5 per cent, 30 per cent and 60 per cent CO conversion was obtained at 250, 300, 350°C, respectively.

Kim *et al*. (2009) investigated Pt-Ce/γ-Al_2O_3 catalyst which was composed of 0.6wt.%Pt and 2.73wt.%Ce. As feed, 6.7vol.%CO, 6.7vol.%CO_2, 33.2vol.%H_2O and H_2 in balance. 0.10 g catalyst and 150 ml/min flow rate were used. As a result, 60 per cent CO conversion was obtained at 650˚C.

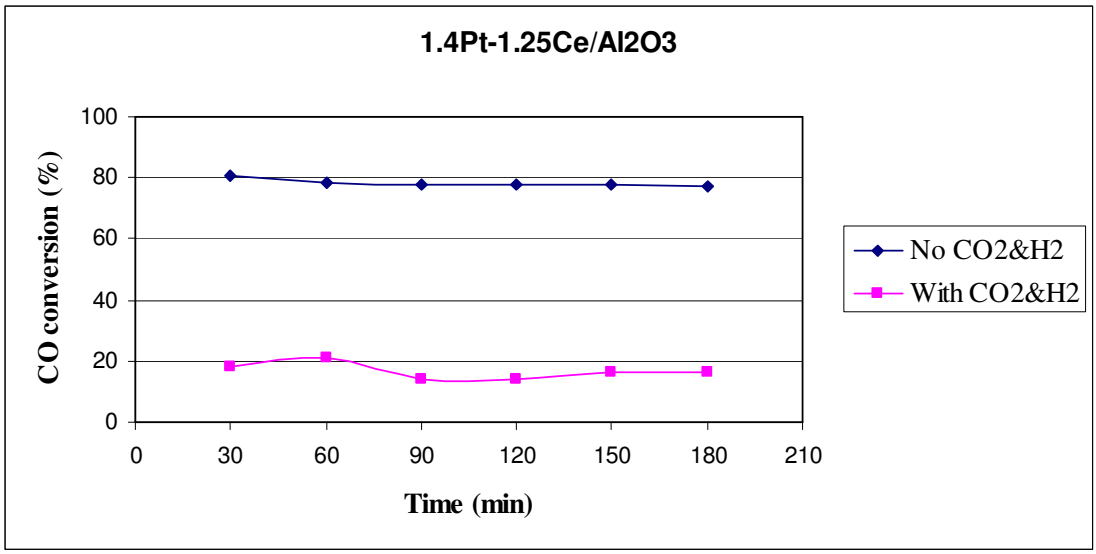

Figure 4.34. CO conversion comparison for Pt-Ce/γ-Al_2O_3 with CO_2&H_2 and without CO_2&H_2 at 300°C

Germani *et al*. (2005) investigated Platinum/ceria/alumina catalyst prepared with sol-gel method between 300 and 400°C. The feed composition was 9.6%CO, 8.4%CO_2, 23%H_2O, 32.2%H_2 and 26.8%Ar. Several catalysts were prepared containing 1-2wt.%Pt and 10-20wt.%CeO_2. They concluded as CO conversion increased above 250°C. Approximately 70 per cent CO conversion was obtained at 370°C with 2wt.%Pt and 10wt.%CeO_2. This conversion was quite close to equilibrium curve.

In the Table 4.29 the conversion results were given for Pt-Co-Ce/Al_2O_3 catalyst. Similar to Pt-Ce/Al_2O_3, the CO_2 and H_2 had a negative effect on CO conversion over Pt-Co-Ce/Al_2O_3. CO conversion increased slightly with time until 90 minutes (Figure 4.35).

Table 4.29. Conversion results for Pt-Co-Ce/γ-Al_2O_3 at 300˚C

Time (min)	% CO conversion
30	12
60	13
90	16.8
120	15.4
150	15.4
180	13.9

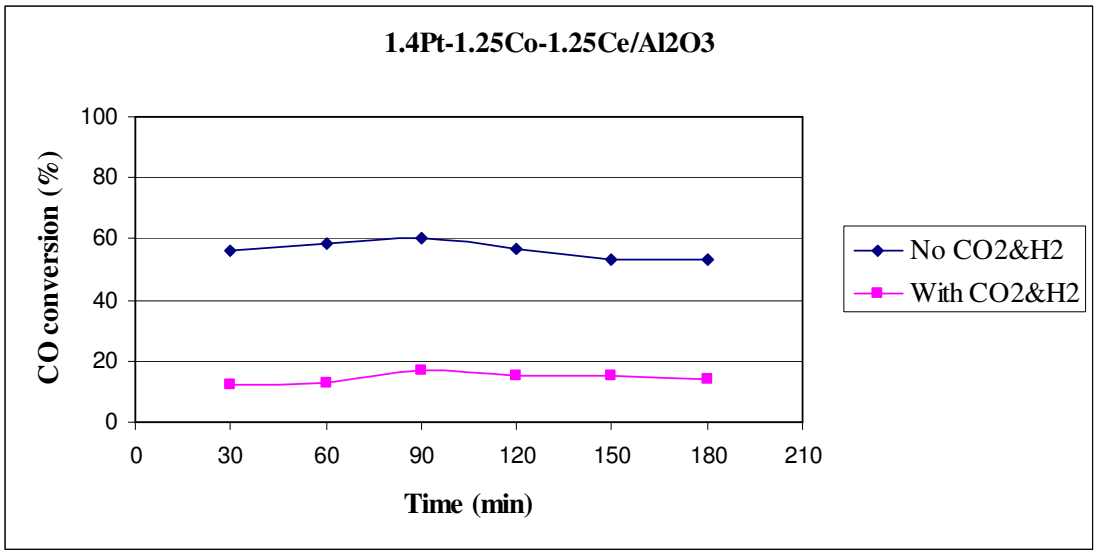

Figure 4.35. CO conversion comparison for Pt-Co-Ce/γ-Al_2O_3 with CO_2&H_2 and without CO_2&H_2 at 300°C

For Pt-K-Ce/Al_2O_3 the negative effect of CO_2 and H_2 was shown in Table 4.30. The CO conversion decreased up to 20.5% after 60 min reaction time, where at the same reaction time it was 60.2% for the gas stream containing no CO_2 and no H_2.

Table 4.30. Conversion results for Pt-K-Ce/γ-Al_2O_3 at 300˚C

Time (min)	% CO conversion
30	17.1
60	20.5
90	18.5
120	19.9
150	15.1
180	18.5

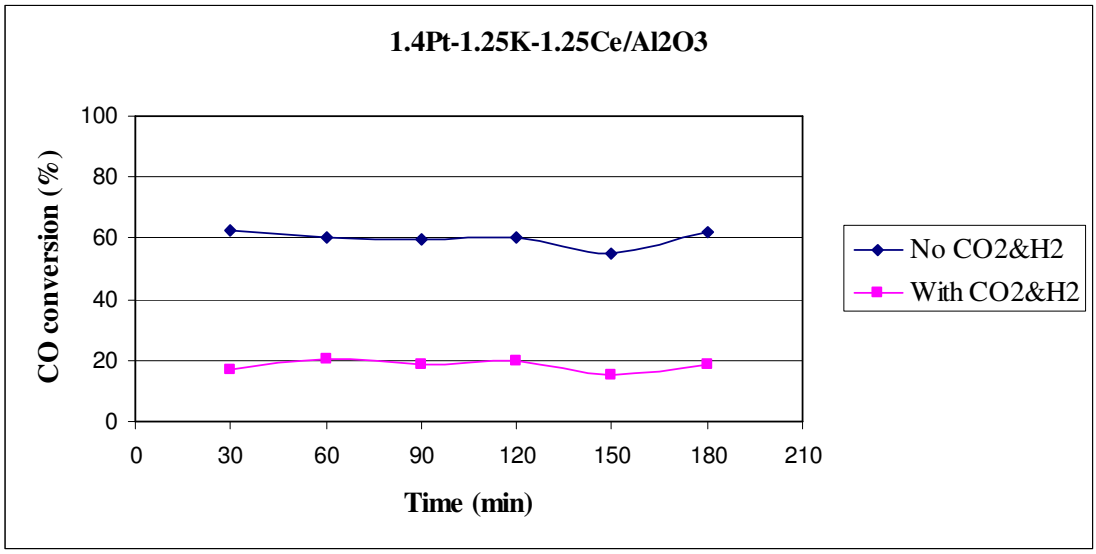

Figure 4.36. CO conversion comparison for Pt-K-Ce/γ-Al_2O_3 with CO_2&H_2 and without CO_2&H_2 at 300°C

Table 4.31 contains the results for Pt-Ni-Ce/Al_2O_3 catalyst in the presence of CO_2 and H_2. 49 per cent decrease was observed after 60 min with the addition of CO_2 and H_2. After that time the conversion started to decrease.

Table 4.31. Conversion results for Pt-Ni-Ce/γ-Al_2O_3 at 300˚C

Time (min)	% CO conversion
30	7
60	13.4
90	12.4
120	10.9
150	11.9
180	12.4

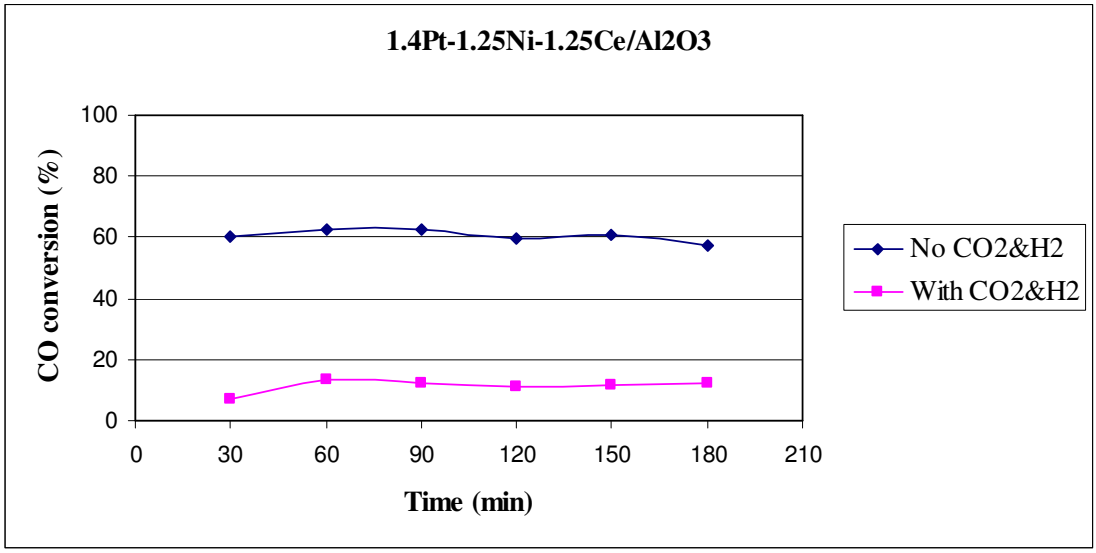

Figure 4.37. CO conversion comparison for Pt-Ni-Ce/γ-Al_2O_3 with CO_2&H_2 and without CO_2&H_2 at 300°C

The CO conversion obtained at the 60th minute time on stream was summarized in Figure 4.38 for all the catalyst tested in the presence of CO_2 and H_2. It is clear that CO_2 and H_2 together had negative effects in all the catalysts. The most affected catalyst was Pt-Ce/Al_2O_3 and less affected was Pt-K-Ce/Al_2O_3 catalyst.

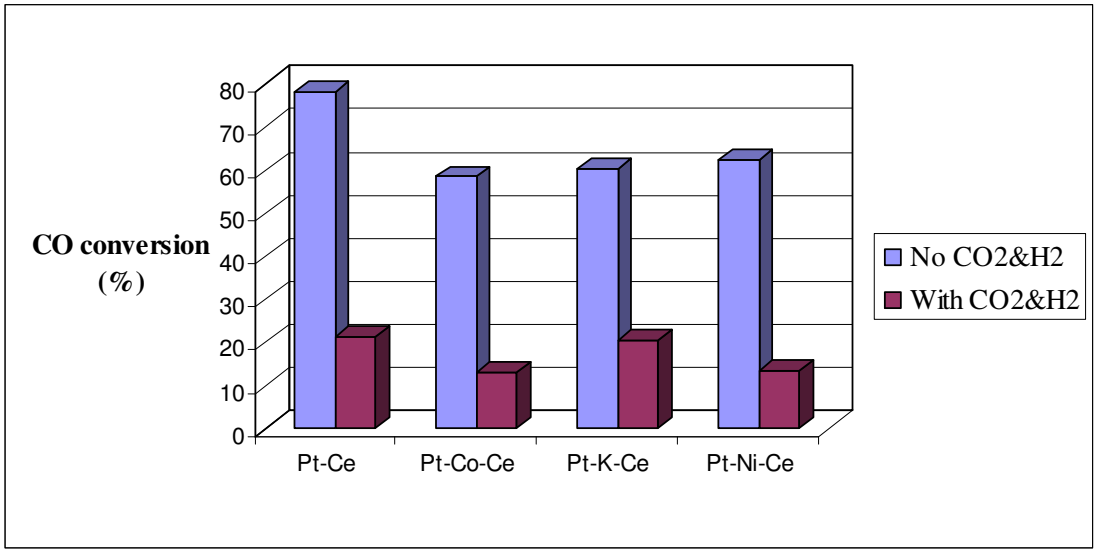

Figure 4.38. CO conversion comparison at the 60th minute for Pt-X-Ce/γ-Al_2O_3 with CO2&H_2 and without CO2&H_2 at 300˚C

4.4.2. 1.4wt.%Pt-1.25wt.%Co-1.25wt.%X/Al_2O_3 (X= None, Ce, Fe, Mg, Mn, Zr) at 300˚C

In this part, the effects of the second promoters in addition to cobalt were tested for their water gas shift activity in the presence of CO_2 and H_2 together. Firstly, Pt-Co/Al_2O_3 results were shown in Table 4.32, and this catalyst had a quite low activity with the realistic gas mixture.

Table 4.32. Conversion results for Pt-Co/γ-Al_2O_3 at 300˚C

Time (min)	% CO conversion
30	0
60	1.9
90	0
120	3.7
150	4.9
180	8.6

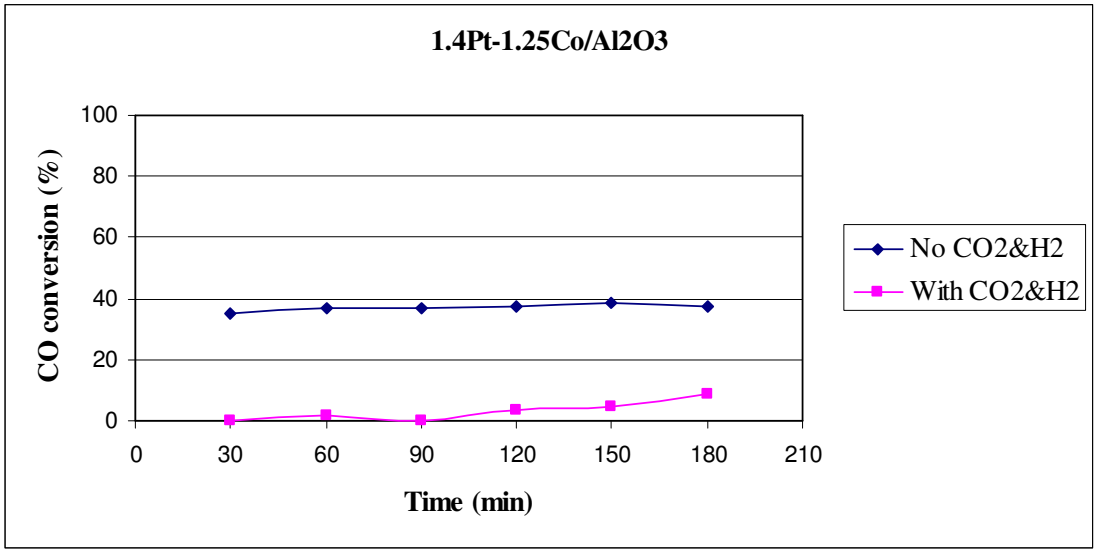

Figure 4.39. CO conversion comparison for Pt-Co/γ-Al_2O_3 with CO_2&H_2 and without CO_2&H_2 at 300°C

A significant activity decrease, which was 48 per cent, was observed in Pt-Co-Fe/Al_2O_3 catalyst with the addition of CO_2 and H_2. The results were shown in Table 4.33 and Figure 4.40. The maximum CO conversion was obtained as 20 per cent after 60 min.

Table 4.33. Conversion results for Pt-Co-Fe/γ-Al_2O_3 at 300˚C

Time (min)	% CO conversion
30	19.7
60	20.2
90	18.7
120	10.8
150	11.3
180	18.7

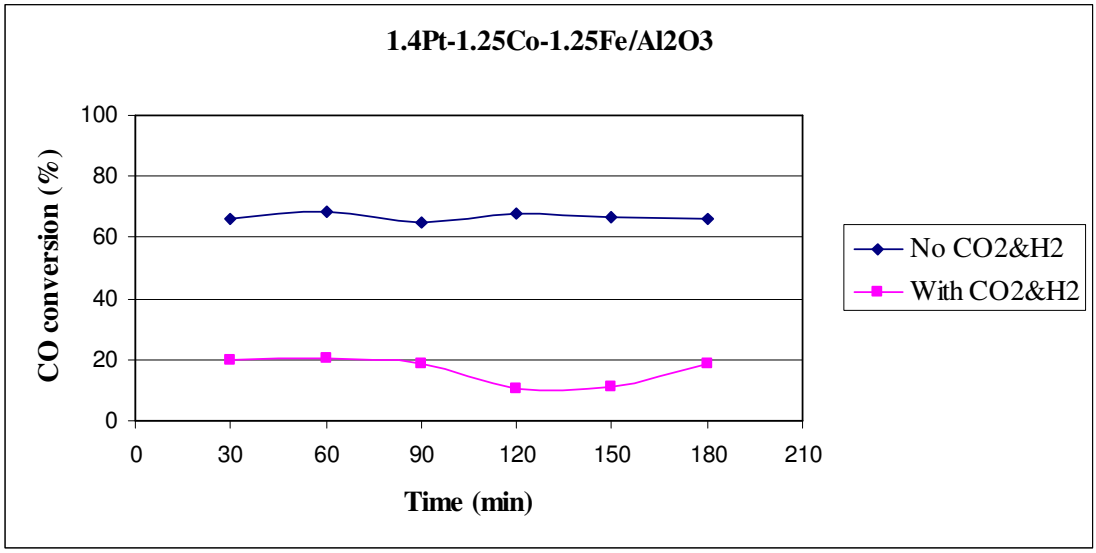

Figure 4.40. CO conversion comparison for Pt-Co-Fe/γ-Al_2O_3 with CO_2&H_2 and without CO_2&H_2 at 300°C

For Pt-Co-Mg/Al_2O_3 the conversion results were given in Table 4.34. 27 per cent activity decrease was observed in the presence of CO_2 and H_2.

Table 4.34. Conversion results for Pt-Co-Mg/γ-Al_2O_3 at 300˚C

Time (min)	% CO conversion
30	7.1
60	8.6
90	9.1
120	9.1
150	9.1
180	9.6

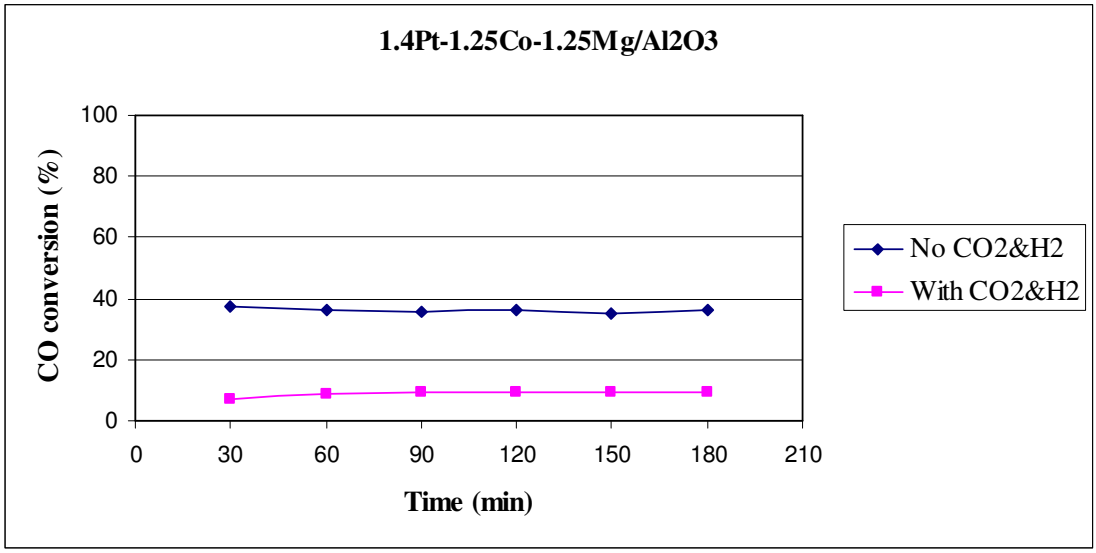

Figure 4.41. CO conversion comparison for Pt-Co-Mg/γ-Al_2O_3 with CO_2&H_2 and without CO_2&H_2 at 300°C

The experiment results for Pt-Co-Mn/Al_2O_3 at 300˚C were given in Table 4.35. It can be also seen from Figure 4.42 that the CO conversion decreased again with the addition of CO_2 and H_2. After 150 min no CO conversion was observed.

Table 4.35. Conversion results for Pt-Co-Mn/γ-Al_2O_3 at 300˚C

Time (min)	% CO conversion
30	10.2
60	13.3
90	8.7
120	11.2
150	1.5
180	0

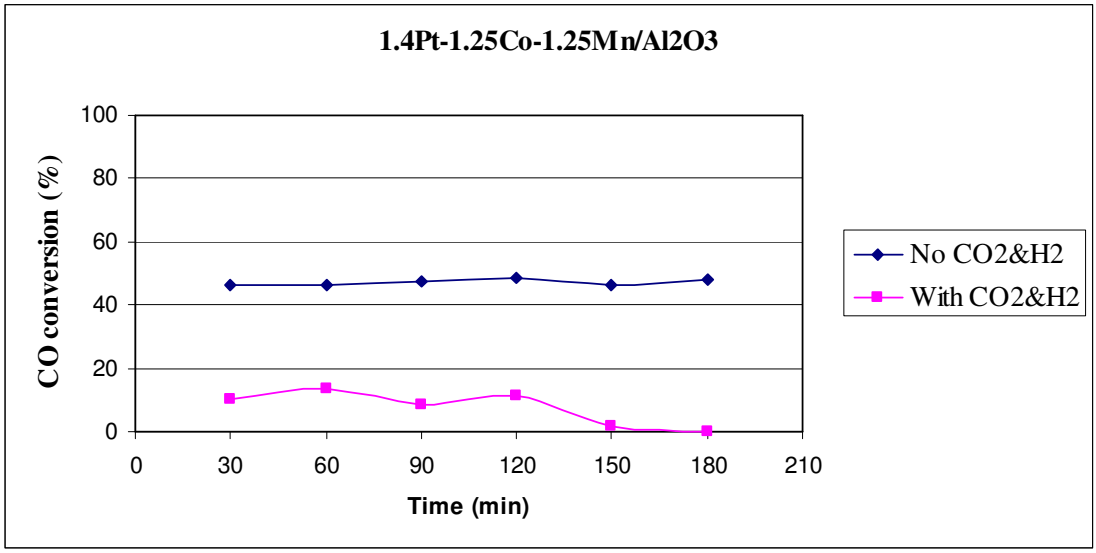

Figure 4.42. CO conversion comparison for Pt-Co-Mn/γ-Al_2O_3 with CO_2&H_2 and without CO_2&H_2 at 300°C

Finally, Pt-Co-Zr/Al_2O_3 was tested in the presence of CO_2 and H_2. The results were shown in Table 4.36. 32 per cent decrease was obtained after 60 min.

Table 4.36. Conversion results for Pt-Co-Zr/γ-Al_2O_3 at 300˚C

Time (min)	% CO conversion
30	5.7
60	7.3
90	10.9
120	10.9
150	8.3
180	9.3

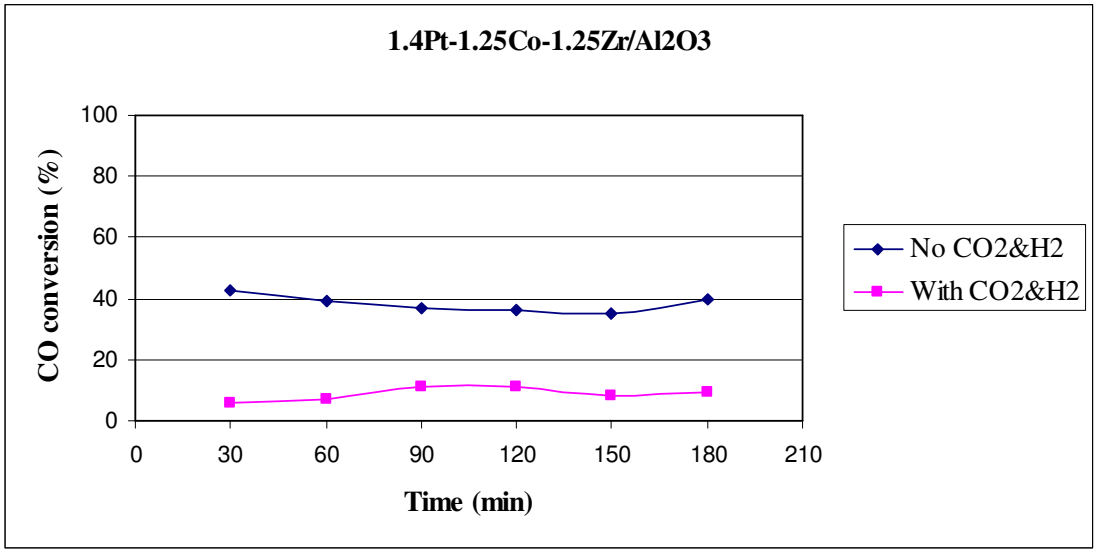

Figure 4.43. CO conversion comparison for Pt-Co-Zr/γ-Al_2O_3 with CO_2&H_2 and without CO_2&H_2 at 300°C

The CO conversion value for all the catalyst tested in the presence of CO_2 and H_2 is summarized in Figure 4.44. The conversion dropped in all the cases as expected. The biggest and lowest decrease was seen in Fe and Mg containing catalyst respectively. Furthermore, the activity of catalyst was increased with the addition of promoter. In these conditions Pt-Co-Fe/Al_2O_3 catalyst was the most active one.

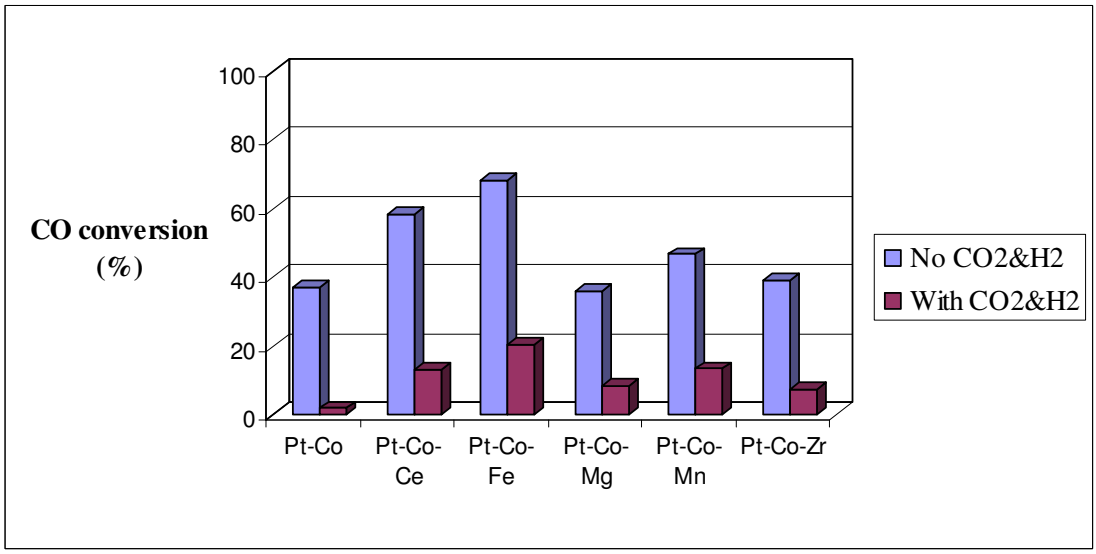

Figure 4.44. CO conversion comparison at the 60th minute for Pt-Co-X/γ-Al_2O_3 with CO_2&H_2 and without CO_2&H_2 at 300˚C

4.5. Effect of Reaction Temperature in the Presence of CO_2 and H_2

Four catalysts which showed high activity in the presence of CO_2 and H_2 were used to investigate the effect of reaction temperature on the catalytic activity. The reaction temperatures were chosen as 300, 275 and 250˚C. The experiments were conducted with 5 per cent CO, 10 per cent H_2O, 10 per cent CO_2, 40 per cent H_2 and He in balance. The equilibrium conversions of CO with respect to temperature were also calculated for this feed gas composition using the computer software HSC4 (HSC Chemistry Version 4.1, Outokumpu Research Oy.) and is presented in Figure 4.45. The water-gas shift reaction is an exothermic reaction; hence the equilibrium CO conversion is higher at lower temperatures, and decreases with increasing temperature.

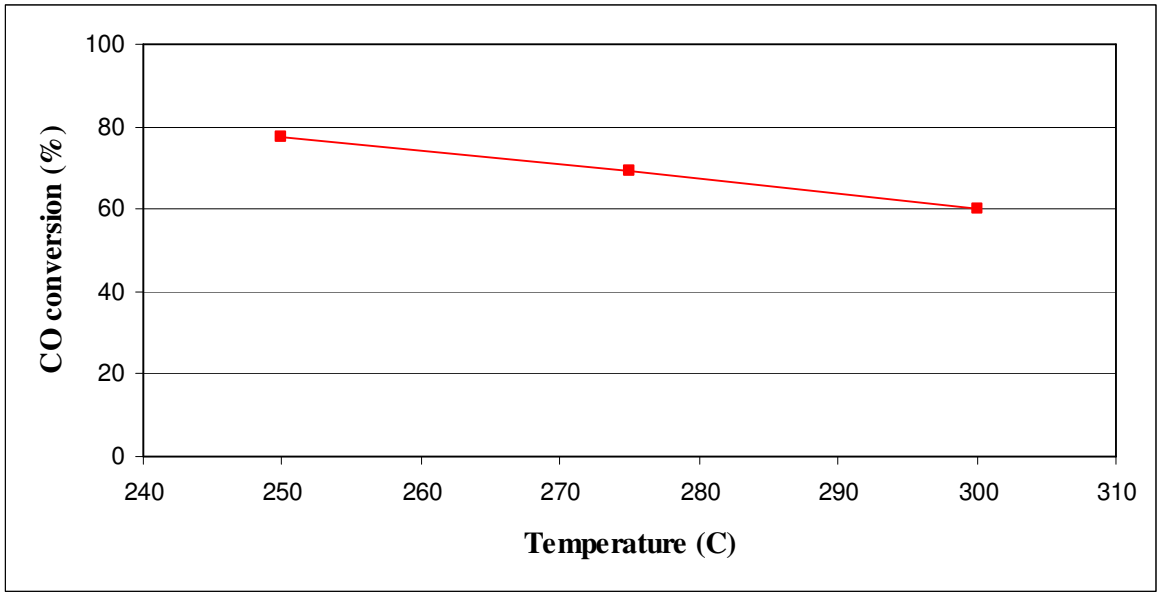

Figure 4.45. Equilibrium curve of the water-gas shift reaction for a feed gas composition of 5%CO, 10% H_2O, 10%CO_2 and 40%H_2 in He

Firstly, the temperature effect over 1.4wt.%Pt-1.25wt.%Ce/Al_2O_3 catalyst was studied. The results are given in Table 4.37 and Figure 4.46. CO conversion decreased with decreasing temperature as expected. Maximum 14.8 and 12 per cent CO conversion was observed at 275 and 250°C, respectively.

Table 4.37. Conversion results for Pt-Ce/γ-Al_2O_3 at different reaction temperatures

Time (min)	CO conversion (%)		
	300°C	275°C	250°C
30	18.2	14.8	12
60	21.2	12.3	7.3
90	13.8	11.3	5.2
120	14.3	9.9	2.6
150	16.3	10.3	2.1
180	16.3	14.3	6.8

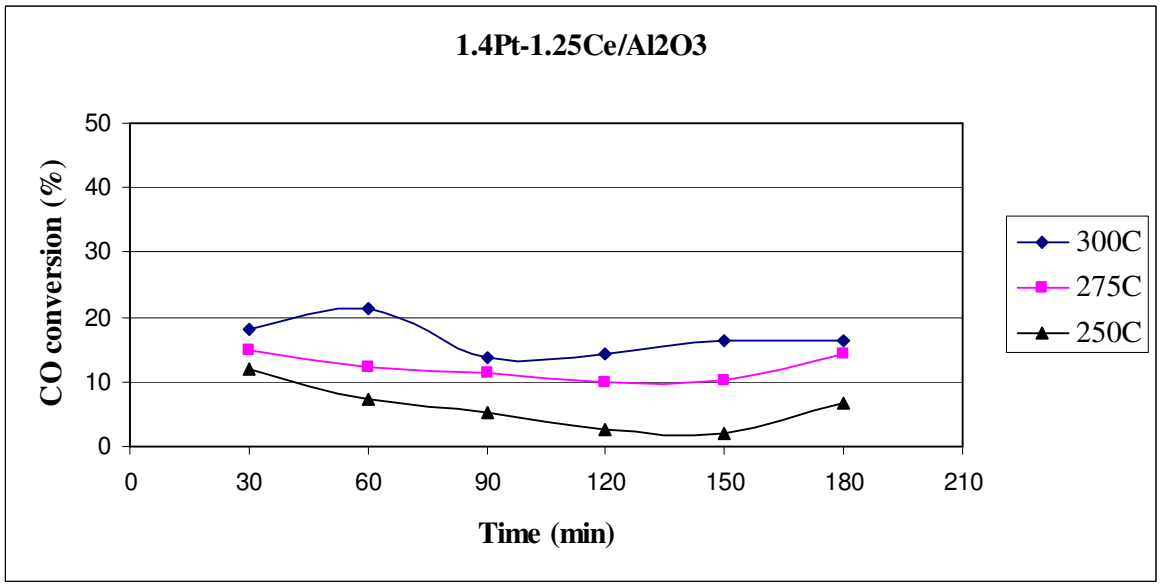

Figure 4.46. CO conversion comparison for Pt-Ce/γ-Al_2O_3 at different temperatures

CO conversion approached the equilibrium curve when temperature was increased. But the reaction was far from the equilibrium under these conditions (Table 4.38 and Figure 4.47).

Table 4.38. CO conversion over 1.4%Pt-1.25%Ce/γ-Al_2O_3 at different reaction temperatures (60 minutes time-on-stream)

Temperature (^oC)	CO conversion (%)
300	21.2
275	12.3
250	7.3

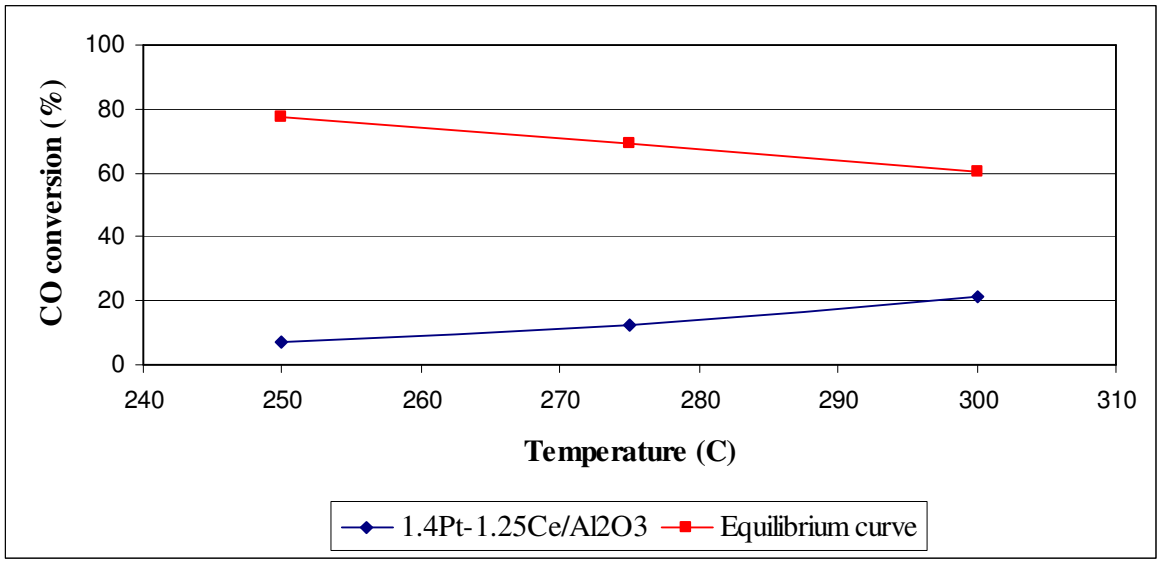

Figure 4.47. CO conversion versus temperature over 1.4wt.%Pt-1.25wt.%Ce/γ-Al_2O_3 with respect to equilibrium (60 minutes time-on-stream)

The effect of temperature was also studied over 1.4wt.%Pt-1.25wt.%Co-1.25wt.%Ce/Al_2O_3 catalyst. Only 4 per cent activity decrease was observed until 90 min. with decreasing temperature from 300 to 275°C. No significant activity was observed at 250°C. The activity of the catalyst is presented in Table 4.39 and Figure 4.48.

Table 4.39. Conversion results for Pt-Co-Ce/γ-Al_2O_3 at different reaction temperatures

Time (min)	CO conversion (%)		
	300°C	275°C	250°C
30	12	8.7	0
60	13	9.2	3.1
90	16.8	11.2	0
120	15.4	8.3	0
150	15.4	6.3	1.6
180	13.9	12.1	2.1

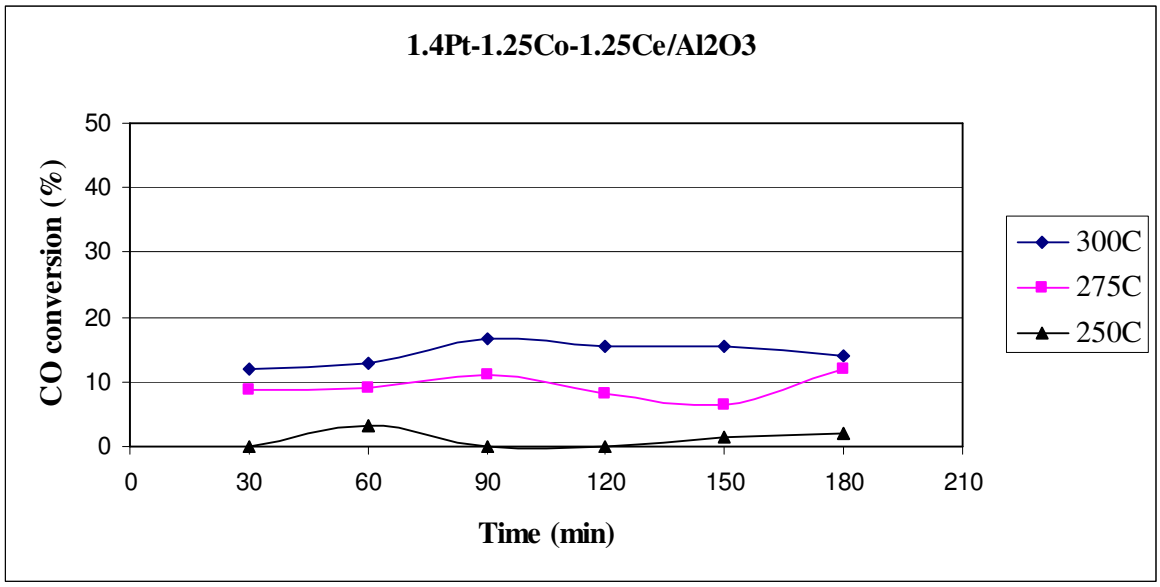

Figure 4.48. CO conversion comparison for Pt-Co-Ce/γ-Al_2O_3 at different temperatures

The CO conversions obtained over this catalyst at 60 minutes time-on-stream was plotted under the equilibrium curve (Table 4.40 and Figure 4.49). Again the reaction was far from the equilibrium.

Table 4.40. CO conversion over 1.4%Pt-1.25%Co-1.25%Ce/γ-Al_2O_3 at different reaction temperatures (60 minutes time-on-stream)

Temperature (°C)	CO conversion (%)
300	13
275	9.2
250	3.1

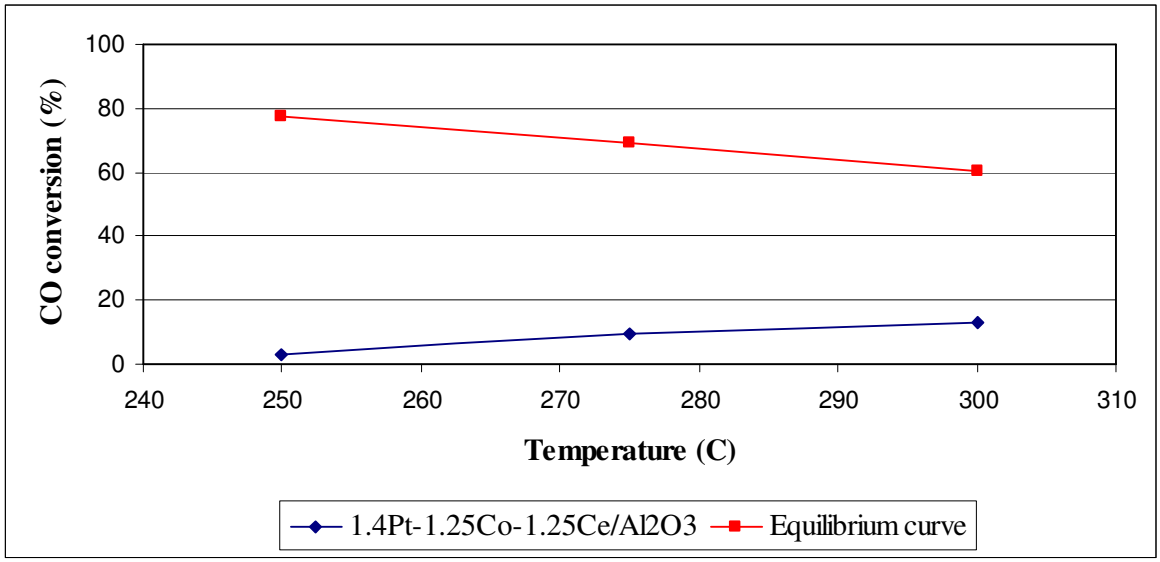

Figure 4.49. CO conversion versus temperature over 1.4wt.%Pt-1.25wt.%Co-1.25wt.%Ce/γ-Al_2O_3 with respect to equilibrium (60 minutes time-on-stream)

Another catalyst investigated was 1.4wt.%Pt-1.25wt.%K-1.25wt.%Ce/Al_2O_3. The activity of catalyst decreased 11 per cent with decreasing temperature from 300 to 275°C. Besides, catalyst had really low activity at 250°C. The results are shown in Table 4.41 and Figure 4.50.

Table 4.41. Conversion results for Pt-K-Ce/γ-Al_2O_3 at different reaction temperatures

Time (min)	CO conversion (%)		
	300°C	275°C	250°C
30	17.1	14.7	0
60	20.5	9.5	1.6
90	18.5	6.8	1.1
120	19.9	3.2	0
150	15.1	3.7	3.7
180	18.5	5.8	1.6

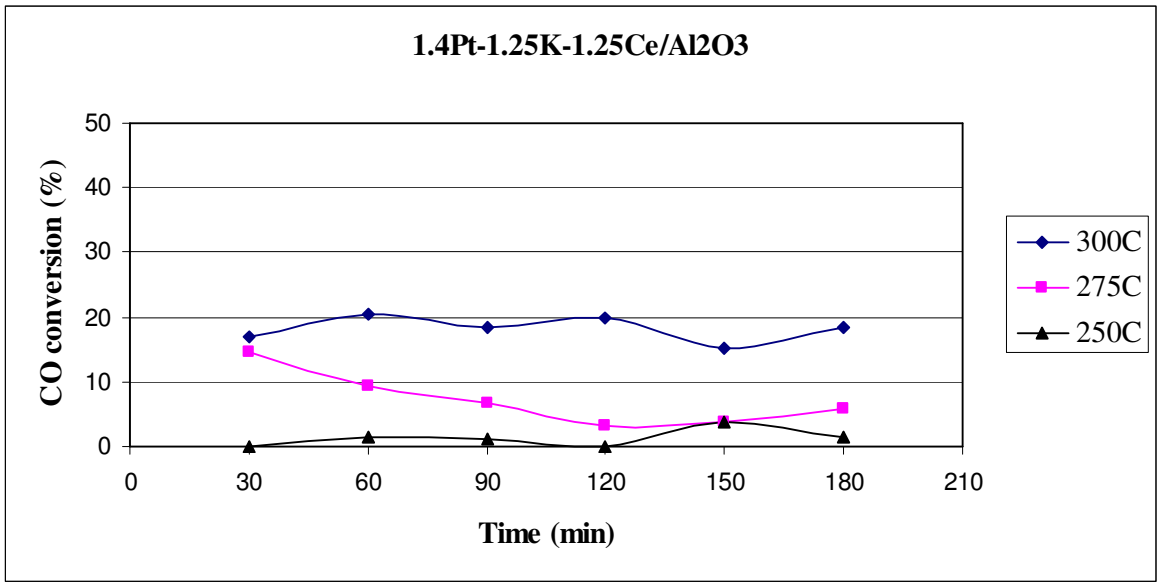

Figure 4.50. CO conversion comparison for Pt-K-Ce/γ-Al_2O_3 at different temperatures

The CO conversions obtained over this catalyst at 60 minutes time-on-stream was plotted under the equilibrium curve (Table 4.42 and Figure 4.51). Again the reaction was not at equilibrium.

Table 4.42. CO conversion over 1.4%Pt-1.25%K-1.25%Ce/γ-Al_2O_3 at different reaction temperatures (60 minutes time-on-stream)

Temperature (^oC)	CO conversion (%)
300	20.5
275	9.5
250	1.6

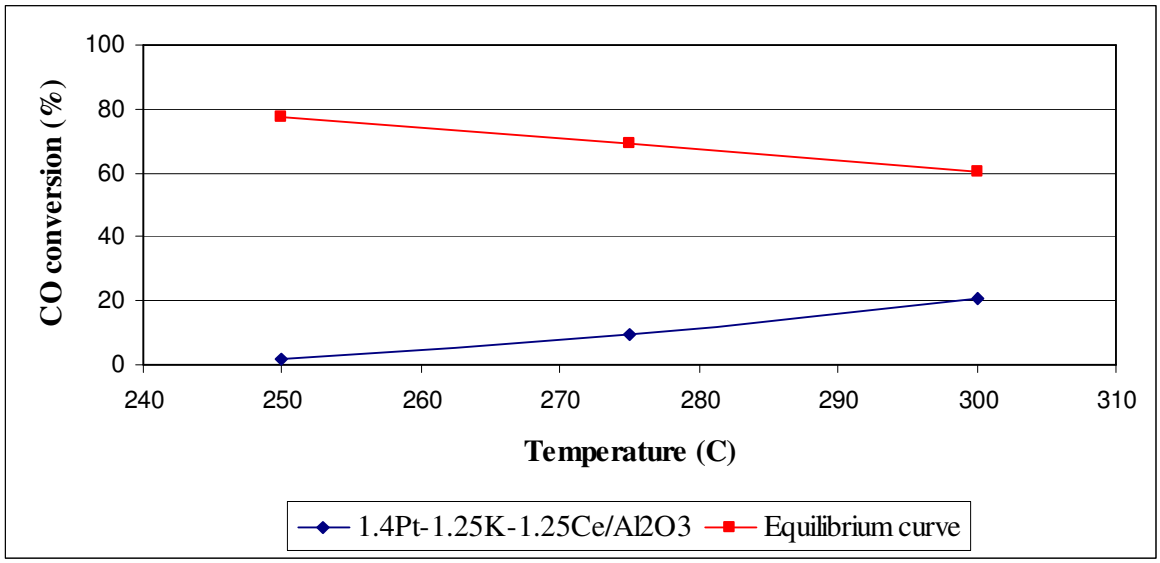

Figure 4.51. CO conversion versus temperature over 1.4wt.%Pt-1.25wt.%K-1.25wt.%Ce/γ-Al_2O_3 with respect to equilibrium (60 minutes time-on-stream)

The last catalyst was 1.4wt.%Pt-1.25wt.%Co-1.25wt.%Fe/Al_2O_3. CO conversion decreased from 20.2% to 17.1% after 60 min when temperature reduced from 300 to 275°C (Table 4.43 and Figure 4.52). At 250°C the catalyst deactivated after 120 min.

Table 4.43. Conversion results for Pt-Co-Fe/γ-Al_2O_3 at different reaction temperatures

Time (min)	CO conversion (%)		
	300°C	275°C	250°C
30	19.7	15.6	8.2
60	20.2	17.1	7.3
90	18.7	16.1	7.3
120	10.8	14.6	5.2
150	11.3	13.1	0
180	18.7	13.1	0

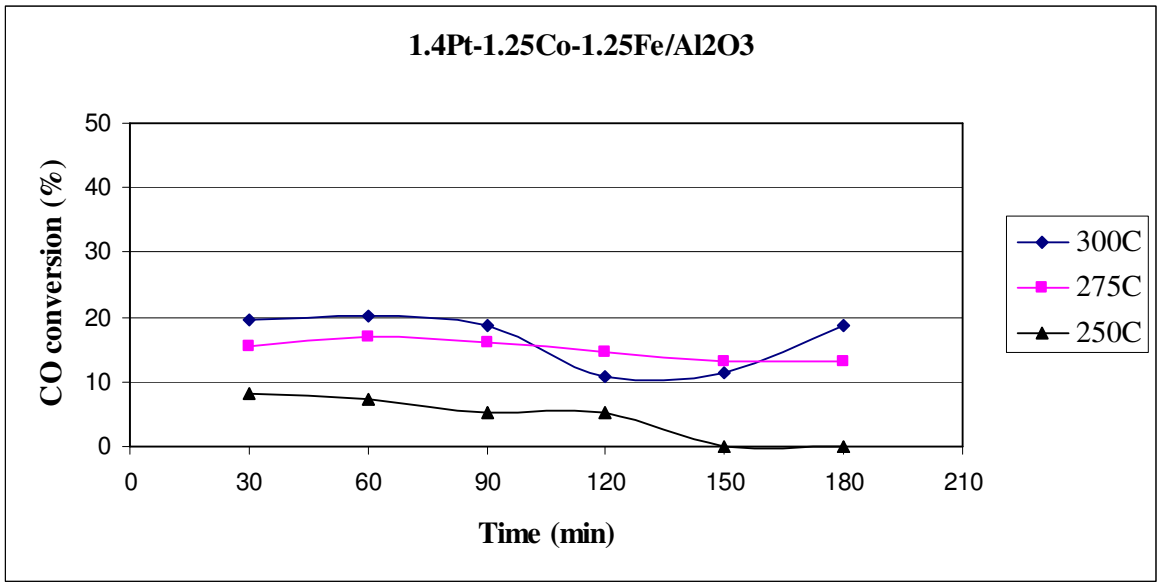

Figure 4.52. CO conversion comparison for Pt-Co-Fe/γ-Al_2O_3 at different temperatures

The CO conversions obtained over this catalyst at 60 minutes time-on-stream was plotted under the equilibrium curve (Table 4.44 and Figure 4.53). Again the reaction was not at equilibrium.

Table 4.44. CO conversion over 1.4%Pt-1.25%Co-1.25%Fe/γ-Al_2O_3 at different reaction temperatures (60 minutes time-on-stream)

Temperature (^oC)	CO conversion (%)
300	20.2
275	17.1
250	7.3

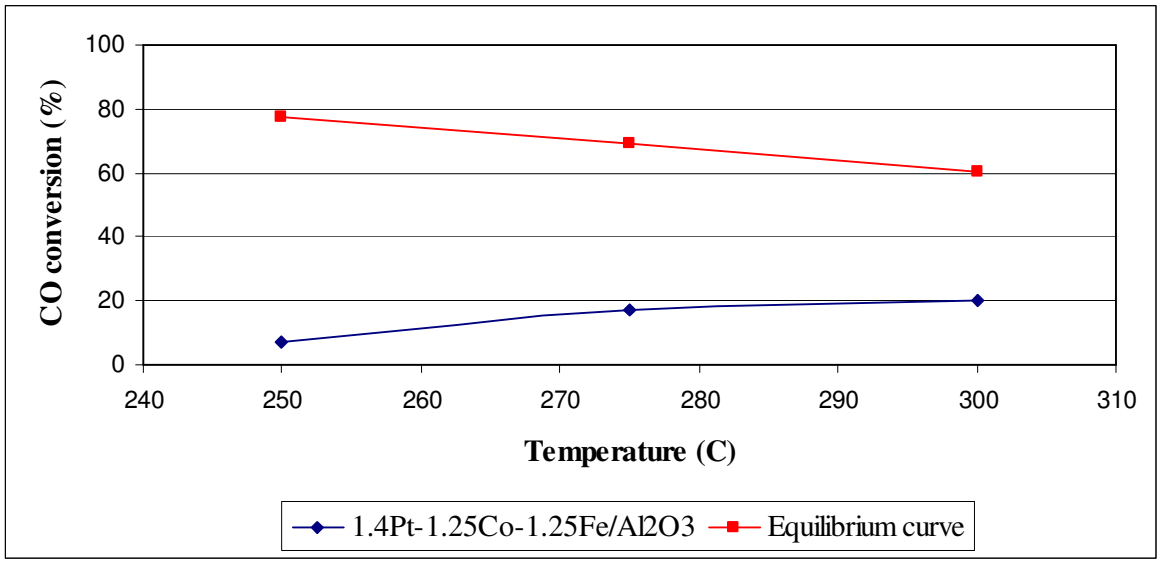

Figure 4.53. CO conversion versus temperature over 1.4wt.%Pt-1.25wt.%Co-1.25wt.%Fe/γ-Al_2O_3 with respect to equilibrium (60 minutes time-on-stream)

The CO conversion value for all the catalyst tested in the presence of CO_2 and H_2 is summarized in Figure 4.54. The conversion decreased with decreasing temperature in all catalysts.

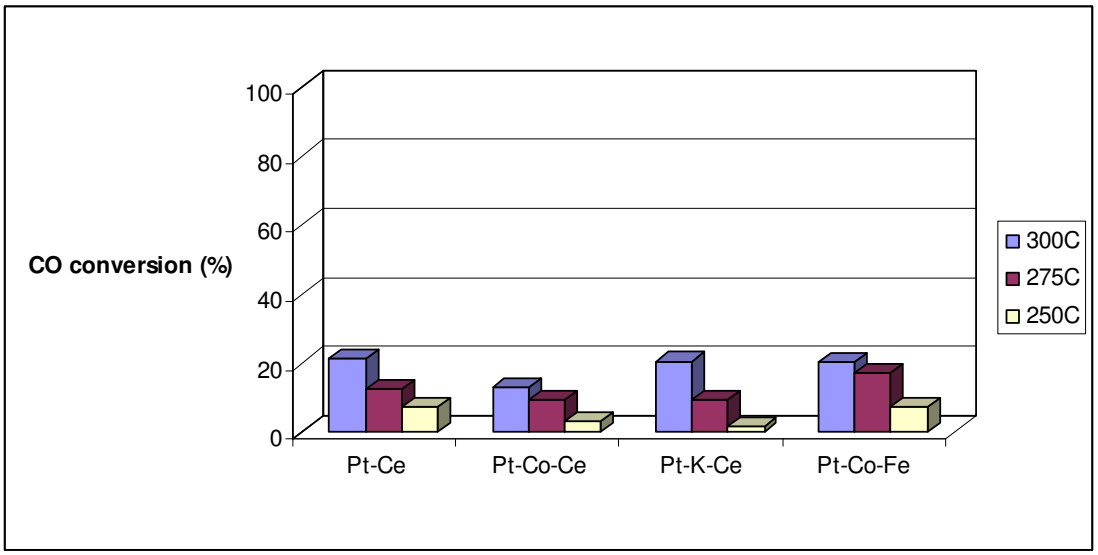

Figure 4.54. CO conversion comparison at the 60th minute for Pt-X-Ce/γ-Al_2O_3 and Pt-Co-X/γ-Al_2O_3 with CO_2&H_2 and without CO_2&H_2 at 300, 275, 250˚C

4.6. Effect of H_2O/CO Ratio in the Presence of CO_2 and H_2

The effect of H_2O/CO ratio was investigated at 275°C over Pt-Ce/Al_2O_3 and Pt-Co-Fe/Al_2O_3 catalysts. In the experiments, 5 per cent CO, 10 or 15 per cent H_2O, 10 per cent CO_2, 40 per cent H_2 and He as balance were used as the feed. In order to get H_2O/CO ratio as 2 and 3, CO was kept as constant and H_2O was changed.

The CO conversions results obtained over Pt-Ce/Al_2O_3 at different H_2O/CO ratios are shown in Table 4.45 and Figure 4.55. The activity of catalyst increased significantly with increasing H_2O/CO ratio from 2 to 3.

Çağlayan and Aksoylu (2009) also investigated the effect of H_2O/CO ratio over bimetallic Pt-Ni/Al_2O_3 catalyst. They found that CO conversion increased with increasing H_2O/CO ratio. Andreeva *et al.* (2002) investigated the Au/CeO_2 catalyst at different H_2O/CO ratio and obtained that Au/CeO_2 catalyst activity increased as increasing H_2O/CO ratio.

Chen *et al.* (2008b) found that CO conversion enhanced with CO/steam ratio was decreased. They tested CO/steam ratios as 1/2, 1/4 and 1/8. As a result, 68%, 90% and 94% conversion was obtained with 1/2, 1/4 and 1/8 CO/steam ratios, respectively.

Table 4.45. Conversion results for Pt-Ce/γ-Al_2O_3 at different H_2O/CO ratios at 275°C

Time (min)	H_2O/CO ratio	
	2	3
	CO conversion (%)	
30	14.8	25.4
60	12.3	24.4
90	11.3	25.4
120	9.9	24.9
150	10.3	23.4
180	14.3	22.8

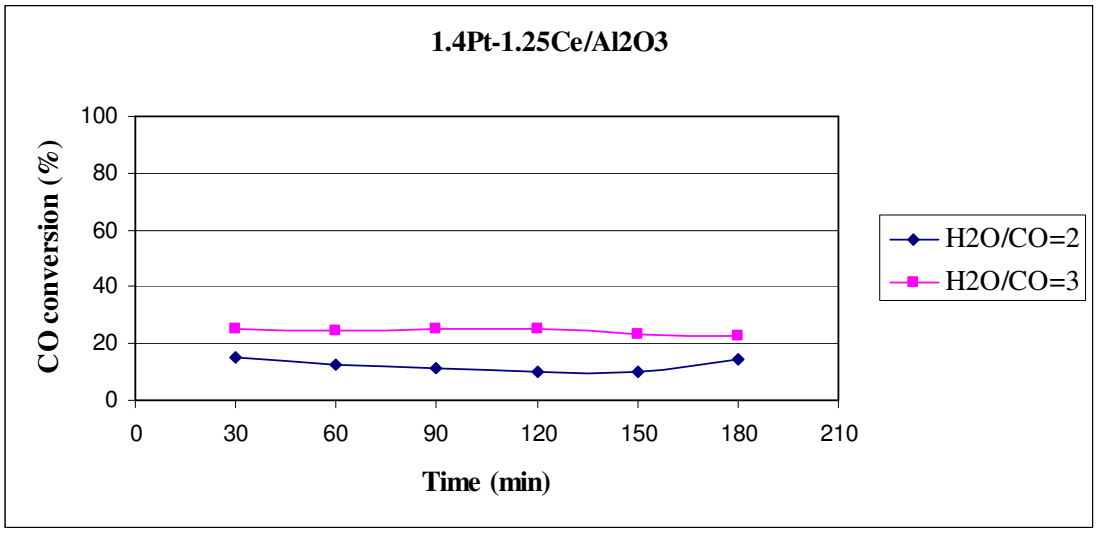

Figure 4.55. Effect of H_2O/CO ratio on CO conversion at 275°C over 1.4wt.%Pt-1.25wt.%Ce/γ-Al_2O_3

The CO conversions results obtained over Pt-Co-Fe/Al_2O_3 at different H_2O/CO ratios are presented in Table 4.46 and Figure 4.56. The activity did not change with increasing H_2O/CO ratio.

Table 4.46. Conversion results for Pt-Co-Fe/γ-Al_2O_3 at different H_2O/CO ratios at 275°C

Time (min)	H_2O/CO ratio	
	2	3
	CO conversion (%)	
30	15.6	15.2
60	17.1	15.2
90	16.1	16.2
120	14.6	15.2
150	13.1	15.7
180	13.1	20.3

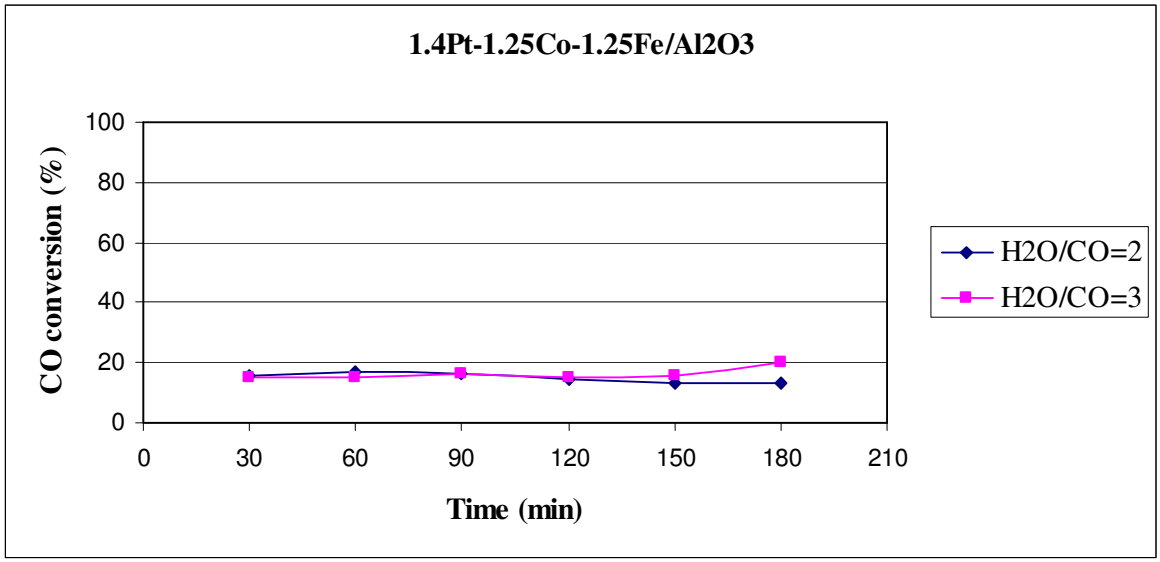

Figure 4.56. Effect of H_2O/CO ratio on CO conversion at 275°C over 1.4wt.%Pt-1.25Co-1.25wt.%Fe/γ-Al_2O_3

5. CONCLUSIONS AND RECOMMENDATIONS

5.1. Conclusions

The purpose of this work was to investigate the second promoter effect on Pt-Ce/Al_2O_3 and Pt-Co/Al_2O_3 for water gas shift reaction. All catalysts were prepared with 1.4wt.%Pt, 1.25wt.% promoter(s) supported on alumina by co-impregnation method. The Co, Ni and K added to Ce while Ce Mg, Mn, Fe, and Zr added to Co as the second promoter. Effect of promoter type in the absence of CO_2 and H_2, in the presence of CO_2, in the presence of both CO_2 and H_2, effect of temperature and the effect of H_2O/CO ratio was investigated at low temperature water gas shift reaction.

The results obtained can be summarized as follows:

- 1.25wt.% Co, K and Ni addition to 1.4wt.%Pt-1.25wt.%Ce/Al_2O_3 had negative effect on CO conversion at 300˚C in the absence of CO_2 and H_2. On the other hand, at 300˚C 1.25wt.%Ce, Fe, Mn and Zr addition to 1.4wt.%Pt-1.25wt.%Co/Al_2O_3 improved the CO conversion while Mg addition did not have any significant result on the catalytic activity.
- The activity decreased with the addition of 10 per cent CO_2 to the feed for all catalysts and this decrease was smaller for the catalysts containing K, Mn, Mg and Zr.
- More decrease in the catalytic activity was observed with the addition of 40%H_2 than 10%CO_2. The influence of the H_2 was most dramatically seen on the Pt-Ce/Al_2O_3 with an about 53 per cent decrease in CO conversion.
- The presence of CO_2 and H_2 together affected all catalysts tested negatively as expected. The performances of Pt-Ce/Al_2O_3, Pt-K-Ce/Al_2O_3 and Pt-Co-Fe/Al_2O_3 catalysts were found to be quite close to each other under these feed conditions at 300°C.
- The reaction temperature had significant effect on CO conversion for all Pt-based catalysts. CO conversion decreased as the reaction temperature decreased from 300 to 275, 250°C.

- The activity of 1.4wt.%Pt-1.25wt.%Ce/γ-Al_2O_3 catalyst increased significantly with increasing H_2O/CO ratio from 2 to 3. On the other hand, no change was observed on 1.4wt.%Pt-1.25wt.%Co-1.25wt.%Fe/γ-Al_2O_3 catalyst.

5.2. Recommendations

According to the results of experiments, the recommendations for low temperature water gas shift reaction are shown as follows:

- Catalytic activity can be improved with changing catalyst preparation method. Sequential impregnation can be employed instead of co-impregnation method.
- Higher platinum and promoters loadings can be tested for higher CO conversions.
- The reduction time under H_2 flow can be increased to obtain more active catalysts.
- Characterization techniques can be helpful to understand the reaction pathways clearly.

REFERENCES

Adrover, M. E., E.Lopez, D.O. Borio and M. N. Pedernera, 2009, "Simulation of a membrane reactor for the WGS reaction: Pressure and thermal effects", *Chemical Engineering Journal,* In Press.

Akın, A. N., 1996, *Development of Coprecipitated Cobalt-Alumina Catalysts for the Production of C_1-C_4 Hydrocarbons by Carbon Monoxide Hydrogenation*, Ph. D. Dissertation, Boğaziçi University.

Andreeva, D., V. Idakiev, T. Tabakova, L. Ilieva, P. Falaras, A. Bourlinos and A. Travlos, 2002, " Low temperature water gas shift reaction over Au/CeO_2 catalysts ", *Catalysis Today*, Vol. 72, pp. 51-57.

Araujo, G. C. and M. C. Rangel, 2000, "An environmental friendly dopant for the high-temperature shift catalysts", *Catalysis Today*, Vol. 62, pp. 201–207.

Azzam, K.G., I.V. Babich, K. Seshan and L. Lefferts, 2007a, "Bifunctional catalysts for single-stage water–gas shift reaction in fuel cell applications. Part 1. Effect of the support on the reaction sequence", *Journal of Catalysis,* Vol. 251, pp. 153–162.

Azzam, K.G., I.V. Babich, K. Seshan and L. Lefferts, 2007b, "A bifunctional catalyst for the single-stage water–gas shift reaction in fuel cell applications. Part 2. Roles of the support and promoter on catalyst activity and stability", *Journal of Catalysis,* Vol. 251, pp. 163-171.

Balakrishnan K. and R. D. Gonzalez, 1994, "Preparation of Bimetallic Pt-Sn/Alumina Catalysts by the Sol-Gel Method", *Langmuir*, Vol. 1*0, pp.* 2487-2490.

Bamwenda, G. R., S. Tsubota, T. Nakamura and M. Haruta, 1997, "The influence of the preparation methods on the catalytic activity of platinum and gold supported on TiO_2 for CO oxidation", *Catal. Lett.*, Vol. 44, pp. 83-87.

Campanati, M., G. Fornasari and A. Vaccari, 2003, "Fundamentals in the preparation of heterogeneous catalysts", *Catalysis Today*, Vol. 77, pp. 299–314.

Chen, W.H., M. R. Lin, T. L. Jiang and M. H.Chen, 2008a, "Modeling and simulation of hydrogen generation from high-temperature and low-temperature water gas shift reactions", *International Journal of hydrogen Energy*, Vol. 33, pp. 6644-6656.

Chen, W.H., T. C. Hsieh and T.L. Jiang, 2008b, "An experimental study on carbon monoxide conversion and hydrogen generation from water gas shift reaction", *Energy Conversion and Management*, Vol. 49, pp. 2801–2808.

Costa, J. L. R., G. S. Marchetti and M. C. Rangel, 2002, "A thorium-doped catalyst for the high temperature shift reaction", *Catalysis Today*, Vol. 77, pp. 205–213.

Çağlayan, B. S. and A. E. Aksoylu, 2009, "Water-gas shift reaction over bimetallic Pt-Ni/Al_2O_3 catalysts", *Turk J Chem*, Vol. 33, pp. 1-8.

Damyanova, S. and J. M. C. Bueno, 2003, "Effect of CeO_2 loading on the surface and catalytic behaviors of CeO_2-Al_2O_3-supported Pt catalysts", *Applied Catalysis A: General*, Vol.253, pp. 135-150.

Ding, O.L. and S.H. Chan, 2009, "Water-gas shift assisted autothermal reforming of methane gas – transient and cold start studies", *International Journal of Hydrogen Energy*, Vol. 34, pp. 270-284.

Djinovic, P., J. Batista and A. Pintar, 2008, "Calcination temperature and CuO loading dependence on CuO-CeO2 catalyst activity for water-gas shift reaction", *Applied Catalysis A: General*, Vol. 347, pp. 23–33.

Du, X., Z. Yuan, L. Cao, C. Zhang and S. Wang, 2008, "Water gas shift reaction over Cu–Mn mixed oxides catalysts: Effects of the third metal", *Fuel Processing Technology*, Vol. 89, pp. 131-138.

Duarte de Farias, A. M., P. Bargelia, C. R. Maria da Graça and M. A. Fraga, 2008, "Vanadium-promoted Pt/CeO_2 catalyst for water gas shift reaction ", *Journal of Catalysis*, Vol. 260, pp. 93-102.

European commission report, 2003, "Hydrogen energy and fuel cells", *EUR 20719 EN.*

Figueiredo, R. T., A. L. D. Ramos, H. M. C. Andrade and J. L. G. Fierro, 2005, "Effect of low steam/carbon ratio on water gas shift reaction", *Catalysis Today*, Vol. 107–108, pp. 671–675.

Fiorot, S., C. Galletti, S. Specchia, G. Saracco and V. Specchia, 2007, "Development of Water Gas Shift Supported Catalysts for Fuel Processor Units", *International Journal of Chemical Reactor Engineering*, Vol. 5, Article A113.

Fuelcell energy, 2008, http://www.fuelcellenergy.com/

Fuel cells, 2008, http://www.lanl.gov/orgs/mpa/mpa11/Green Power.pdf

Fuel cell handbook (Fifth Edition), 2000, *EG&G Services Parsons, Inc. Science Applications International Corporation.*

Fuel cell handbook (Seventh Edition), 2004, *EG&G Technical Services, Inc.*

Germani, G., P. Alphonse, M. Courty, Y. Schuurman and C. Mirodatos, 2005, "Platinum/ceria/alumina catalysts on microstructures for carbon monoxide conversion", *Catalysis Today*, Vol. 110, pp. 114–120.

Goerke, O., P. Pfeifer and K. Schubert, 2004, "Water gas shift reaction and selective oxidation of CO in microreactors", *Applied Catalysis A: General*, Vol. 263, pp. 11–18.

Goguet, A., F. Meunier, J.P. Breen, R. Burch, M.I. Petch, and A. F. Ghenciu, 2004, "Study of the origin of the deactivation of a Pt/CeO_2 catalyst during reverse water gas shift (RWGS) reaction", *Journal of Catalysis,* Vol. 226, pp. 382–392.

Gonzalez, I. D., R.M. Navarro, M.C. Alvarez-Galvan, F. Rosa and J.L.G. Fierro, 2008, "Performance enhancement in the water–gas shift reaction of platinum deposited over a cerium-modified TiO_2 support", *Catalysis Communications*, Vol. 9, pp. 1759–1765.

Guo, P., L. Chen, Q. Yang, M. Qiao, H. Li, H. Li, H. Xu and K. Fan, 2009, "$Cu/ZnO/Al_2O_3$ water–gas shift catalysts for practical fuel cell applications: the performance in shut-down/start-up operation", *International Journal of Hydrogen Energy*, Vol. 34, pp. 2361-2368.

Halim, N. A., N. S. Nasri and A. R. Songip, 2005, "Characterization of CoNi based catalyst for Water Gas Shift Reaction", *ICCBP/SOMChE.*

Haryanto, A., S. D. Fernando, S. D. F. To, P. H. Steele, L. Pordesimo and S. Adhikari, 2009, "Hydrogen production through the water-gas shift reaction: Thermodynamic equilibrium versus experimental results over supported Ni catalysts", Energy & Fuels, In Press.

Hu, Y., H. Jin, J. Liu and D. Hao, 2000, "Reactive behaviors of iron-based shift catalyst promoted by ceria", *Chemical Engineering Journal*, Vol. 78, pp. 147–152.

Idakiev, V., T. Tabakova, K. Tenchev, Z. Y. Yuan, T. Z. Ren and B. L. Su, 2007, " Gold nanoparticles supported on ceria-modified mesoporous titania as highly active catalysts for low-temperature water gas shift reaction ", *Catalysis Today*, Vol. 128, pp. 223-229.

Iida, H. and A. Igarashi, 2006, "Structure characterization of $Pt\text{-}Re/TiO_2$ (rutile) and $Pt\text{-}Re/ZrO_2$ catalysts for water gas shift reaction at low-temperature", *Applied Catalysis A: General*, Vol.303, pp. 192–198.

Iida, H., K. Kondo and A. Igarashi, 2006, "Effect of Pt precursors on catalytic activity of Pt/TiO_2 (rutile) for water gas shift reaction at low-temperature", *Catalysis Communications*, Vol. 7, pp. 240–244.

İnce, T., 2004, "*Low temperature oxidation of carbon monoxide over a Pt-CeO_2-Co_3O_4/Al_2O_3 catalyst in H_2-rich streams*", MS. Thesis, Boğaziçi University.

Jo, M.-C., G.-H. Kwon, W. Li and A. M. Lane, 2009, "Preparation and characteristic of pretreated Pt/alumina catalysts for the preferential oxidation of carbon monoxide", Journal of Industrial and Engineering Chemistry, In Press.

Kappen, P., J.-D. Grunwaldt, B. S. Hammershoi, L. Tröger and B. S. Clause, 2001, "The State of Cu Promoter Atoms in High-Temperature Shift Catalysts—An in Situ Fluorescence XAFS Study", *Journal of Catalysis*, Vol. 198, pp. 56–65.

Kim, Y. T., E. D. Park, H. C. Lee, D. Lee and K. H. Lee, 2009, "Water-gas shift reaction over supported Pt-CeO_x catalysts", *Applied Catalysis B: Environmental*, In Press.

Ladebeck, J. R. and J. P. Wagner, 2003, "Catalyst development for water-gas shift", *Handbook of Fuel Cells – Fundamentals, Technology and Applications*, Vol.3, pp. 190-201.

Lee, C.-H. and Y.-W. Chen, 1997, "Effect of support on a catalytic converter for removing CO and HC emissions from a two-stroke motorcycle", *Ind. Eng. Chem. Res,* Vol. 3*6, pp.* 5160-5169.

Lei, Y., N. W. Cant and D. L. Trimm, 2006, "The origin of rhodium promotion of Fe_3O_4–Cr_2O_3 catalysts for the high temperature water–gas shift reaction", *Journal of Catalysis*, Vol. 239, pp. 227–236.

Lei, Y., N. W. Cant and D. L. Trimm, 2005, "Activity patterns for the water gas shift reaction over supported precious metal catalysts", *Catalysis Letters*, Vol. 103, pp. 133-136.

Li, Y., Q. Fu and M. Flytzani-Stephanopoulos, 2000, "Low-temperature water-gas shift reaction over Cu- and Ni-loaded cerium oxide catalysts", *Applied Catalysis B: Environmental*, Vol. 27, pp. 179–191.

Lilong, J., Y. Binghuo and W. Kemei, 2008, "Effects of CeO_2 on structure and properties of Ni-Mn-K/bauxite catalysts for water-gas shift reaction", *Journal of Rare Earths*, Vol. 26, pp. 352.

Lim, S., J. Bae and K. Kim, 2009, "Study of activity and effectiveness factor of noble metal catalysts for water–gas shift reaction", *International Journal of hydrogen Energy*, Vol. 34, pp. 870-876.

Liu, Q., W. Ma, R. He and Z. Mu, 2005, "Reaction and characterization studies of an industrial Cr-free iron-based catalyst for high-temperature water gas shift reaction", *Catalysis Today*, Vol. 106, pp. 52–56.

Lögdberg, S. L., D. Tristantini, O. Borg, L. Ilver, B. Gevert, S. Jaras, E. A. Blekkan and A. Holmen, 2009, "Hydrocarbon production via Fischer–Tropsch synthesis from H_2-poor syngas over different Fe-Co/ γ-Al_2O_3 bimetallic catalysts", Applied Catalysis B: Environmental, Vol. 89, pp. 167–182.

Luengnaruemitchai, A., S. Osuwan and E. Gulari, 2003, "Comparative studies of low-temperature water–gas shift reaction over Pt/CeO_2, Au/CeO_2, and Au/Fe_2O_3 catalysts", *Catalysis Communications*, Vol. 4, pp. 215-221.

Luhui, W., Z. Shaoxing and L. Yuan, 2008, "Reverse water gas shift reaction over Co-precipitated Ni-CeO_2 catalysts", *Journal of Rare Earths*, Vol. 26, pp. 66-70.

Mhadeshwar, A. B. and D. G.Vlachos, 2005, "Is the water-gas shift reaction on Pt simple? Computer-aided microkinetic model reduction, lumped rate expression, and rate-determining step, *Catalysis Today*, Vol. 105, pp. 162-172.

Mitsui, T., T. Matsui, H. Miyata, T. Kanazawa, I. Hachisuka, R. Kikuchi and K. Eguchi, 2008, "Formation of layered Al_2O_3 and its inhibitory effect on the sintering of supported platinum particles", *Applied Catalysis A: General*, Vol. 348, pp. 121–128.

Mohamed, M. M., T. M. Salama, A. I. Othman and G. A. El-Shobaky, 2005, "Low temperature water-gas shift reaction on cerium containing mordenites prepared by different methods", *Applied Catalysis A: General*, Vol. 279, pp. 23–33.

Nagai, M., A. Md. Zahidul and K. Matsuda, 2006, "Nano-structured nickel–molybdenum carbide catalyst for low-temperature water-gas shift reaction", *Applied Catalysis A: General*, Vol. 313, pp. 137–145.

Natesakhawat, S., X. Wang, L. Zhang and U. S. Ozkan, 2006, "Development of chromium-free iron-based catalysts for high-temperature water-gas shift reaction", *Journal of Molecular Catalysis A: Chemical*, Vol. 260, pp. 82-94.

Önsan, Z. I., 2007, "Catalytic Processes for Clean Hydrogen Production from Hydrocarbons", *Turk J Chem*, Vol. 31, pp. 531 – 550.

Panagiotopoulou, P., J. Papavasiliou and G. Avgouropoulos, 2007, "Water–gas shift activity of doped Pt/CeO_2 catalysts", *Chemical Engineering Journal*, Vol. 134, pp. 16–22.

Panagiotopoulou, P. and D. I. Kondarides, 2006, "Effect of the nature of the support on the catalytic performance of noble metal catalysts for the water–gas shift reaction", *Catalysis Today*, Vol. 112, pp. 49–52.

Panagiotopoulou, P. and D. I. Kondarides, 2007, "A comparative study of the water-gas shift activity of Pt catalysts supported on single (MO_x) and composite (MO_x/Al_2O_3, MO_x/TiO_2) metal oxide carriers", *Catalysis Today*, Vol. 127, pp. 319–329.

Pecchi, G., M. Morales, and P. Reyes, 1997, "Pt/SiO_2 catalysts obtained by the sol-gel method. Influence of the pH of gelation on the surface and catalytic properties", React. Kinet. *Catal. Lett.*, Vol. 61, pp. 237-244.

Pereira, A. L. C., G. J. P. Berrocal , S. G. Marchetti, A. Albornoz, A. O. Souza and M. C. Rangel, 2008, "A comparison between the precipitation and impregnation methods for water gas shift catalysts", *Journal of Molecular Catalysis A: Chemical*, Vol. 281, pp. 66–72.

Pierre, D., W. Deng and M. Flytzani-Stephanopoulos, 2007, "The Importance of Strongly Bound Pt–CeO*x* Species for the Water-gas Shift Reaction: Catalyst Activity and Stability Evaluation", *Top Catal*, Vol. 46, pp. 363-373.

Radhakrishnan, R**.**, R.R. Willigan, Z. Dardas and T.H. Vanderspurt, 2006, **"**Water gas shift activity and kinetics of Pt/Re catalysts supported on ceria-zirconia oxides", *Applied Catalysis B: Environmental*, Vol. 66, pp. 23-28.

Rhodes, C., B. P. Williams, F. King and G. J. Hutchings, 2002, " Promotion of Fe_3O_4/Cr_2O_3 high temperature water gas shift catalyst ", *Catalysis Communications*, Vol. 3, pp. 381-384.

Ruettinger, W., O. Ilinich and R. J. Farrauto, 2003, "A new generation of water gas shift catalysts for fuel cell applications", *Journal of Power Sources*, Vol. 118, pp. 61-65.

Quadro, E.B., M. L. R. Dias, A. M. M. Amorim and M. C. Rangel, 1999*,* "Chromium and Copper-Doped Magnetite Catalysts for the High Temperature Shift Reaction", *J. Braz. Chem. Soc.*, Vol. 10, pp. 51-59.

Querino, P. S., J. R. C. Bispo and M. C. Rangel, 2005, "The effect of cerium on the properties of Pt/ZrO_2 catalysts in the WGSR", *Catalysis Today*, Vol. 107–108, pp. 920–925.

Sekine, Y., H. Takamatsu, S. Aramaki, K. Ichishima, M. Takada, M. Matsukata and E. Kikuchi, 2009, "Synergistic effect of Pt or Pd and perovskite oxide for water gas shift reaction", *Applied Catalysis A: General*, Vol. 352, pp. 214–222.

Silva, A.M., A. M. Duarte de Farias, L. O. O. Costa, A. P.M.G. Barandas, L. V. Mattos, M. A. Fraga and F. B. Noronha, 2008, "Partial oxidation and water–gas shift reaction in an integrated system for hydrogen production from ethanol", *Applied Catalysis A: General* Vol. 334, pp. 179–186.

Şen, Ö., 2008, *Construction and testing of a low-temperature water-gas shift reaction system*, M. S. Thesis, Boğaziçi University, Istanbul.

Tabakova, T., V. Idakiev, D. Andreeva and I. Mitov, 2000, "Influence of the microscopic properties of the support on the catalytic activity of Au/ZnO, Au/ZrO_2, Au/Fe_2O_3, Au/Fe_2O_3–ZnO, Au/Fe_2O_3–ZrO_2 catalysts for the WGS reaction", *Applied Catalysis A: General*, Vol. 202, pp. 91–97.

Thinon, O., F. Diehl, P. Avenier and Y. Schuurman, 2008, "Screening of bifunctional water-gas shift catalysts", *Catalysis Today*, Vol. 137, pp. 29-35.

Uğuz, K. E., 2007, *Effects of promoters on selective CO oxidation in hydrogen-rich streams over Pt/Al_2O_3 catalysts*, M. S. Thesis, Boğaziçi University, Istanbul.

Venugopal, A., J. Aluha, D. Mogano and M. S. Scurrell, 2003, " The Gold-ruthenium-iron oxide catalytic system for the low temperature water-gas-shift reaction: The examination of gold-ruthenium interaction ", *Applied Catalysis A*: General, Vol. 245, pp. 149-158.

Wee, J. H., 2007, "Applications of proton exchange membrane fuel cell systems", *Renewable and Sustainable Energy Reviews*, Vol.11, pp. 1720–1738.

Yablonsky, G. S., R. Pilasombat, J. P. Breen, R. Burch, S. Hengrasmee, 2009, "Cycles across an equilibrium: Studies of the reverse and forward WGS reaction over a

2%Pt/CeO_2 catalyst (Experimental data and 'kinetic resistance' analysis)", *International Workshop.*

Yahiro, H., K. Murawaki, K. Saiki, T.Yamamoto and H. Yamaura, 2007, "Study on the supported Cu-based catalysts for the low-temperature water–gas shift reaction", *Catalysis Today*, Vol. 126, pp. 436–440.

Yahiro, H., K. Nakaya, T. Yamamoto, K. Saiki and H. Yamaura, 2006, "Effect of calcination temperature on the catalytic activity of copper supported on γ-alumina for the water-gas-shift reaction", *Catalysis Communications*, Vol. 7, pp. 228–231.

Yang, J., Y. Sun, Y. Tang, Y. Liu, H. Wang, L. Tian, H Wang, Z. Zhang, H. Xiang and Y. Li, 2006, "Effect of magnesium promoter on iron-based catalyst for Fischer–Tropsch synthesis", *Journal of Molecular Catalysis A: Chemical*, Vol. 245, pp. 26–36.

Yeragi, D. C., N. C. Pradhan and A. K. Dalai, 2006, "Low-temperature water-gas shift reaction over Mn-promoted Cu/Al_2O_3 catalysts", *Catalysis Letters*, Vol. 112, pp. 139-148.

Zhou, L., Y. Guo, M. Yagi, M. Sakurai and H. Kameyama, 2009, "Investigation of a novel porous anodic alumina plate for methane steam reforming: Hydrothermal stability, electrical heating possibility and reforming reactivity", *International Journal of hydrogen Energy*, Vol. 34, pp. 844-858.

Zhang,L., X. Wang, J.-M. M. Millet, P. H. Matter and U. S. Ozkan, 2008, "Investigation of highly active Fe-Al-Cu catalysts for water-gas shift reaction", *Applied Catalysis A: General*, Vol. 351, pp. 1–8.